https://theses.gla.ac.uk/

Theses Digitisation:

https://www.gla.ac.uk/myglasgow/research/enlighten/theses/digitisation/

This is a digitised version of the original print thesis.

Copyright and moral rights for this work are retained by the author

A copy can be downloaded for personal non-commercial research or study, without prior permission or charge

This work cannot be reproduced or quoted extensively from without first obtaining permission in writing from the author

The content must not be changed in any way or sold commercially in any format or medium without the formal permission of the author

When referring to this work, full bibliographic details including the author, title, awarding institution and date of the thesis must be given

Enlighten: Theses
https://theses.gla.ac.uk/
research-enlighten@glasgow.ac.uk

CRYSTALLISATION KINETICS OF POLYMER SOLUTIONS

ProQuest Number: 10647845

All rights reserved

INFORMATION TO ALL USERS
The quality of this reproduction is dependent upon the quality of the copy submitted.

In the unlikely event that the author did not send a complete manuscript
and there are missing pages, these will be noted. Also, if material had to be removed,
a note will indicate the deletion.

ProQuest 10647845

Published by ProQuest LLC (2017). Copyright of the Dissertation is held by the Author.

All rights reserved.
This work is protected against unauthorized copying under Title 17, United States Code
Microform Edition © ProQuest LLC.

ProQuest LLC.
789 East Eisenhower Parkway
P.O. Box 1346
Ann Arbor, MI 48106 – 1346

T H E S I S

submitted to

THE UNIVERSITY OF GLASGOW

in accordance with the regulations

governing the award of the degree of

DOCTOR OF PHILOSOPHY

BY

N. L. JAIN

MARCH, 1964

ACKNOWLEDGEMENTS

The author wishes to express his thanks to Dr. F. L. Swinton for his encouraging instructions and guidance throughout this work, to Professor P. L. Pauson for providing facilities to work in his laboratories and awarding a grant during major part of these studies, and to the Education Department, Government of Madhya Pradesh, Bhopal (India) for according Leave of Absence.

Thanks are also extended to Miss G. Forrest and Mr. R. K. Selot for their valuable assistance.

S U M M A R Y

During the past two decades, it has been established that the crystallisation process in polymers is a phase transformation phenomenon akin to that occurring in low molecular weight compounds. The experimental crystallisation isotherms have been shown to obey, with a reasonable degree of precision, the Avrami equation,

$$\ln \theta = -Kt^n \simeq -(NG^3).t^n.$$

θ is the weight fraction of material remaining uncrystallised at time t. The time exponent, 'n', is usually found to have an integral value in the range of 1 to 4 and K is the rate constant involving both nucleation and growth processes. This equation, when derived theoretically is based on three main assumptions,

(1) The nucleation is random in space and constant with respect to time.

(2) The growth rate is constant and a linear function of time.

(3) The density of the growing crystalline phase is constant throughout the whole process.

The above equation requires that 'n' should be an integer and sigmoidal curves should be obtained on plotting θ against log t.

Two types of experimental techniques have been used. Dilatometric measurements enabled the overall crystallisation process to be studied while microscopic observations of the separate growth and nucleation processes enable the rate constant to be measured by an independent method.

Most of the early experimental work seemed to indicate integral values of the time exponent, 'n', and these values were, then, used to provide information about the detailed crystallisation mechanism. Recent and more accurate work has led to fractional values of 'n' being found experimentally, and only one experimental dilatometric study has been made of the crystallisation of polymer-diluent mixtures from concentrated or moderately concentrated solutions. The results of this study deviated considerably from the original Avrami equation.

The object of the present work was to obtain more data on the crystallisation of polymer-diluent systems using both dilatometry and microscopy to try and gain some insight into the mechanism of the process. The system selected for study was polyethylene oxide-diethyl sebacate. The polymer was chosen because it is known[111] to form large spherulitic structures rather easily which facilitates microscopic determination of growth and nucleation rates.

The pure polymer was studied first and at all temperatures, the crystallisation followed the simple Avrami equation with a constant value of $n = 2.5 \pm 0.1$ throughout the whole process. Non-integral values of 'n' cannot arise from the Avrami equation and as the first two basic assumptions noted above have been tested experimentally, doubt was cast on the experimental validity of the last. Various density-time relationships were used to modify the theoretical rate equation, but none gave a constant value of n equal to 2.5.

The results on the polymer-diluent systems showed that the nucleation process was basically heterogeneous as for the pure polymer, and the growth rate was linear with respect to time. The dilatometric results gave values of 'n' which were a function of θ, the weight fraction of unchanged material over a large portion of the crystallisation process. The initial value of 'n' was 2.5, as in the case of pure polymer, but after remaining at this value for a certain time which depended on the concentration of polymer in the mixture, 'n' fell in a reasonably linear manner to 1.3 ± 0.1.

A reasonable interpretation of these results is that the crystalline phase begins to grow as a structure similar to that forming in pure polymer, but after a certain time, the diluent is incorporated into the crystalline phase leading to a reduced value of 'n'. Once again, any physically reasonable density-time relationship failed to give a theoretical equation which fitted the experimental results.

CONTENTS

C H A P T E R 1.

I N T R O D U C T I O N

Crystallinity in Polymers

Polymers are composed of a large number of molecular chain units covalently linked together. The polymer molecules may be dis-oriented with respect to one another as in the pure liquid state or arranged in a regular, ordered fashion. Branching[1], cross-linking[2] or steric irregularity[3] are found to inhibit this type of order. The ordered state has been termed crystalline. Various factors such as the presence of different molecular sizes and the large number of chain units make it difficult for the polymer molecule to crystallise completely and uniformly. As a result, a large number of polymers are semicrystalline with a crystallinity range varying between 10 and 90 per cent.

Crystallinity in a polymer determines its fibre forming qualities[4] and the amount of crystallinity has a bearing on its physical and mechanical properties. It has been found[5] that the extent of crystallinity is directly proportional to the increase in rigidity, modulus of elasticity[6], tensile strength[7], change in density and the decay in strain[8] of a polymer sample. The phenomenon, consequently, has been the subject of a large amount of theoretical as well as experimental studies and several reviews[9-15] have been published describing general and special aspects of the problem. Despite these studies, it has not been possible to define the term uniquely. Often poor quantitative agreement is found for the numerical values of the percentage crystallinity of the same sample of polymer when it is determined by different methods.[16]

The earliest attempt to define the percentage crystallinity was based on x-rays which produce selective diffraction from ordered and disordered regions. It was later found that smaller crystallites could not be included in these diffractions because of their highly diffuse scattering. The Patterson function,

$$P(u) = \int P(r + u).P.r(dr)$$

Where $P(r)$ is the electron density at r, gives a better definition[17] than the one based on molecular sharpness only. Here, with a large value of u, $P(u)$ would measure the persistence of regularity of the lattice.

The thermodynamic definition of crystallinity is based on the assumption of the existence of two distinct phases within the bulk polymer, the crystalline phase being defined as any unit volume wherein all the chain groups behave as a unit under an externally applied force. This phase will behave differently from the amorphous phase present with it in the sample. In this case, the crystallinity (X) may be defined by the equation

$$X = \frac{P_l - P_x}{P_l - P_c}$$

Where P may be a property such as enthalpy, volume or x-ray intensity of the polymer in its various states. The subscripts refer to liquid (l), crystalline (c) and mixed (x) states respectively. This definition ignores surface energy and internal disorders.

A mechanical definition[18] of crystallinity has also been proposed. The Markoff chain structure, where chains trace out paths in a cubic lattice with their vectors having only preferred directions along the axes, is characterised by two amorphous (r_+, r_-) and three crystalline (h_+, h_- and h_0) states with the matrix of transition probabilities for x-vectors. The fractions of components existing in h_+, h_-, h_0 states is given b

$$\frac{P}{1 - \alpha + P}$$

the expression which defines the crystallinity.

Till[19] has referred to (a) chain entanglements, (b) heterogeneous chain lengths, (c) side chains, (d) randomness in polymerisation and (e) randomness in disposition of substituents as the factors influencing the crystallinity of polymers. According to him linear polymers will be more crystalline because of the absence of factors (c - e). The intermolecular forces, segmental mobility and size, molecular weight, annealing conditions, structural regularity and temperature are also factors influenci the extent of crystallisation in polymers. Consequantly, crystallinity is rarely determined by only one factor. This is the reason why the results obtained by the various methods are not completely in agreement. A review of methods for determining the degree of crystallisation has recently been given by Magill,[20] where he has enumerated eight influencing factors.

The qualitative and quantitative aspects of the process have been studied extensively during the past two decades. They have followed two main directions, each supplementing the other. In the first case, kinetic studies have been made to determine the crystallisation rate and, subsequently, to deduce the mechanism of the process. These studies relate the crystallisation process to one of the many physical properties undergoing change when molten polymer is allowed to crystallise. The change in volume (or Sp. volume) and density have been used in preference to many others because of the experimental simplicity of such measurements. It has been found that the degree of crystallinity is extremely sensitive to temperature. Studies, therefore, have been made under isothermal conditions at various temperatures. Change of specific heat, refractive index, light depolarisation, infrared spectra either of crystalline bands, or amorphous ones have also been employed for kinetic studies. The thermograms obtained by differential thermal analysis and nuclear magnetic resonance studies have also been used recently.

The other type of study is the direct observation of the physical features of the crystallising polymer by the light or polarising microscope, x-ray diffraction and electron microscope. During the past ten years, the quantitative study of these morphological features have supplied data on rates of growth (G) and nucleation densities (N) of crystallising polymer at various temperatures. This enables rate constants (K) to be measured as in the first method and the experimental values of rate constants obtained by the two methods have been compared. Studies by the latter method have been concerned mainly with bulk polymers of all types and the kinetic data obtained have been in quite reasonable agreement with data obtained by other method. However, no attempt has been made to supplement the kinetic data on polymer-diluent mixtures by microscopic results. The work presented here is an attempt to obtain such data and to find out whether the results are in agreement with the comparative studies on bulk polymers.

Morphology of Semi-crystalline Polymers.

X-ray examination of thin films of polymers reveal that most of them are poly-crystalline and show two types of diffraction pattern characteristic of amorphous and crystalline substances of low molecular weight. The broader crystalline reflections suggest that the crystallites have linear dimensions of the order of ten to one hundred Angstrom-units. It is natural to assume that one molecule may pass through several crystallites and that these crystallites are embedded in the rest of the amorphous part. This simple model was known as the Fringed Miscelle Model'. This could explain some physical properties of polymers such as the melting temperature range, swelling, absorption effects, mechanical behaviour and density defects.[21] It was, however, unable to explain the experimental observation of spherulites in polymers.

Spherulites have long been known to be formed from viscous melts of metals and minerals,[22] but their existence in polymers i.e. polythene - was first reported by Bunn and Alcock[23] in 1945. Since then, spherulitic structure has been confirmed to be a more or less general feature of the morphology of semi-crystalline polymers.

When viewed as thin films under a polarising microscope, the spherulites appear to be circular birefringent areas of radiating fibrillar structure with a dark maltese cross of about 10 microns in diameter in the centre. Optically, it is known that the refractive index for the direction of vibration perpendicular to the polymer molecule is lower than it is along the chain axis. If the larger refractive index is radial, the spherulite is termed as positive and if it is tangential, it is termed as negative. Normally, polymers with polar groups or hydrogen bonds give positive spherulites while polythenes, polypropylene etc. give negative ones. It has, however, been found that many polymers such as PETP,[24] PHMS,[25] PHMA,[26] and polypropylene[27] can form different types of spherulites under different conditions of fusion and crystallisation. Detailed studies have shown that their size and number are extremely temperature sensitive and affect the transparency,[28] yield point[29] and impact strength.[30]

The observation of spherulites in polymers suggested an ordered structure on a larger scale than that expected from the fringed miscelle model. In PETP and Polyethylene Sebacate, diameters up to 75,000-100,000Å have been observed.[4] Microbeam x-rays have confirmed that diffraction is caused only by spherulites, though, in many cases, the crystals may be imperfect or not fully oriented. The statistical theory of polymer crystallisation[31] suggested a two phase model wherein distinct phases - amorphous and crystalline - were in thermodynamic equilibrium. The existence of a definite melting point (T°_m) and depression of T°_m by impurities, diluents and co-polymers according to well-defined formulae were confirmed by experimental observation. Keller[11] considers that the fringed miscelle model is now obsolete while Stuart[21] doubts the validity of the two phase model and suggests that the two phases are regions of different order. A crystal defect model[14] has been proposed by Lindenmeyer while a complete crystalline model has been suggeste by Zaukelies[32] where he has explained the difference of 7.3% in x-ray and observed densities of nylon crystals as due to vacancies within the lattice, dislocation and grain boundaries.

The spherulites have been confirmed to be the products of the crystallisation process. The observations of Richard and Hawkins[33] on polythene and the calculations of Price[34] on PTFE from x-ray date indicate that they form as a secondary process. The results of Morgan[24] et al and of many others, on kinetics of crystallisation indicate that spherulites are the primary products of crystallisation while their growth proceeds through a secondary nucleation mechanism at the surface of existing spherulites. The persistence of nucleii at temperatures well above the melting point has been found experimentally in many cases depending upon temperature and melt conditions.

The spherulites have been assumed to grow from the homogeneous melt in the case of PETP, PHA, PDMS but the recent results of Price[35] on PEO and Sharples[36] et al. on polythene show that growth proceeds out of heterogenesities in these two polymers. Ravisiaka and Kovacs[37] have concluded that the growth of spherulites can be both - homogeneous and heterogeneous - in polythene.

There has been considerable work on the formation of spherulitic shape during the process of crystallisation. Morgan[13a] suggested that polymer crystallites are fibrillar rather than miscellar on the basis of x-ray reflections and microscopic and electron microscopic results. The size and arrangement of these fibrils depend upon the actual conditions of the melt and the crystallisation process. At higher temperatures, they increase in size while at lower temperatures, their size is small and they induce secondary nucleation at their sides. On repetition, this process gives rise to a sheaf-like structure This, subsequently, develops into a spherulitic one - consisting of fibrillar aggregations all lying in radial direction. The five stage process suggested by Bernauer[38] for non-polymeric substances is applicable to polymeric systems. The initial sheaf-like structures, are generally, visible under the electron microscope. They have also been observed through the optical microscope at 200 diameter magnifications in the case of PETP at 240-250°C. The fibrosity of spherulites has been confirmed by Khoury,[39] Gahler[40], Zenckel[41] and coworkers, Kellar and Waring[42] and others in many polymers. This then, confirms that a spherulite develops by a well-defined growth mechanism from a nucleus. Electron microscopy has revealed an inter twinning fibrillar structure of smaller fibril dimensions of 100Å and Fischer,[43] Cleaver and others[44] have observed laminar or ribbonlike structures in many polymers. These conclusions are also confirmed by the light scattering studies of Kean and Stein[45] and Price. Price[46] concluded that the light scattering entities are rods, 8×10^{-5} cm. long and 15×10^{-10} $cm.^2$ in cross section. Hedritic[47] and dendritic[48,54] structures have also been observed in some polymers as a precursor of spherulitic formation.

Detailed studies of spherulites have shown the existence of some abnormal structures. The arms of the maltese cross have been found to be zigzag[49] or concentric rings[50] in the case of PEA, PETP, PE, PHMA and other polymers. They also showed consecutive and periodic extinction patterns. These effects have been explained on the basis of long range periodic ordering[51] of the crystal units along the radius of the spherulites rather than by assuming periodically varying composition[52] or alternation of phases.[53] It has been confirmed that these effects are caused by a helical arrangement of the crystallites. Keith and Padden[54] assume the twisting of ribbonlike structures in polythene while Keller[55] prefers a helicoidal structure supported by Point[50] and Price[56] in the same polymer. The spherulites have also been found to have dendritic growth when grown at higher temperatures or smaller super-coolings.

Despite the earlier observation of single crystals of α-guttapercha from its benzene solution or of β-polyoxymethylene, single crystals of polymer molecules were generally assumed to be improbable. Jacoline,[57] Till[58] and Keller[59] however, independent of each other, were able to grow thin platelets of polythene from dilute solutions (.01-0.1%) in xylene in 1957. These plates had thicknesses of 100-150Å and showed the characteristic electron diffraction patterns for single crystals. The polymer axis was found to be perpendicular to the platelets and growth was spiral. This could be explained by terraced growth through a screw dislocation mechanism suggested for non-polymeric substances by Frank[60] in 1952. Since then, single crystals have been obtained for some twenty polymers including PEO, PVA, isofactic polypropylene, PMP, cell. Triacetate, cellulose II and branched polythenes usually grown from their solutions. In polythene, the single crystals are about 100Å thick whereas the normal length of the molecule is 6000Å. This leads one to assume that the polymer chains fold[59] forward and backward during the growth of single crystals which grow as hollow pyramids[61-63] rather than flat platelets. The pyramids, then, either break or flatten to form single crystals as has been shown by many workers and confirmed by fracture experiments. Lindenmeyer[14] believes that under suitable solvent and temperature conditions, any polymer can be made to form single crystals. It has been established that by varying the conditions of crystallisation, all stages between lozenges and dendrites can be obtained and the thickness or terrace height has been shown to be a function of temperature of crystallisation (T_c).

Fischer[64] and Anderson[14] have observed lamellar single crystals from fractured surfaces of high or low molecular weight polythene and PTFE. These have also been obtained from melt crystallisation of thin films. It is now presumed that this form is the preferred method of crystallisation from the melt. It has been found that the small angle x-ray spacings are almost identical in single crystals grown from solution or the melt. This indicates that melt crystallised lamellae and solution grown single crystal lamellae are very similar and they grow through a chain folding mechanism which has been explained on the basis of a thermodynamic approach by Peterlin and Fischer[65] and a kinetic treatment of Lauritzen and Hoffmann,[66] and of Price.[67] Fischer and Stuart[68] have proposed a laminar growth mechanism for solution grown single crystals.

The relationship between single crystals and spherulites is not yet well defined. Kargin[69] has shown how by changing the conditions of melt, temperature of crystallisation, and the solvent, one can obtain various morphological shapesin which polymer crystallises ribbonlike, lamellar, fibrillar, spherulitic - from polythene, isotactic polyproylene, PTFE, and polystyrene. He has shown that polyproylene spherulites formed at higher temperature were lamellar while they were fibriller at low temperature. He observed spherulitic structures together with single crystals in the same film of bulk polymers like polypropylene, polyamides and polycaprolactam. Furthermore, he transformed single crystals of polythene into spherulites between 110-118°C with increase in molecular mobility while in the reverse process, he obtained single crystals by heating the spherulitic film below the melting point for 2-3 min. and keeping it at 70°C for 2.5 hr. Voegelsong[70] has also recently confirmed polymorphism in nylons. The above view is quite in contrast with earlier views,[71,36] where a spherulite has been described as a complex or organised[36] array of ribbon-like single crystals, though Keller[11] referred to several intermediate structures preceding it.

In conclusion, it may be said that spherulites are not basic structures. They are formed out of smaller structures which might be ribbon like, lamellar or fibrillar depending upon the condition of the melt and the crystallisation process. They can also grow out of single crystals through a screw dislocation mechanism.

CHAPTER II

Crystallisation Kinetics of Polymers in Bulk

MATHEMATICAL THEORY

The kinetic analysis of some early experiments[72] on rubber showed that the process of crystallisation in polymers could be treated as a phase transformation phenomenon. Accordingly, it should be possible to apply the theoretical treatment applicable to the crystallisation of simple low molecular weight compounds.

The classical theory[73] of crystallisation of low molecular weight materials assumes that the process consists of two stages, namely:

(i) nucleation, and (ii) growth,

which are concurrent and initiated at $t = o$.

The theory states that in order for the crystalline phase to appear, stable nuclei of a certain critical size must form out of an equilibrium array of associated molecules which are present in the molten substance above its melting point (T_m). These nuclei, then, begin to grow until they are retarded or stopped by abutment against other crystallites. The kinetics of crystallisation, therefore, can be described under three sections as follows,

(a) Kinetics of nucleation,

(b) Kinetics of growth,

(c) Overall kinetics including both nucleation and growth factors.

Kinetics of Nucleationn

According to the classical nucleation theory of Becker and Doring,[74] and Turnbull and Fischer,[75] the rate of nuclei formation in a condensed system is given by the equation,

$$N = N_c(T) \exp\left(-\frac{E_D}{RT} - \frac{\Delta F}{RT}\right) \quad \ldots\ldots\ldots\ldots\ldots\ldots(1$$

where

N is the Nucleation Rate and

E_D = Activation energy of viscous flow which is required for a unit to pass from the liquid to the crystal surface.

ΔF = The free energy barrier or the difference between the free energies of the liquid and crystalline states.

N_0 - A frequency factor which is almost independent of temperature.

The free energy change in the formation of a nucleus possesses a maximum value with respect to the size of the nucleous. The ΔF_{max} is the height of the free energy barrier which must be overcome before stable nuclei are formed. Nuclei smaller than the size corresponding to $\Delta F_{max.}$ are thermodynamically unstable and redissolve, larger nuclei grow spontaneously.

For the rate of nucleation of critical size nuclei, then, the equation (1) assumes the form,

$$N = N_0(T) \exp\left[-\frac{E_D}{RT} - \frac{\Delta F(max)}{RT}\right] \quad \ldots\ldots\ldots\ldots\ldots\ldots($$

Expressions for $\Delta F_{max.}$

The free energy term ΔF in (1) is the resultant of two opposing forces.

(a) The surface free energy associated with the new surface which is positive and proportional to the surface area.

(b) The bulk free energy of fusion which is negative and proportional to the volume.

The values of ΔF depend upon the geometry of the nuclei developed. The free energy of formation of a spherical nucleus is given by,

$$\Delta F_S = 4\pi r^2 \sigma_s - \frac{4}{3}\pi r^3 \Delta f_0 \qquad \ldots\ldots\ldots\ldots\ldots(3)$$

where r is the radius of the sphere and

σ_s - The interfacial free energy per unit area between the crystal and liquid surfaces.

Δf_0 - Bulk free energy of fusion per mole of substance.

For the disc-shaped, cylindrical nucleus $\Delta F = \Delta F_d$ and,

$$\Delta F_D = 2\pi r l \sigma_s + 2\pi r^2 \sigma_E - \pi r^2 l \Delta f_0 \qquad \ldots\ldots\ldots\ldots\ldots(4)$$

where σ_s - the interfacial free energy per unit area for curved surface.

σ_E - The interfacial free energy per unit area for the two end surfaces.

r, l - the radius and thickness of the disc respectively.

The equations (3) or (4) can be used to evaluate the value of $\Delta F_{max.}$ in (2) corresponding to the maximum value of r - the critical size of the nucleus. Δf_0 can be evaluated thermodynamically as,

$$\Delta f_0 = \Delta Hu - T \Delta S = \Delta Hu - T . \frac{\Delta Hu}{T_m}$$

$$= \Delta Hu \left(1 - T/T_m\right) = \Delta Hu . \frac{\Delta T}{T_m} \qquad \ldots\ldots\ldots\ldots\ldots\ldots\ldots (5)$$

where, Hu = heat of fusion per mole of substance

T_m = melting point of the substance

T = Temperature of crystallisation

ΔT = Degree of supercooling.

Now, on substitution of (5) in (3) or (4) and maximising it with respect to r, we get,

$$\Delta F_{s\,(max)} = \frac{16\pi}{3} \frac{\sigma_s^3}{(\Delta Hu)^2} \frac{T_m^2}{(\Delta T)^2} \qquad \ldots\ldots\ldots\ldots (6)$$

and $$r_{max.} = \frac{2\sigma_s . T_m}{\Delta Hu . \Delta T} \qquad \ldots\ldots\ldots\ldots\ldots\ldots\ldots (6a)$$

for the spherical nucleus and for the disc nucleus,

$$\Delta F_{D\,(max)} = \frac{8\pi \sigma_s^2 \sigma_E}{\Delta Hu} . \frac{T_m^2}{(\Delta T)^2} \qquad \ldots\ldots\ldots\ldots (7)$$

and $$l = \frac{4\sigma_E . T_m}{\Delta Hu . \Delta T} \qquad \ldots\ldots\ldots\ldots\ldots\ldots\ldots (7a)$$

$$r_{max.} = \frac{2\sigma_s . T_m}{\Delta Hu . \Delta T} \qquad \ldots\ldots\ldots\ldots\ldots\ldots\ldots (7b)$$

Now, substituting the values of $F_{d\ max.}$ or F_s max. in equation (2), we get,

$$N = N_c(T)\exp - \left[\frac{E_D}{RT} + \frac{16\pi}{3RT}\cdot\frac{\sigma_s^3}{(\Delta H_u)^2}\frac{T_m^2}{(\Delta T)^2}\right] \qquad (8a)$$

$$N = N_c(T)\exp - \left[\frac{E_D}{RT} + \frac{8\pi}{RT}\cdot\frac{\sigma_s^2\cdot\sigma_E\cdot T_m^2}{(\Delta H_u)^2(\Delta T)^2}\right] \qquad (8b)$$

for the spherical and disc-shaped nuclei respectively. It has, however, been found that the activation energy for viscous flow, i.e. E_D does not vary appreciably, just below T_m and could be assumed to be temperature independent.

It can be seen from (8a - b) that a plot of log N versus $T_m^2/T\Delta T^2$ should be linear in both cases.

Similar expressions have been obtained for linear or two-dimensional nuclei where the factor $T_m^2/T\Delta T^2$ in (8a-b) is replaced by $T_m/T\Delta T$.

Application of the Nucleation Theory to Polymeric Systems

Mandelkern[79] first showed how the above theory can be applied to polymeric systems. Assuming that nucleation rates obey equations (2), the free energy of formation of, say, a disc-shaped cylindrical nucleus will be

F_d = Surface free energy (cylinder + sides) − bulk free energy of fusion.

If we assume that a polymer disc nucleus consists of P polymer chains with ζ repeating units in length l of the disc, then,

$$F_d = \zeta P \sigma_s \quad - \quad \Delta F_f(\zeta P) \qquad \ldots\ldots\ldots\ldots\ldots \text{(9)}$$

Where ΔF_f includes the bulk free energy of fusion (Δf_o) and the surface free energy at the ends. On consideration of the volume and surface area of each unit, it can be shown that the number of repeating units on the surface,

$$\zeta P_s = \zeta . 2 (\pi P)^{\frac{1}{2}} \qquad \ldots\ldots\ldots\ldots\ldots\ldots \text{(1}$$

Similarly by applying the statistical theory of polymers, ΔF_f can be evaluated for a system having N polymer molecules of x repeating units each,

$$\frac{\Delta F_f}{xN} = \left(\frac{\zeta P}{xN}\right) \Delta f_o + RT \left\{ \frac{1}{x} \ln\left(1 - \frac{\zeta P}{xN}\right) + \frac{P}{xN} \left[\ln D + \left(\frac{x - \zeta + 1}{x}\right) \right] \right\} \qquad \text{(1}$$

where D is a parameter varying between 0 and 1. The expression (11) could be put in the following simpler form on the assump-tio that the number of repeating units in the length of a nucleus must be much less than x. Since the crystallite length is much less than the molecular length of the polymer*,

$$\Delta F_f = \zeta P \Delta f_0 \quad + RTPlnD \quad \ldots\ldots\ldots\ldots\ldots\ldots\ldots (12)$$

Thus, $$F_d = 2\zeta \sigma_s (\pi P)^{1/2} - \zeta P \Delta f_0 + RT.P.lnD \ldots\ldots\ldots\ldots\ldots\ldots (13)$$

Maximising this expression (13) in the usual way, we have,

$$\Delta F_{d\,(max)} = 4\pi \sigma_s^2 \gamma . \frac{Tm^2}{(\Delta Hu . \Delta T)^2} \ldots\ldots\ldots\ldots (14)$$

where γ = -RTlnD and, $\Delta f_0 = \frac{\Delta Hu . \Delta T}{Tm}$

On comparing equation (14) with (7), an expression for D is obtained,

$$D = \exp\left(-\frac{2\sigma_E}{RT}\right)$$

The above expressions enable the dimension of the critical size nucleus to be calculated,

$$\zeta = 4\sigma_E / \Delta f_0 = \frac{4\sigma_E}{\Delta Hu} . \frac{Tm}{\Delta T}$$

$$P = \frac{4\pi \sigma_s^2}{\Delta f_0^2} = \frac{4\pi \sigma_s^2}{\Delta Hu^2} . \frac{Tm^2}{\Delta T^2}$$

wherefrom one can obtain (14) in the form,

$$\Delta F_{d\ max.} = \frac{8\pi \sigma_E \sigma_s^2}{\Delta Hu^2} \quad \frac{T_m^2}{\Delta T^2} \quad \ldots\ldots\ldots\ldots\ldots\ldots\ldots (14a)$$

Equation (14a) is almost identical to (7) above.

Kinetics of Growth

The growth of an existing nucleus will depend upon the geometry of the nucleus and will follow either of the two paths,

(a) Three dimensional or spherical growth.

(b) Two dimensional growth, where it is assumed that the growth process consists of repeated secondary nucleations on the surface of the original nucleus.

The growth process is, in many ways, a continuation of the nucleation process and it is found that the theoretical equations for the growth are similar to those already derived for the nucleation mechanism. The essential difference between growth and nucleation is the different free energies required for each. $\Delta F_{max.}$ for growth turns out to be less than for nucleation.

The rate determining step for the growth process is the viscous flow of the polymer molecules from the surrounding melt. If we define, G as the growth rate and replace N in (1), we get,

$$G = G_o(T) \cdot \exp - \left(\frac{E_D}{RT} + \frac{\Delta F}{RT} \right) \quad \ldots\ldots\ldots\ldots (15)$$

Defining F as before and calculating $F_{max.}$ by maximising it with respect to r, we obtain the required expressions for the different modes of growth.

Three-dimensional growth

On rearranging (15) and substituting $F_{max.}$ for spherical growth, as described before, we have the following expression for three dimensional growth,

$$\log \frac{G}{T} = \log G_0 - \frac{E_D}{RT} - \frac{16\pi\sigma_s^3 \cdot T_m^2}{3RT \cdot \Delta H_u^2 \Delta T^2} \quad \ldots\ldots (16)$$

The expression (16) shows that a plot of log $G/T - T_m^2/T\Delta T^2$ Should be linear.

Two-dimensional growth

Two obvious, distinct possibilities arise in this case, a two dimensional growth following a three-dimensional nucleation process and two dimensional growth following a two dimensional nucleation.

Several different theoretical treatments have been given recently giving rise to final equations in which the growth rate G has a different temperature dependence. It is proposed to give one of these treatments, that of Burnet and McDevit in fair detail and simply to quote the results of the other theories.

Burnet-McDevit Treatment[76]

Assuming the growth to proceed by a two dimensional surface nucleation we can define F in (15) as follows,

$$\Delta F = 2\pi r l \sigma_s - \pi r^2 l \Delta f_0 \quad \ldots\ldots (17)$$

where on differentiation, and maximising F with respect to r, we obtain,

$$\frac{dF}{dr} = 2\pi l \sigma_s - 2\pi r l \, \Delta f_0 = 0 \quad \ldots\ldots (18)$$

$$\text{Or, } r = \frac{\sigma_s}{\Delta f_0} = \frac{\sigma_s \cdot T_m}{\Delta H_u \cdot \Delta T} \quad \ldots\ldots (19)$$

when Δf_0 is equated to $\frac{\Delta T}{T_m} . \Delta H_u$ on the assumption that over the temperature interval of interest, the entropy and heat of fusion remain constant.

Now substituting the critical value of r from (19) in (17) andthat of Δf_0, we get,

$$\Delta F_{(max)} = \pi l \sigma_s^2 \cdot \frac{T_m}{\Delta H_u . \Delta T}$$

$$- \pi l \sigma_s^3 . \frac{T_m^2}{(\Delta H_u . \Delta T)^2} \times \frac{\Delta T . \Delta H_u}{T_m}$$

so that,

$$\Delta F_{(max)} = 2\pi l \sigma_s^2 \cdot \frac{T_m}{\Delta H_u . \Delta T} \quad \ldots\ldots\ldots\ldots\ldots (20$$

substituting (20) in (15), we get,

$$G = G_o(T) \exp - \left(\frac{E_D}{RT} + \frac{\pi l \sigma_s^2 \cdot T_m}{RT . \Delta H_u \Delta T} \right) \ldots\ldots\ldots\ldots (21$$

which on rearranging,

$$\log \frac{G}{T} = \log G_o - \frac{E_D}{2.3 RT} - \frac{\pi l \sigma_s^2}{2.3 R . \Delta H_u} \frac{T_m}{T \Delta T} \ . (22$$

Which can be simplified to,

$$\log \frac{G}{T} = \log G_o - \frac{A}{T} - \frac{B . T_m}{T \Delta T} \quad \ldots\ldots\ldots\ldots\ldots (22$$

where . $A = \frac{E_D}{2.3R}$; and $B = \frac{\pi r \sigma_s^2}{2.3R \Delta H_u}$

Equation (22a) is similar to that developed by other workers[70,8] for similar growth.

It is clear that at high temperature or low ΔT, the factor

$T_m/_{T\Delta T}$ will be changing more rapidly than $^1/_T$, while at low temperature or high ΔT-values, the opposite will be the case. Consequently, one could expect a maximum in the G versus T curve. Also, a plot of log $G/_T$ against $T_m/_{T\Delta T}$ should be linear, the slope of the line being proportional to $\sigma s^2/_{\Delta Hu}$

Other treatments.

Barnes *et al*[35] have based their treatment on the fact that spherulites are formed by dendritic growth and that new crystals are constantly nucleated on the surface of the old ones, increasing the volume of the crystals. The growth takes place in radial direction.

Their final equation is,

$$\ln G = \ln G_0 - \frac{\Delta F^{\circ}}{RT} \qquad \ldots\ldots\ldots\ldots(23)$$

where it is assumed that for nucleation controlled growth, the spherulitic growth rate is proportional to the nucleation rate and that entire temperature dependence of N or G lies in the last exponential term F° of the Turnbull expression. In expression (23), $G_0 = \alpha . \theta NO . e^{-ED/RT}$ where α is the fraction of area available for new crystals, and θ is a constant.

The equation (23) indicates that plots of log G against $\frac{1}{T\Delta T}$ should be linear for two dimensional growth. Also, it points out that log G Vs. $\frac{1}{T\Delta T^2}$ should be linear for three dimensional growth.

The treatment of Hirai[77] is based on the following assumptions. A two dimensional nucleus is generated on the surface and grows rapidly to a critical size. When it covers the whole surface, it stops growing. A new nucleus is generated on the surface of the first and the process is repeated to give a layer-like structure.

This treatment further assumes that as the interfacial energy terms (σ_s, σ_E) used in previous theories are practically impossible to measure, they should not appear in the final equations of any theory.

The final equation for the growth rate is,

$$G = \left(4KT/d_1 D_3 . n_L\right)\left[1 - \exp\left\{-\frac{\Delta H_m \Delta T}{RT.T_m}\right\}\left\{\exp - 1/18\,\frac{\Delta H_m . T_m}{RT.\Delta T}\right\}\right] \ldots\ldots(24)$$

where, d_1, d_3 are the width and the length of a rectangular parellopiped segment, ΔH_m is the heat of fusion per mole of the segment and n_L is the melt viscosity near the crystal surface.

The equation can be simplified as follows,

(a) If $\Delta H_m . \Delta T$ is $\ggg R.T.T_m$, then,

$$G = \left(4KT/d_1, d_3, n_L\right) \exp\left(-1/18\,\frac{\Delta H_m . T_m}{RT.\Delta T}\right) \ldots\ldots\ldots\ldots\ldots\ldots(25)$$

(b) If $\Delta H_m . \Delta T$ is $\lll RT.T_m$, then,

$$G = 4/d_1, d_3, n_L\,\frac{\Delta H_m . \Delta T}{T_m} . \frac{1}{N} \exp\left(-\frac{1}{18}\frac{\Delta H_m}{R} . \frac{T_m}{T\Delta T}\right) \ldots\ldots\ldots\ldots(26)$$

If $\Delta T > 50$, equation (25) will be applicable, while in cases where $\Delta T < 50$, the G will be given by (26). In more general cases, it is clear that log $G/_{\Delta T}$ against $^{T_m}/_{T \Delta T}$ should be linear and the slope of the line should enable the values for ΔH_m to be calculated.

Overall crystallisation kinetics: Basis of Avrami Equation

Avrami developed an expression for the overall crystallisation rate of low molecular weight materials by combining the effects of nucleus formation and the impingement of the growing centres.

It is assumed that the new phase is nucleated by the germ nuclei which exist in the old phase. Their effective number can be altered by the temperature and the duration of the supercooling They are generally heterogeneous and of subcritical size.

It is, further, supposed that these nuclei soon pass the region of slow growth beyond which the rate becomes constant and, therefore, the incubation period can be neglected. The germ nucle tend to decrease in two ways - (I) by becoming active growth nucle as a result of free energy fluctuations and (II) by being absorbed by the growing crystalline phase.

Avrami Equation

Avrami deduced the following expression for the crystallisation process in simple compounds.

$$\theta = \frac{W_L}{W_0} = \frac{V_L}{V_0} = \exp\left(-Kt^n\right) \qquad \ldots\ldots\ldots\ldots\ldots\ldots(27)$$

$$\text{or } \log(-\log\theta) = \frac{\log K}{2.3} + n.\log t. \qquad \ldots\ldots\ldots\ldots\ldots\ldots(27a)$$

where, θ is the fraction remaining uncrystallised at any time, t;

K, the overall rate constant including growth and nucleation factors and 'n' is an integral rate parameter varying between 1 and 4 depending upon the mode of growth.

θ can be expressed either as a weight fraction (W) or volume fraction (V) where the subscript L and O refer to the liquid or uncrystallised amount at time t = t and at t = 0 respectively.

The derivation of the equation given by Avrami is mathematically extremely complex, but Evans[78] has derived the equation using simple mathematical techniques based on the pioneer work of Poisson.

For a 2-dimensional system, Evans, like Poisson, assumed that nuclei appear sporadically on the plane surface giving rise to a system of expanding circles. The chance for these circles, numbering n, to pass over a point P within a certain time, t, is given by the Poisson's formula,

$$\exp\left(-E \cdot \frac{E^n}{\lfloor n}\right) \qquad \ldots\ldots\ldots\ldots\ldots\ldots\ldots\ldots(28)$$

where E is the expected number,

Let dE be the expected number arising from nuclei occurring in an annulus of width dr at a radial distance, r, from point P. E is obtained by integration from r = o to r = vt where v is the constant radial velocity of each expanding circle.

The annulus has an area of $2\pi r.dr$. Any point, within the annulus, will be capable of nucleating circles reaching the point P during a period equal to $(t - r/v)$. Thus the elementary contribution dE will be,

$$dE = 2\pi r . dr . N \left(t - \frac{r}{v}\right) \qquad \text{.....................(29}$$

where N is a two-dimensional nucleation rate. If we define N by stating that the number of nuclei, formed in time dt and area dA, will be equal to N.dA.dt., then,

$$E = 2\pi N \int_0^{t,r} \left(t . r - \frac{r^3}{v}\right) . dr = \pi N v^2 \frac{t^3}{3} \qquad \text{......(30}$$

Now, the chance that the point P will escape being crossed by a circle initiated after t=0, is clearly,

$$\exp\left(-E . \frac{E^n}{Ln}\right) = \exp(-E) \qquad \text{...................(31}$$

as under this condition, n = 0 and, therefore, E^n and Ln are both unity. If this probability is α, we have

$$\alpha = e^{-E} = e^{-\pi N v^2 \frac{t^3}{3}} = e^{-Kt^3} \qquad \text{.........(32}$$

where $K = \pi N v^2/3$.

If dust particles or other inclusions present are responsible for nucleating the expanding circles, then, the relation between α and t will be different. In this case, the number of circles will be indicated by the nucleation density (ω) which can be given in terms of the number of nuclei in an area dA, which is ω.dA. Also, as the nuclei are fixed from t = 0 to the end of the process, the conception of time in this case does not arise. Hence, the elementary contribution dE, in this case, is

$$dE = 2\pi r . dr . \omega \qquad \text{....................(33)}$$

so that,

$$E = 2\pi\omega\int_0^{v_1 t} r.\,dr = \pi\omega.\,v^2t^2 \quad\ldots\ldots\ldots\ldots\ldots(34)$$

and,

$$\alpha = e^{-E} = e^{-\pi\omega v^2 t^2} = e^{-K t^2} \quad\ldots\ldots\ldots\ldots(35)$$

where $K = \pi.\omega v^2$

Based on the above principles and applying the necessary shape factors, the following expressions of Table 1 for α can be derived,

TABLE 1. Expressions for α for various shape factors.

Growth	Nucleation			
	Predetermined	n	Sporadic	n
1 3-dimensional spherulite	$\exp\left(-\frac{4\pi\omega.v^3t^3}{3}\right)$	3-4	$\exp\left(-\frac{\pi N v^3 t^4}{3}\right)$	4
2 2-dimensional circles	$\exp\left(-\pi\omega\, v^2.t^2\right)$	2-3	$\exp\left(-\frac{\pi N v^2.t^3}{3}\right)$	3
3 " fibrilar	$\exp\left(-\frac{\pi d^2\omega v.t}{2}\right)$	1-2	$\exp\left(-\frac{\pi d^2 N v t^2}{4}\right)$	2
4 Sheaf	$\exp\left(-K^{v} t^5\right)$	4	$\exp\left(-K^{vi} t^6\right)$	4-7

where d is the diameter of the fibrils and the other terms have their normal significance. If we designate the power of t as 'n' and all the other terms except t as K, all these expressions can be put into the form,

$$\alpha = e^{-Kt^n} \quad\ldots\ldots\ldots\ldots\ldots\ldots\ldots\ldots\ldots\ldots(36)$$

where α has the same meaning as θ in the Avrami equation.

Avrami Equation for Polymeric Systems

Mandelkern[79] et al applied the principles on which Avrami based his equation for simple substances, to polymeric systems, and derived a similar expression for the crystallisation kinetics of such systems.

In any polymeric system undergoing crystallisation at a constant temperature, after a certain fraction of the material has crystallised, nucleation can only occur in the molten part and not throughout the whole bulk of the polymer. Also, there will always be impingement and other factors, leading to the retardation of ideal growth of crystals. Thus under such conditions, the actual amount of mass transformed from liquid phase to the crystal phase (dw_c) will be less than the ideal or effective mass (dw_c') transformed. Because the nucleation is random, it can be assumed that in the vicinity of growing centres, the fraction of mass remaining untransformed is the same as the total fraction untransformed.

Consider a polymeric system of mass w_0 in which w_c and w_L are the masses transformed and untransformed respectively at time t. If dw_c is the mass that is transformed in a time interval dt and dw_c' is the effective mass that could be transformed in the same time interval, then, it can be assumed that the mass fraction transformed at t will be proportional to the mass fraction remaining untransformed. Moreover, the actual fraction that is transformed is also assumed to be proportional to the effective fraction transformed, the proportionality factor being $1/X_W$, the reciprocal of th equilibrium degree of crystallinity or the mass fraction of the total system which eventually becomes transformed.

On the basis of the above assumptions, the following expression can be derived,

$$dW_c \propto dW_c' \qquad \text{.........................(37)}$$

$$\frac{dW_c}{dW_c'} \propto 1 - \frac{W_c}{W_o} \qquad \text{.........................(38)}$$

combining (37) and (38), we get,

$$\frac{dW_c}{dW_c'} = 1/X_W (1 - W_c/W_o) = 1/X_W \cdot \frac{W_L}{W_o} \qquad \text{..................(39)}$$

$[\text{as } W_o - W_c = W_L]$

If now, we assume ideal growth conditions with a linear radial growth rate G, then, the volume v_c', (t,z) of a spherically growing centre at time t, which was initiated at time Z (where $z \ll t$), can be given by,

$$v_c'(t,z) \cong \frac{4\pi}{3} \cdot G^3 \cdot (t-z)^3 \qquad \text{...........(40)}$$

Similarly, the effective mass W_c' transformed at 't', is given by,

$$W_c'(t) = W_o . N \int_0^t W_c'(t,z) . dz \qquad \text{........(41)}$$

$$= W_o N \frac{\rho_c}{\rho_L} \int_0^t v_c'(t,z) . dz \qquad \text{........(41a)}$$

where N is the nucleation rate per unit mass or volume and ρ_L, ρ_c are densities of the liquid and crystalline polymer respectively.

By substituting (40) in (41a), we have,

$$W_i'(t) = W_0 N \frac{\rho_e}{\rho_l} \int_0^t \frac{4\pi}{3} G^3 (t-z)^3 dz$$

$$= W_0 N \cdot \frac{4\pi}{3} \frac{\rho_e}{\rho_l} G^3 \left\{ \left[\frac{t-z}{4} \right]^4 \right\}_0^t$$

$$= \frac{\pi}{3} \frac{\rho_e}{\rho_l} \cdot W_0 N G^3 t^4 \qquad \ldots\ldots\ldots(42)$$

Now, differentiating (42) with respect to 't', we get,

$$dW_i'(t) = \frac{\rho_e}{\rho_l} \cdot \frac{4\pi}{3} W_0 N G^3 t^3 \qquad \ldots\ldots\ldots\ldots \quad (43)$$

Under ideal conditions, equation (38) becomes,

$$\frac{dW_e}{dW_e'} = \frac{W_i}{W_0} \qquad \ldots\ldots\ldots\ldots\ldots\ldots(38a)$$

Now, on substituting (43) in (38a), we obtain,

$$dW_e = \frac{W_i}{W_0} \cdot \frac{4\pi}{3} \frac{\rho_e}{\rho_l} \cdot W_0 \cdot N \cdot G^3 \cdot t^3$$

$$= (W_0 - W_e) \cdot \frac{4\pi}{3} \cdot \frac{\rho_e}{\rho_l} \cdot N \cdot G^3 \cdot t^3$$

or, or

$$\frac{dW_e}{W_0 - W_e} = \frac{4\pi}{3} \cdot \frac{\rho_e}{\rho_l} \cdot N \cdot G^3 t^3 \qquad \ldots\ldots\ldots(44)$$

The equation (44), on integration, gives,

$$-\log (W_0 - W_e) = \frac{\pi}{3} \frac{\rho_e}{\rho_l} \cdot N G^3 t^4 + K \qquad \ldots\ldots\ldots(45)$$

When $t = 0$, $W_e = 0$, so that,

$K = -\log W_0$

Hence we obtain,

$$\log \frac{W_0}{W_0 - W_e} = \frac{\rho_e}{\rho_l} \cdot \frac{\pi}{3} \cdot N G^3 t^4 \qquad \ldots\ldots\ldots\ldots(46)$$

Now, if we substitute the volume terms in place of weight terms in (46) as,

$$W_0 = p_L v_0,\ W_c = p_c v_c,\ \delta = \rho_L/\rho_c \quad \text{and}$$

$$X_W = W_c/W_0\ (t = \infty),$$

then, we obtain,

$$\log \frac{X_W(\delta - 1)}{X_W(\delta - 1) - (\frac{v_L}{v_0} - 1)} = \frac{1}{X_W} \cdot \frac{\pi}{3} \cdot NG^3 \cdot t^4$$

$$= \frac{1}{X_W} \cdot K \cdot t^4 \quad \ldots\ldots\ldots\ldots\ldots\ldots\ldots (47)$$

Where $K = \frac{\pi}{3\delta} \cdot N \cdot G^3$ and may be called the overall rate constant The effect of $X_W \leq 1$ will be minor except for low values of X_W. Also, the values of X_W in pure polymeric systems under examination for the small temperature interval of interest do not effect the values of overall rate constant K, as X_W, generally, has a high value. X_W might become important in systems such as polymer-diluent mixtures or copolymer-polymer mixtures where X_W may be small. These cases are discussed later.

In a process involving cylindrical growth, the following expression is obtained.

$$\log \frac{\delta - 1}{\delta - v_t/v_0} = 1/X_W \cdot \pi/3\delta\ l_c \cdot N \cdot G^2 t^3 = 1/X_W K \cdot t^3 \quad \ldots\ldots\ldots\ldots (48)$$

where l_c is the thickness of the disc and $K = \frac{\pi}{3\delta} l_c N \cdot G^2$, is the rate constant.

Expressions used for Experimental Verification

The theoretical expressions developed above can be expressed in a form which can be subjected to direct experimental verification.

If we substitute the following,

$X_W = \frac{W_c}{W_0}(t = \infty)$, $W_c = p_c v_c$, $W_c\ (t = \infty) = p_c v_c\ (t = \infty)$

and $v_{c(t)} = \frac{\delta}{\delta - 1}\ (v_t - v_0)$, then, we obtain,

$$\log \frac{v_\infty - v_0}{v_\infty - v_t} = \frac{1}{X_W} \cdot K \cdot t^n \qquad \text{.......................(49)}$$

where K = rate constant for spherical or cylindrical growth, and 'n' denotes the integer which appears in equations (47) and (48) above.

The expression (49) can be related to θ in the following way. θ is the volume fraction remaining uncrystallised at time t, which, by definition, will be,

$$\frac{v_t - v_\infty}{v_0 - v_\infty}$$

whereby one obtains, that the expression,

$$\frac{v_\infty - v_0}{v_\infty - v_t} = - \frac{1}{\theta}$$

Equation (49), now, assumes the form,

$$\log \theta = - \frac{1}{X_W} \cdot K \cdot t^n \cong - Kt^n \qquad \text{......................(49a)}$$

assuming that the effect of X_y is small except at low values as explained earlier.

The Avrami expression suggests that plots of Θ against log t should be sigmoidal and a plot of the values of $\log(-\log \Theta)$ against log t should be linear. In the latter case, the slope of the line will define the parameter 'n' characteristic of the mode of growth and its intercept will give the values for K which includes both the nucleation and growth factors.

If one assumes the values of 'n' arbitrarily, and plots Θ against $\log t^n$, one will obtain plots for vaious values of 'n' which may be compared with the experimentally observed plots. Also, Θ against log t plots should be superposable by rescaling each plot on the time scale, if the crystallisation mechanism remains constant throughout at all temperatures.

The expression (49a) suggests, alternatively, that values of 'n' can be obtained for each stage of the crystallisation process by differentiating the original equation, thus obtaining the expression[80]

$$n = \frac{dh_t}{dt} \Big/ (h_\infty - h_t) \ln \frac{h_0 - h_\infty}{h_t - h_\infty} \quad \ldots\ldots\ldots\ldots\ldots\ldots (49b)$$

Values of dh_t/dt can be obtained from successive pairs of results. A plot of 'n' against $h_t - h_\infty / h_0 - h_\infty$ will confirm whether n is constant or variable throughout the process.

Relation between Microscopic Results and Overall Kinetics

It is clear from the above derivation (47) that the rate constant,

$$K = \frac{\pi}{3} \frac{\rho_c}{\rho_l} . N G^3$$

for three-dimensional spherical growth indicating it to be a combined effect of density, nucleation and growth factors during the crystallisation process. If we assume that the density of the two phases remains constant during the process, and the shape also remains the same after nucleation, we find that,

$$K \cong N . G^3 \qquad \text{.........................(50)}$$

The microscopic observations supply the necessary data regarding the nucleation rate per unit volume and the growth rates of spherulites at different temperatures. Hence it is possible to calculate independently, the rate constant, K, from microscopic data.

It is, then, interesting to compare the values of K obtained by this method and by the intercepts of the Avrami plots. This procedure enables information about the actual growth mechanism to be obtained.

Comparison of Experiment and Theory

The mathematical theory described above has been applied to interpret the results obtained for the crystallisation of many types of polymer. Mandelkern attempted to define the nucleation and growth mechanism for the crystallisation of poly-decamethylene-sebacate on the basis of the results of McIntyre. He found that both the plots of log G against $T_m^2/T\,\Delta T^2$ and log G vs $T_m/T\,\Delta T$ were reasonably linear and, thus, he was unable to choose between the two possible mechanisms. The results of Price[36] and others,[76,77] however, are in better agreement with a two-dimensional growth mechanism, though, if the experimental values of $T_m°$ are increased slightly (i.e. $T_m°$ = T + 3-5°C), the results may satisfy the three dimensional mechanism. The recent comparative study by Limbert and Baer[81] on various polymers have confirmed the two dimensional growth mechanism which could be represented by any of the various linear plots devised for the process. However, they have pointed out that ΔH_u values obtained from slopes of the plots are nearly double the directly measured value when the Hirai equations are used.

The experimental results confirm the dependence of N and G on temperature and a maximum in G has been found in those cases where large temperature ranges have been studied.[34] It has been found that with larger ΔT's, the number of nuclei increases while their size diminishes.

Mandelkern has interpreted his results on the basis of homogeneous nucleation. However, persistence of nuclei in the melt above $T_m°$ has been found in many cases.[34,82] The studies on catalysed and induced nucleation have also been found to obey the Avrami expression except that they reduce the value of rate parameter n by 1 or more than 1 unit.[23] Moreover, at lower ΔT's, homogeneous nucleation seems to be preferred.

The rate parameter-n

The experimental results of the kinetic analysis of the crystallisation process in polymers show that the major part of the process follows the Avrami equation provided there are no complicating factors such as secondary crystallisation and simultaneous growth. The temperature dependence of the process shows it to be nucleation controlled. The θ against log t plots have been, generally, found to be superposable except in the case of branched polythene[46] and polymer-diluent systems [84] at low ΔT's.

The Avrami expression defines the mechanism of the process where the rate parameter, 'n', is assumed or known. The earlier results gave values of n varying between 2 and 4. But recently abnormal values, i.e. below 2 and above 4,[88] and fractional values[86] have been reported in many cases. The cause of this behaviour remains to be explained. It has also been suggested that n varies with temperature according to the expression,[9b]

$$\log K = A - \frac{n \cdot B}{\Delta T^2} \qquad \text{................(51)}$$

Morgan[4] reported that at higher temperatures, the process might be sporadic (i.e. n = 4) or pre-determined (n = 3), but with the increase in ΔT, there is change in the kinetics of crystallisation from n = 4 to n = 3 or 2 in the case of PETP between 248-249°C and PHMA between 160-170°C. Barnes[86] et al also report change in 'n' values in PEO, from the initial to final stage of the crystallisation process at the same temperature. Also, it has been found in some cases, besides being fractional, n has a maximum value at some ΔT, below and above which it decreases.[87] The fractional values of n have been subject to much critical examination recently.[88]

The earlier results have included induction period in the time scale. It has been suggested that this inclusion causes n to be fractional. Allen[89] studied PHMA and obtained Avrami plots excluding the induction period. But the values of 'n' are found to be less than the values obtained by direct observation of the growth process. Recently Magill[90] has reported the same results. Rybnikar, however, finds that fractional values of 'n' disappear on exclusion of the induction period from the time scale.

Avrami plots reported in the literature have generally been non-linear at the initial and final stages at low ΔT. This fact was not taken into account until recently as most of the process - up to 97 per cent - was linear - and the fractional values of n were assumed to be due to experimental uncertainty. The results of Hutamo and Kambara,[87] Sharples and others,[92] however, have now indicated that fractional and constant values of 'n' at the same ΔT's are a general rule rather than an exception.

Suggested Modifications

The non-linearity of Avrami plots and the fractional values of the rate parameter suggest that there is need to introduce some additional parameter besides K and n in the Avrami equation Ravioka and Kovacs[87] suggested simultaneous nucleation occurring during the process and suggested a modified plot on the basis of reduced crystallinity Z. Keith and Padden[87] mention a decrease in molecular mobility as possible cause for these variations. Sharples *et al*[88] have recently rejected the idea of simultaneous occurring processes in the case of PDTP and PE. It is suggested that out of the three assumptions, i.e. (a) a random and constant nucleation; (b) constant rate of growth and (c) constant density of the crystalline phase, on which the Avrami equation is based, one - the last one, must be in error. Johnson and Farrow[109] have also shown that in drawn PETP, the absence of a linear relationship between specific volume and crystallinity indicates that the density of the amorphous material might not be remaining constant. A modified Avrami equation, including a contribution from this factor has been proposed,

$$\theta = \frac{W_L}{W_0} = \frac{v_L}{v_0} = \exp(-Kt^4, At^{-m}) \qquad \ldots\ldots\ldots\ldots\ldots\ldots\ldots\ldots(52)$$

where K is the rate constant excluding density contribution which are At^{-m}. At $m = 0$, $n = 4$, but when $m > 0$, n will have smaller and generally fractional values. This expression awaits experimental verification.

Comparison with Microscopic Results

Morgan[26] obtained K values for PHMA and PETP by both density change and microscopic methods. These values were of the same order of magnitude. McIntyre[81] also obtained a similar order of magnitude in the K values of polydecamethylene sebacate by dilatometry and microscopy. Their microscopic results also support the assumption that the growth rate is linear and constant at any ΔT. The number of nuclei per unit volume also becomes constant after a short initial stage. These observations give support to the assumptions made in the derivation of the Avrami equation.

It has, recently, been found[82-85] that the values of the rate parameter n obtained dilatometrically, do not, in some cases, agree with microscopic observations. These results lead to a value of 3 or 4 for n according as the growth is predetermined or sporadic. But actual dilatometric experiments have given values of 1 - 2.

C H A P T E R III

Crystallisation Kinetics of Polymer-Diluent Systems

MATHEMATICAL THEORY

Melting points of Polymer-diluent Systems

The addition of a low molecular weight diluent to a semi-crystalline polymer depresses the melting point of the polymer according to the formula.[51,84]

$$\frac{1}{T_m} - \frac{1}{T_m^0} = \frac{R}{\Delta H_u} \cdot \frac{V_u}{V_D} \cdot v_1 - \frac{V_u}{\Delta H_u} \cdot \frac{B}{T_m} \cdot v_1^2 \quad \ldots\ldots\ldots\ldots\ldots (52\,(b))$$

where ,

T_m^0, T_m = melting points of polymer and polymer-diluent system respectively.

V_u = Molar volume of the repeating unit.

V_D = Molar volume of the diluent.

ΔH_u = Heat of fusion per mole of repeating unit.

v_1 = Volume fraction of the diluent

B = Interaction Parameter

R = = Gas Constant

The expression (52) is analogous to the equation relating the variation of the freezing point of a binary liquid mixture to the composition of the mixture.

From equation (52(b)), it can be seen that a plot of $\left(\frac{1}{T_m} - \frac{1}{T_m^0}\right)/v_1$ versus $\frac{v_1}{T_m}$ Should be linear, enabling values of ΔH_u and B to be calculated from experimentally measured melting points. ΔH_u ought to be independent of the nature of the diluent.

Kinetic treatment of Polymer-diluent Systems.

The addition of diluent to a polymer causes the viscosity of the system to decrease which tends to an increase in crystallisation rate ($K_{\ }$). Also, it might be expected that the rate of nucleation might decrease owing to the presence of the diluent. These two concentration dependent and opposing forces are, therefore, operative in such systems and it is the dominance of one or the other which defines the overall rate.

Mandelkern[84] observed that polymer-diluent systems should follow the same general principles as bulk polymer systems. The crystallisation process, therefore, can be explained on the basis of expressions developed in the previous chapter with some extra terms included to take into account the presence of the diluents.

The two basic additional assumptions are,

(a) The added diluent, generally of lower molecular weight, is assumed to be excluded from the crystal lattice formed by the polymer.

(b) The nuclei are assumed to grow randomly throughout the mass and the actual crystallisation rate is calculated by considering the increase in mass of an average growing centre developing in the space actually available for transformation.

The nucleation rate is given by the Turnbull expression, as before,

$$N = N_0(T) \exp - \left(\frac{E_D + \Delta E}{RT} \right)$$

The formation of a critical size nucleus requires the replacement of F_D by $F_{max.}$. This value has been evaluated on the principles already described, and can be expressed[9b]

$$\Delta F_{(max)} = \frac{8\pi \sigma_s^2 \sigma_E T_m^2}{\Delta H_u^2 \cdot \Delta T^2} - \frac{4RT \sigma_s^2 \cdot T_m^2 \ln v_2}{\Delta H_u^2 \cdot \Delta T^2} \quad \ldots\ldots(53)$$

where v_2 is the volume fraction of the polymer. The first term in this expression is identical to that for bulk polymers while the second term arises from the consideration of the probability of selecting the number of polymer segments required to form a critical size nucleus from the polymer diluent mixture.

By substituting ΔF_{max} in the nucleation rate expression above, we get

$$N = N_0(T)\exp\left\{ - \frac{E_D}{RT} - \frac{8\pi \sigma_s^2 \sigma_e \cdot T_m^2}{R \cdot \Delta H_u^2 T \cdot \Delta T^2} + \left(\frac{4\pi \sigma_s^2 \cdot T_m^2}{\Delta H_u^2 \cdot \Delta T^2} \right) \ln v_2 \right\} \quad \ldots(54)$$

which describes the process of nucleation in the polymer-diluent system.

The growth of the critical size nucleus can be treated similarly.

$$G = G_0 \exp -\left(\frac{E_D + \Delta F}{RT} \right)$$

In polymer-diluent systems, G_0 and E_D will vary with composition while it may be assumed that they are temperature independent, over the small temperature range of interest. Thus for the disc shaped nucleus to grow spherically,

$$G = G_0 \exp\left(-{}^{4E_D}/_{RT} - \frac{8\pi\sigma_s^2 \cdot \sigma_e \cdot T_m^2}{RT \cdot \Delta H_u^2 \cdot \Delta T^2} + A\right)$$

and for the same nucleus accompanied by disc growth,

$$G = G_0 \exp\left(-\frac{3E_D}{RT} - \frac{8\pi\sigma_s^2 \sigma_e \cdot T_m^2}{RT \cdot \Delta H_u^2 \cdot \Delta T^2} + A\right)$$

Where $A = 4\pi\sigma_s^2 \cdot T_m^2 \cdot \ln v_2 / \Delta H_u^2 \cdot \Delta T^2$

These expressions have only minor differences in the first term of the exponential and lead to nearly the same temperature coefficient of the rate constant (Ks or Kd).

These expressions indicate that a plot of log G against ${T_m^2}/{T\Delta T^2}$ should be linear and its slope should be greater with larger amount of diluent.

Expression for two dimensional growth of the nucleus can be derived which are similar to the bulk polymer systems in which case log $G - \frac{T_m}{T\Delta T}$ should be linear.

Overall Crystallisation Rate

The kinetic studies on polymer-diluent systems have shown that these systems also follow the Avrami expression during the crystallisation process subject to the assumptions described earlier. If X_w is assumed to be the fraction of the total mass, - polymer and diluent, that is crystalline at equilibrium, then, we have as before,

$$\ln\theta = \ln\frac{v_\infty - v_t}{v_\infty - v_0} = -\frac{1}{X_w} K t^n$$

where K is the rate constant including N, G and density terms.

The expression indicates that the process should follow a sigmoidal path and that log(-log θ) against log t should be linear. The slope of the line will define 'n' while the intercept will give values for K- the rate constant.

Comparison with Experimental Results.

Flory[92], Mandelkern and co-workers[93 a,b] have made experimental dilatometric studies on a few polymer-diluent systems and have applied the theoretical considerations described above to their results. The melting process of these systems has been observed to be broadened in range by a factor of 2 in contrast to bulk polymers. The thermodynamic studies have confirmed the linear relationship between $\left(\frac{1}{T_m} - \frac{1}{T_m^\circ}\right)/v_1$ and v_1/T_m. Their plots have been applied to deduce values of ΔH_u and B. It has been found that ΔH_u, being a molecular property of the crystallising unit is independent of the nature of the diluent.

The studies on crystallisation kinetics of polymer-diluent systems indicate that these systems follow a sigmoidal path during the process when θ is plotted against log t. These isotherms are reasonably superposable. But as the concentration of the diluent increases, this superposability becomes qualitative rather than quantitative. In most cases, the Avrami plots are curved and only approximate values of n and K can be obtained.

For a given degree of supercooling (ΔT), the overall values of K for the more concentrated solutions are similar to those obtained for pure polymer. This agreement disappears at higher dilution. It seems it becomes more difficult for crystallinity to develop as the concentration of diluent increases.

Results[9b] have been reported where superposable plots have been obtained in very dilute solutions ~0.25 per cent. It has been found that in dilute solutions, the crystallinity develops at a measurable rate much nearer to T_m than in bulk polymers.

Reasons for Present Work.

It is seen from above that only dilatometric results have been obtained for polymer-diluent systems. This method alone is not sufficient to give all the information required to define the mechanism of growth and nucleation. Microscopic data are clearly required. In a brief exploratory project, Park[24] studied a polyox-diphenyl ether (1:1) system in this way and was able to confirm qualitatively that the rate constants expressed by

$$K \simeq NG^3$$

Could be related and that log K against $T_m^2/T\Delta T^2$ is linear. The present studies have been initiated by these observations. They are aimed at examining the kinetic behaviour of polymer and polymer-diluent systems in more detail and to see whether dilatometric results could be correlated with microscopic ones as has been done for bulk polymers.

The available evidence seemed to indicate that polymer-diluent systems at moderate concentrations do not obey the simple Avrami equation leading to the conclusion that at least one of the basic assumptions in the development of the equation is in error. The two most obvious being (a) constant rate of growth of spherulites and (b) constant rate of nucleation.

Microscopic results enable these two assumptions to be tested and if either or both are found to be disobeyed, a modified form of the Avrami equation might be suggested to take this into account.

In order that self-consistent results be obtained, a full dilatometric study should be carried out using exactly the same materials.

C H A P T E R   XV

E X P E R I M E N T A L

Materials

Poly(ethylene oxide) polymer was supplied by Union Carbide Co. Ltd. under their trade name Polyox-WSR-35. The polymer was used throughout these studies as received. The sample has been found to be up to 95 per cent crystalline and to have an average density of 1.20 gm. cm.$^{-3}$ [95]. The equilibrium melting point, T_m^o, of this polymer was found by dilatometry to be 66.0°C in exact agreement with Mandelkern[94] and a little less than the value reported by Sharples[82] for the same material but with a different thermal history.

Di-ethyl sebacate - with code No. 4252 under British Specifications (H and W) was used as diluent without further purification. The densities of the molten polymer and the diluent were measured at two temperatures and the density was assumed to vary linearly with temperature. The densities of various polymer-diluent mixtures in the molten state was calculated by assuming no volume change on mixing.

Polymer-diluent Mixtures

The polymer - diluent mixtures were prepared by weighing the required amounts of the polymer and the diluent in a clean and dried dish and melting the mixture at 100 ± 5°C for 15-20 minutes. Stirring was continued until the mixing was complete. After a uniform mixture was obtained, it was again heated for 5-10 minutes and then allowed to cool under gradual but uncontrolled conditions. It was observed that visible spherulites formed at different spots in the melt. The cool mixture was then weighed and the loss in weight was assumed to be due to loss of diluent. A consequent correction was applied to calculate the weight per cent composition of the mixture. These mixtures were used for dilatometric studies.

Dilatometry.

The equilibrium melting temperatures of the bulk and diluent blended polymer were determined by dilatometry. The same method was also used to obtain plots of volume change against time to study the rate of crystallisation at different temperatures.

The dilatometer (fig. 1) used was a modified form[86] of the conventional sealed or U-type described by Wood and Bekkedahl[96] and Barnes et al.[86] It consisted of two different parts

(a) The bulb and

(b) the measuring capillary

The bulb was a stainless steel cylinder, 5.1 cm. high 1.5 cm. o.d. and 1.3 cm. i d. with a flanged top 0.50 cm. high and 2.50 cm. in diameter. This held approximately 4-5 gm. material, about half that described earlier.[86]

FIG 1 DILATOMETER

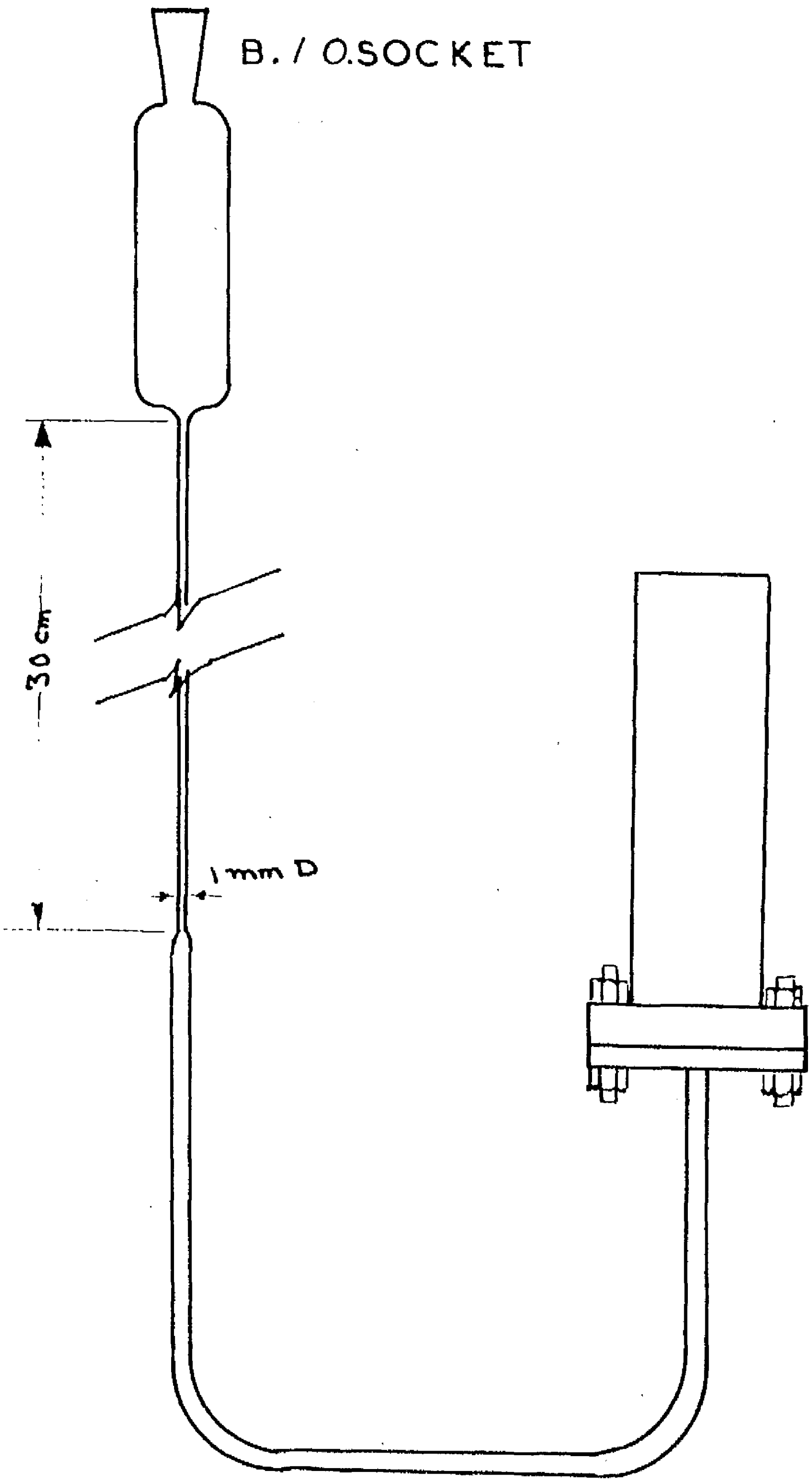

The capillary consisted of a 35-40 cm. length of 1.00 mm. internal diameter precision bore Veridia glass tubing sealed to a B-10 socket at one end and to a Quickfit flange on the other. The two parts were connected through the flanged joints clamped tightly together, which were lightly greased with silicone vacuum grease to render them vacuum-tight.

Filling of Dilatometer

To fill the dilatometer, the bulb was washed several times with chloroform and dried. The required amount of about 1.0 gm. of bulk polymer or a similar bulk-equivalent weight of polymer-diluent mixture was put into the bulb and weighed accurately. The bulb was then kept in the oven at 100 ± 5°C for 15-20 min. and allowed to cool slowly, the thermal history being similar to that described before.[84] It was reweighed to confirm constancy in weight. The capillary was then connected to it.

The dilatometer was afterwards, evacuated for two hours and filled with mercury, in the usual way, under vacuum. The weight of mercury in the dilatometer could be determined by the difference in the weights of mercury before and after the filling.

Working Technique.

The dilatometer was placed in a boiling water bath for exactly 30 min. prior to each kinetic experiment. The height of the mercury column in the capillary as a function of time was measured using a 1-metre cathetometer manufactured by the Precision Tool and Instrument Company. This could be read to ± 0.01 mm.

When filled with bulk polymer, the dilatometer took almost [redacted] three minutes to reach thermal equilibrium with the thermostat bath, after which readings could begin. When filled with polymer-diluent mixtures, the equilibration time increased to about six minutes in the worst case.

The crystallisation or melting experiments were carried out in a rectangular thermostat of conventional design. Water was used as the thermostat fluid in contrast to silicone oil baths used earlier. Constant temperature was maintained using a mercury-toluene regulator in conjunction with a Sunvic hot wire switch, to within ± 0.01°C over periods of several days.

<u>Microscopy - (a) Sample Preparation</u>

The samples of the bulk polymer or polymer-diluent mixtures, prepared as described above were used without any further treatment for microscopic examination.

The cover glasses used for this work were obtained from Chance Bros. They were 16 mm. in diameter, and they weighed 0.015 gm. each on average with an average thickness of

0.15 mm. These cover slips were washed many times with 95% alcohol and then polished with soft KIMWIPE tissue papers before they were used. They were, then, kept in xylene and used when required. This cleaning and polishing process was adopted to exclude heterogeneities from the surface and has been used earlier.[91]

Bulk-Polymer Sample

A small amount (0.1 mg.) of the polymer was placed on a clean and dry coverglass and was allowed to melt for not less than 10 minutes (max. 15 min.) at 100 $\pm$ 2°C when the melt seemed to be uniform. Another cover slip was, then, placed on this melt, and pressed so as to spread the melt uniformly over the whole area. The heating was continued for about five minutes more and the sample was, then, quickly transferred (1 second) to the thermostatted block for examination.

Polymer-diluent Samples

These samples were prepared in a similar way, but as the dilution increased, the time required for melting was very much reduced. The melting time up to a 1:3 mixture was approximately a minute but for the more dilute solutions, only 10 seconds heating was used to avoid loss of diluent. At the highest diluent concentration, the loss in weight due to diluent vaporisation was less than 5 per cent. It appeared, however, that the melting was complete and uniform.

In all the microscopic experiments, the samples were kept in a dessicator prior to their use and they were discarded if more than seven days old. Preliminary work showed that each sample could be used up to three successive times without any degradative changes. Occasionally different samples, of what was apparently the same material, showed varying growth rates. Up to 50 per cent variation was observed in extreme cases. The results presented later are the averages of from 3 to 5 separate experiments.

To minimise stray heat losses or cooling air currents on the surface of the samples, a covering device was used in all the microscopic experiments.

<u>Growth Rate Measurements - Microscope</u>

These were made on a Beck Model 5000 - microscope with X6 eyepiece and X15 objective. The field of observation was 2.32 mm. which could be read from a microscale put under the eyepiece, each division of which corresponded to 0.0232 mm. The microscope was fitted with a device by which the readings could be taken under direct light or polarised light.

<u>Hot-stage.</u>

The hot-stage of the microscope was designed in these laboratories and is shown in figure (2).

It consists of a rectangular brass block with a central

FIG 2 HOT STAGE

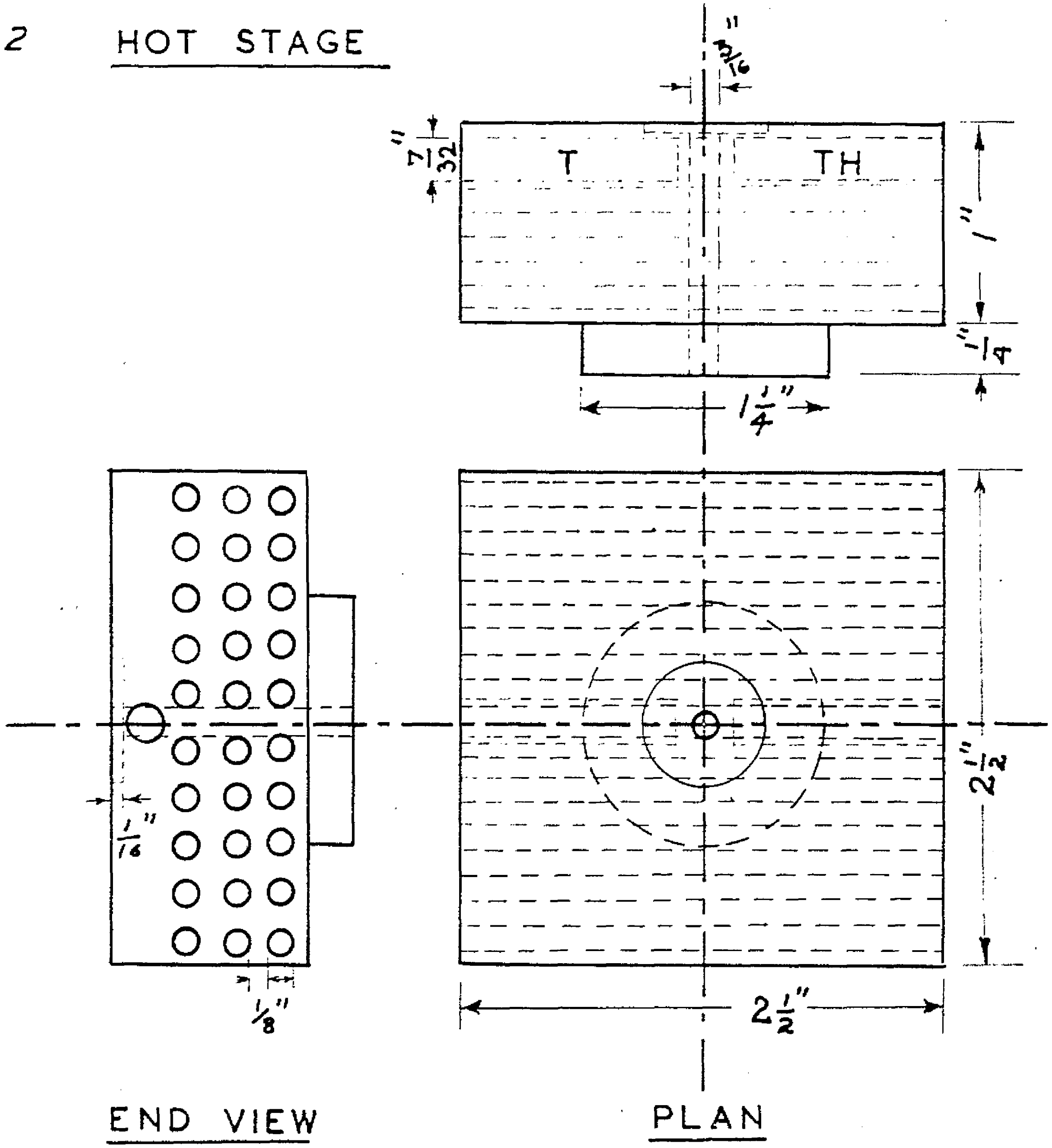

observation hole and two holes drilled in its sides horizontally. The thermometer for recording the temperature is placed in one of these holes and in the other is fitted the thermistor which was used to regulate the temperature. (Shown as T and TH in Fig.2)

The heating element was a thin nichrome wire which was passed through a series of circular holes into the brass block. This was kept insulated from the block by small porcelain beads. The ends of these wires were connected to the automatic control system described below, through two variac transformers. The heating block was thermally insulated by a 5mm. thick jacket of compressed asbestos powder.

The light source for the microscope was a 6 volt, 48 watt Mazda projector lamp.

Automatic Temperature Control System.

The thermistor, placed in one of the cavities of the heating block, was made one arm of a Wheatstone bridge. When the bridge was balanced, the light reflected from the spot-galvanometer in the circuit fell on a photocell. The photocell was connected to the electronic relay which caused the current through the block-heater to increase. The increase in temperature and consequent decrease in the resistance of the thermistor caused an out-of-balance current to flow through the spot galvanometer. The light spot moved off the photo-cell and the current through the block heater was decreased. The temperature control of the system was better than $\pm$ 0.05°C

Experimental Observation of Growth Rate

The samples used for growth rate (G) measurements were approximately 100μ thick. The thickness of the samples was measured using a micrometer after an experiment was performed. The effect of the sample thickness on growth rate was studied.

When the molten samples were transferred to the thermostatte hot stage, the field of view was initially dark when viewed betwee the crossed polaroids. The field gradually brightened and, depending upon the temperature, the spherulites began to appear at random points. At the lower temperatures, i.e. $\Delta T > 15$°C, the number of spherulites, appearing, was large, but at higher temperatures, usually only one spherulite appeared in the field of view. The growth-rate of a selected spherulite was measured using the built-in eye-piece scale. The necessary plots of spherulite radius as a function of time were, then, obtained at different temperatures.

The reproducibility of the growth rates for the same sample was good but it varied for different samples. Repeat experiments on the same samples at a constant temperature showed the spherulites appearing in the same position as before. A sample used for repeated measurements at different temperatures behaved, as expected, the growth rate varying by a factor of approximately 2 per 2°C change in the temperature.

Determination of Nucleation Rate

The nucleation rates were determined by counting the number of spherulites formed in the samples kept between cover slips at each particular temperature. The number of spherulites was observed through a magnifying glass. The thickness of the sample was known from the difference between the total thickness and the thickness of the slides. The volume of the specimen was calculated by,

$$V = \frac{\pi . d^2 . h}{4}$$

where 'd' is the diameter of the slips (16 mm.)

As with growth rates, the nucleation rate also varied with temperature at approximately the same rate, the number of nucleii becoming less and less at the higher temperatures. It was seen, however, that the nucleation started at the sides rather than in the centre of the samples. These experiments had also a range of variability and it is the average of three to five experiments on the same sample at the same temperature which is presented later in the results section.

Photographic Experiments

Some of the microscopic observations have been recorded photographically using a Beck-microscope camera which could be fitted on to the polarising microscope in place of the eye-piece. The camera was provided with an automatic exposure-time control system. FP3 film was used throughout the work with 3-4 seconds time of exposure.

The photographs presented in this thesis were taken to obtain structural details of the spherulites and to verify the effect of abutment of two spherulites. The nucleation of two spherulites was effected by allowing a suitable time-interval (10-55 seconds) during the transfer of the slides from the hot plate at 100°C to the thermostatted block.

CHAPTER V

RESULTS

RESULTS

The results of the present studies are presented in three sections, namely,

(1) Dilatometric

(2) Microscopic and

(3) Photographic

The inter-relationship of the three types of measurement will be established in the Discussion Section.

DILATOMETRIC RESULTS

Measurement of Equilibrium Melting Points (T_m°)

Slow heating rates (1°C rise in 12 hr.) were employed for the determination of the equilibrium melting temperatures. The results shown in figure (3) are similar to those observed by previous workers in that the melting range is about 5°C in the case of the bulk polymer and about 10°C for the polymer-diluent mixtures. It is seen that a plot of T_m° against v_1 is linear (fig 3A) and, thus equation (5.2) can be used to obtain values of ΔH_u and B (Fig. 3B). Values of T_m°, ΔH_u and B are given in the Table (2). The value of ΔH_u compares reasonably well with the values obtained by Mandelkern[79] for the same polymer, but of different mol. wt.

FIG - 3 VOLUME-TEMPERATURE CURVES

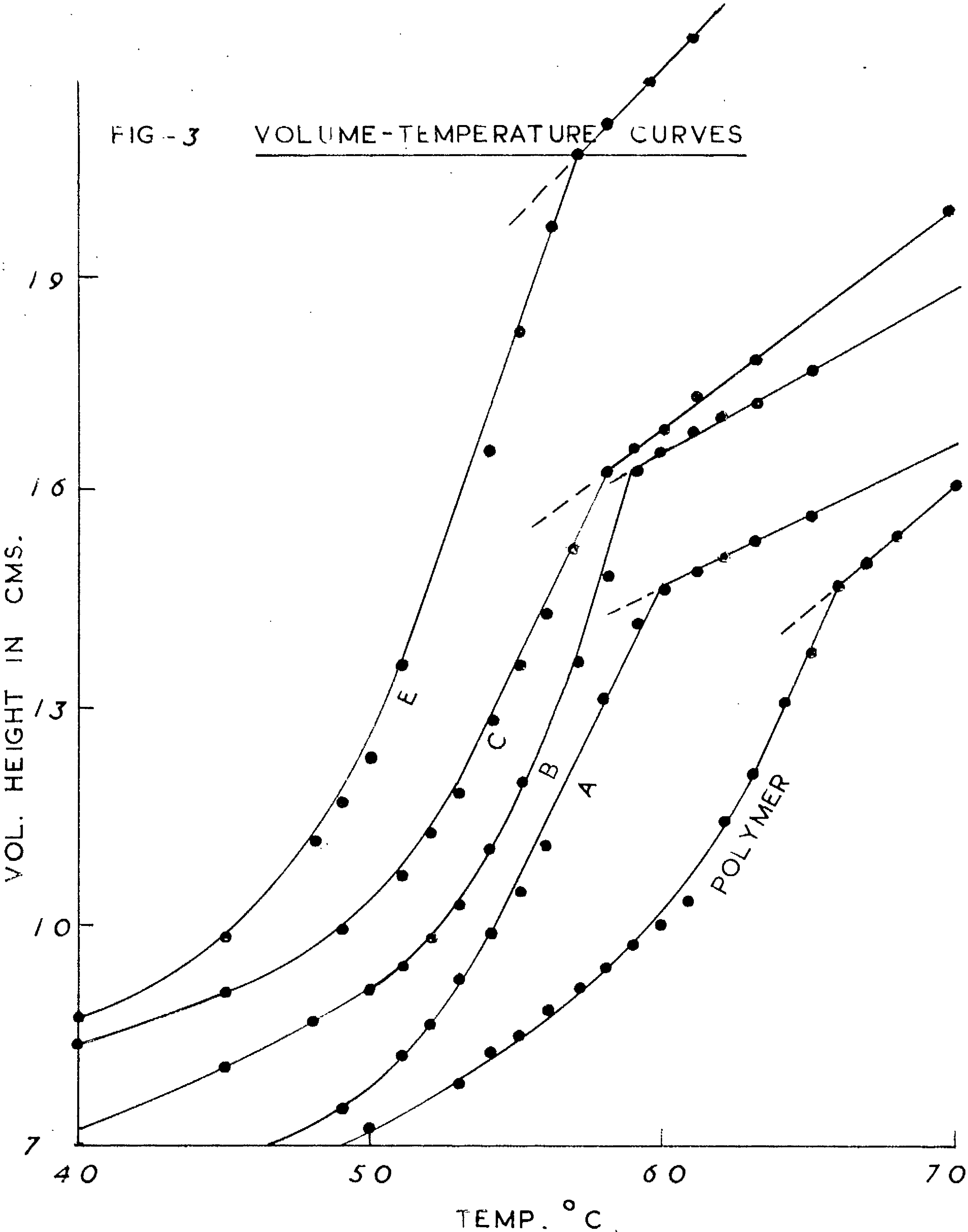

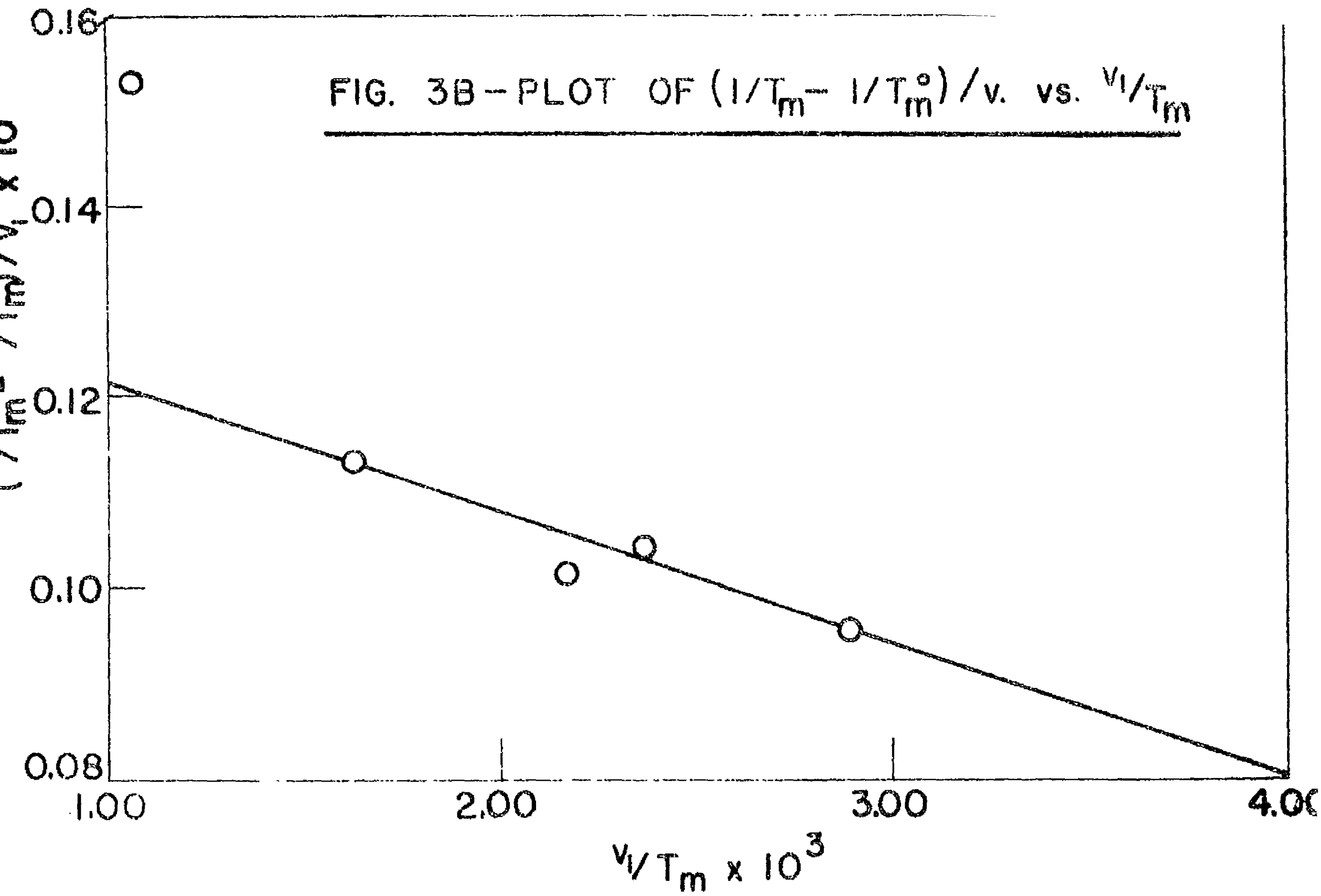
FIG. 3B - PLOT OF $(1/T_m - 1/T_m^{\circ})/v_1$ vs. v_1/T_m
$(1/T_m - 1/T_m^{\circ})/v_1 \times 10^3$
0.16
0.14
0.12
0.10
0.08
1.00
2.00
3.00
4.00
$v_1/T_m \times 10^3$

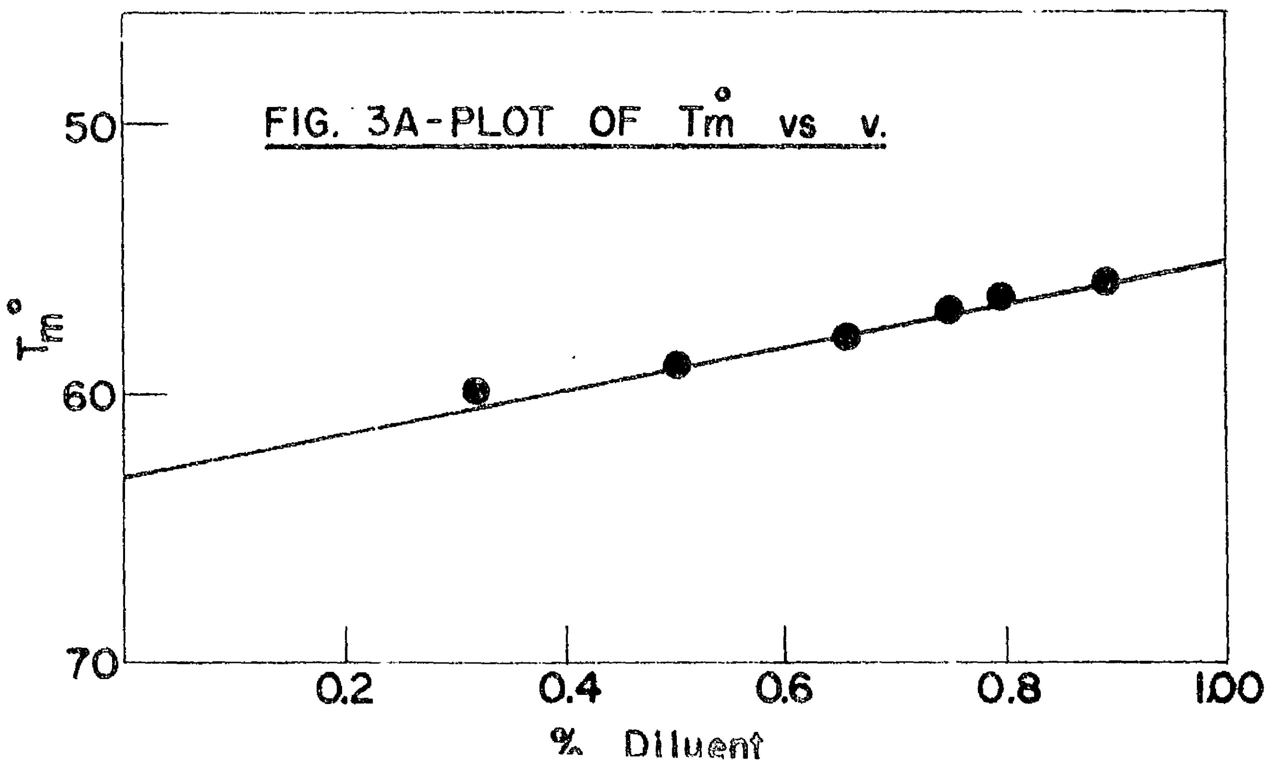
FIG. 3A - PLOT OF T_m° vs v_1
T_m°
50
60
70
0.2
0.4
0.6
0.8
1.00
% Diluent

TABLE 2 Characteristics of Polymer/Polymer-diluent Systems

Symbol	System	Polyox g.	Diluent g.	Weight fraction	T_m °C	Max volume Change in cm^3 per cm^3 polymer	Remarks.
-	Pure Polymer	1.0308	-	1.00	66.0	0.0407	
-	Pure Repeat	1.0308	-	1.00		0.0418	
A	2:1	0.8041	0.4470	0.6603	60.0	0.0622	(i) ΔH_u = 2050 cal/ mole of repeating unit.
B	1:1	0.6869	0.7605	0.4601	59.0	0.0630	
C	1:2	0.7937	1.6465	0.3253	58.0	0.0648	
D	1:3	0.7332	2.2079	0.2494	57.0	0.0670	(ii) B = 1.8 cal/cm^3
E	1:4	0.8214	3.3010	0.1988	56.5	0.0660	
F	1:8	0.5770	4.6100	0.1128	56.0	0.0680	

Overall Crystallisation Rate of the Bulk Polymer

The rates of crystallisation at various temperatures below the equilibrium melting temperature, T_m^o, can be calculated from the change in volume with time during the process. In practice, and for convenience, the relative values of volume change in the crystallising polymer with time could be calculated directly from the dilatometric heights, i.e.

$$\frac{v_t - v_\infty}{v_0 - v_\infty} = \frac{h_t - h_\infty}{h_0 - h_\infty}$$

A typical set of data has been given in table (3) with the corresponding plots in figure (4). The heights have been adjusted to the same initial level for better presentation. It can be concluded from the observations that PEO does not show any secondary crystallisation or other abnormality. It is, however, clear that the crystallinity developed in the polymer below 50°C is about 5 percent higher than the crystallinity developed above that temperature. The apparent induction period which occurs before a detectable amount of crystallinity sets in, can also be seen from the figure (4). This induction period has been shown to vary as $\left(1/\Delta T\right)$.[9] The plots show that the rate of crystallisation, at the beginning, is very slow, but gradually it increases to a maximum and then slows down as the crystallisation ceases.

TABLE 9.

Typical Dilatometric Data for Bulk Polymer crystallised at different temperatures (T_c)

Wt. of sample 1.0308 gm. T_m^0 = 66° = 339°K

Initial dilatometric height = h_0 = 6.47 cm.

T_c = 49°		51°C		53°C	
Time	ht	Time	ht	Time	ht
0 – 8	6.47	0 – 19	6.47	0 – 63	6.47
10	6.39	23	6.42	76	6.42
12	6.27	30	6.33	91	6.35
15	6.02	37	6.20	110	6.28
16	5.91	40	6.10	132	6.20
19	5.49	44	5.98	158	6.05
21	5.22	48	5.82	174	5.94
23	4.91	53	5.61	191	5.79
25	4.65	58	5.39	210	5.62
27	4.38	63	5.18	232	5.39
30	3.96	69	4.86	250	5.20
33	3.59	76	4.53	274	4.95
36	3.27	84	4.18	300	4.63
40	2.94	91	3.90	330	4.27
45	2.64	101	3.45	360	3.97
49	2.45	110	3.18	400	3.59
54	2.34	122	2.92	440	3.26
58	2.27	132	2.75	480	2.92
63	2.20	145	2.54	530	2.72
76 – ∞	2.11	159	2.40	630	2.50
		176 – ∞	2.29	910 – ∞	2.29
$h_t - h_0$ =	4.36		4.18		4.18
$t_{1/2}$	28		80		320

FIG. 4 DILATOMETRIC RESULTS FOR PURE POLYMER

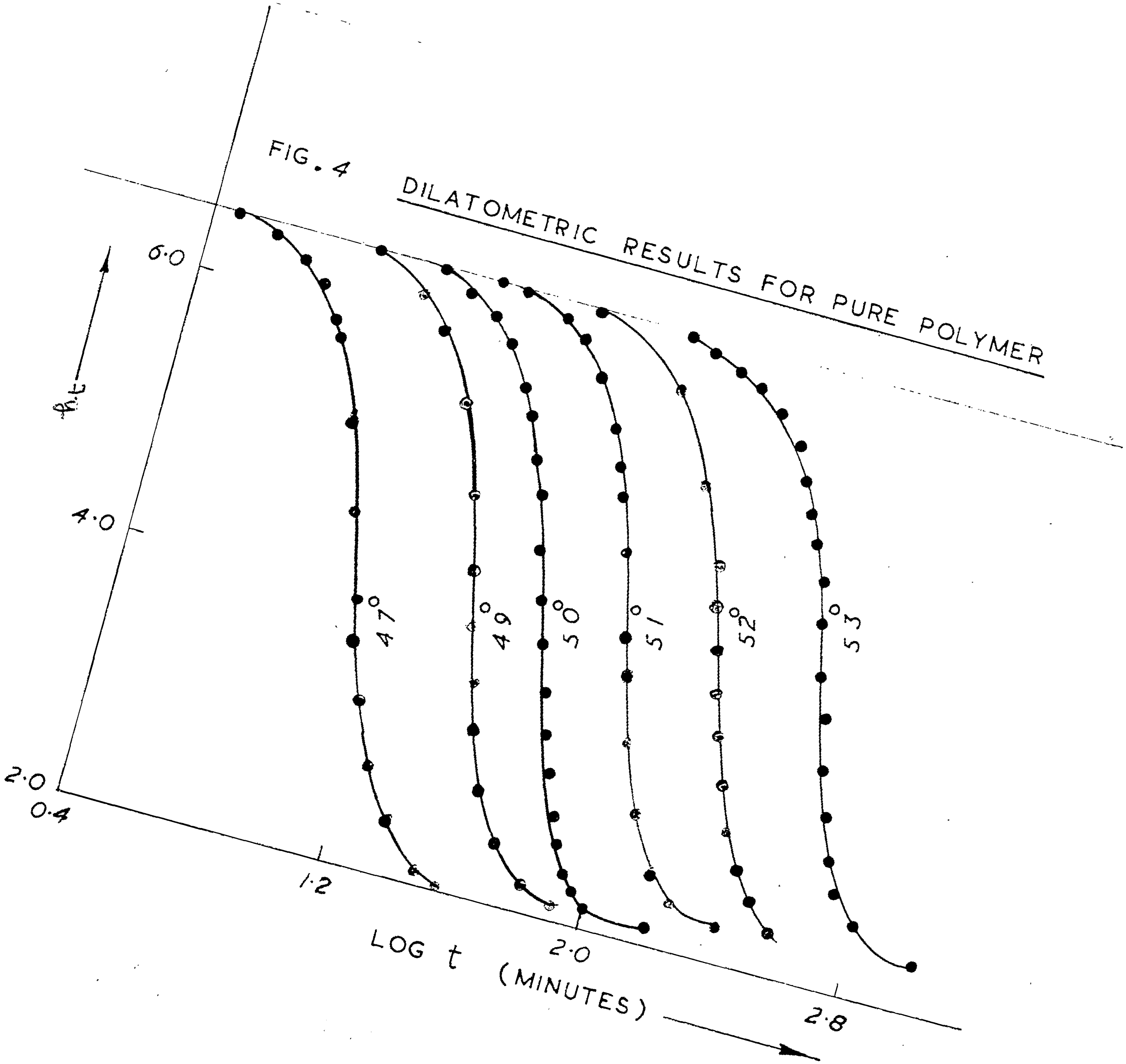

TABLE 4 - Summary of runs on Bulk Polymer

Crystallisation Temp T_c	ΔT	Sample 1 $h_0 - h_\infty$	r_i	n	Sample 11 $h_0 - h_\infty$	r_i	n	Repeat Sample 1 $h_0 - h_\infty$	r_i	n
49	17	4.36	8	2.39	4.36	5	2.37	5.22	-	2.36
50	16	4.36	10	2.39	-	-	-	5.11	6	2.39
51	15	4.18	19	2.62	4.21	16	2.65	4.91	9	2.50
52	14	4.18	36	2.44	-	-	-	4.91	19	2.48
53	13	4.18	63	2.54	4.19	53	2.55	-	-	-

FIG.5 DILATOMETRIC RESULTS FOR PURE POLYMER REPEAT

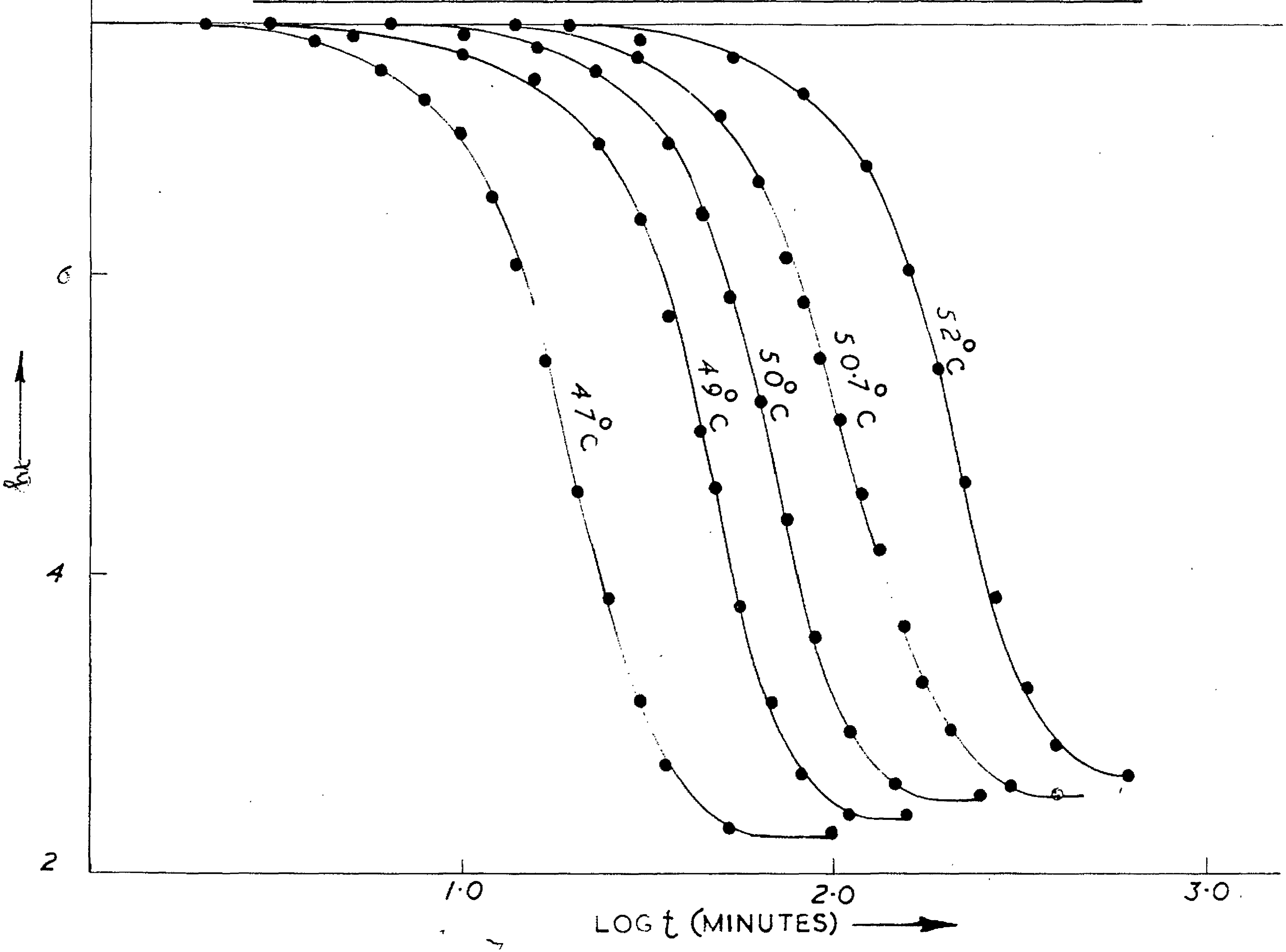

The experiments were repeated on the same sample (fig. 5) and on a fresh sample and table 4 summarises the results, showing the reproducibility and change in crystallisation behaviour of the samples. The weight of the fresh sample was almost identical to that of the first sample.

The sample with the same thermal history behaves in the same way at the same temperature with about 3-5 per cent variation, but the kinetics of the repeat samples seem to be different. Higher crystallinity is developed and the $\tau_{\frac{1}{2}}$ values are also reduced. 'n' is reasonably constant for all samples and repeat.

The limit of temperature range for the dilatometric studies has been from 47°C to 53°C, requiring from 40 to 910 minutes for completion of the runs. Below 47°C, the crystallisation would be too fast to study accurately and above 53°C, too slow.

<u>Overall Crystallisation of Polymer-diluent Systems</u>

The isothermal rates of crystallisation of the polyox-diethyl sebacate system in the concentration range of 30-89 weight per cent diluent were studied. A selection of representative results is shown in figures (6-11) depicting the dilatometric results for the mixtures, and each run is summarised in tables 5 to 10.

TABLE 5 - Summary of Dilatometric Results: Mixture A

T_c	ΔT	$h_0 - h_\infty$	r_1	$t_{1/2}$	
43.1	16.9	5.19	3	19.5	Constant Vol. Change up to $\Delta T = 14$
44.1	15.9	5.16	6	29.5	
44.8	15.2	5.15	8	39.0	
46.2	13.8	5.15	11	83.0	
47.1	12.9	5.03	16	150.0	
48.1	11.9	4.76	30	250.0	
49.1	10.9	4.61	53	530.0	

TABLE 6 - Summary of Dilatometric Results: Mixture B

T_c	ΔT	$h_0 - h_\infty$	r_1	$t_{1/2}$	
42.0	17	4.56	7	21	Constant vol. Change up to $\Delta T = 13$
43.0	16	4.56	10	35	
44.0	15	4.56	13	52	
45.0	14	4.56	21	99	
46.0	13	4.56	30	156	
47.0	12	4.35	40	274	
48.0	11	4.15	53	440	

FIG. 6 DILATOMETRIC RESULTS FOR MIXTURE A

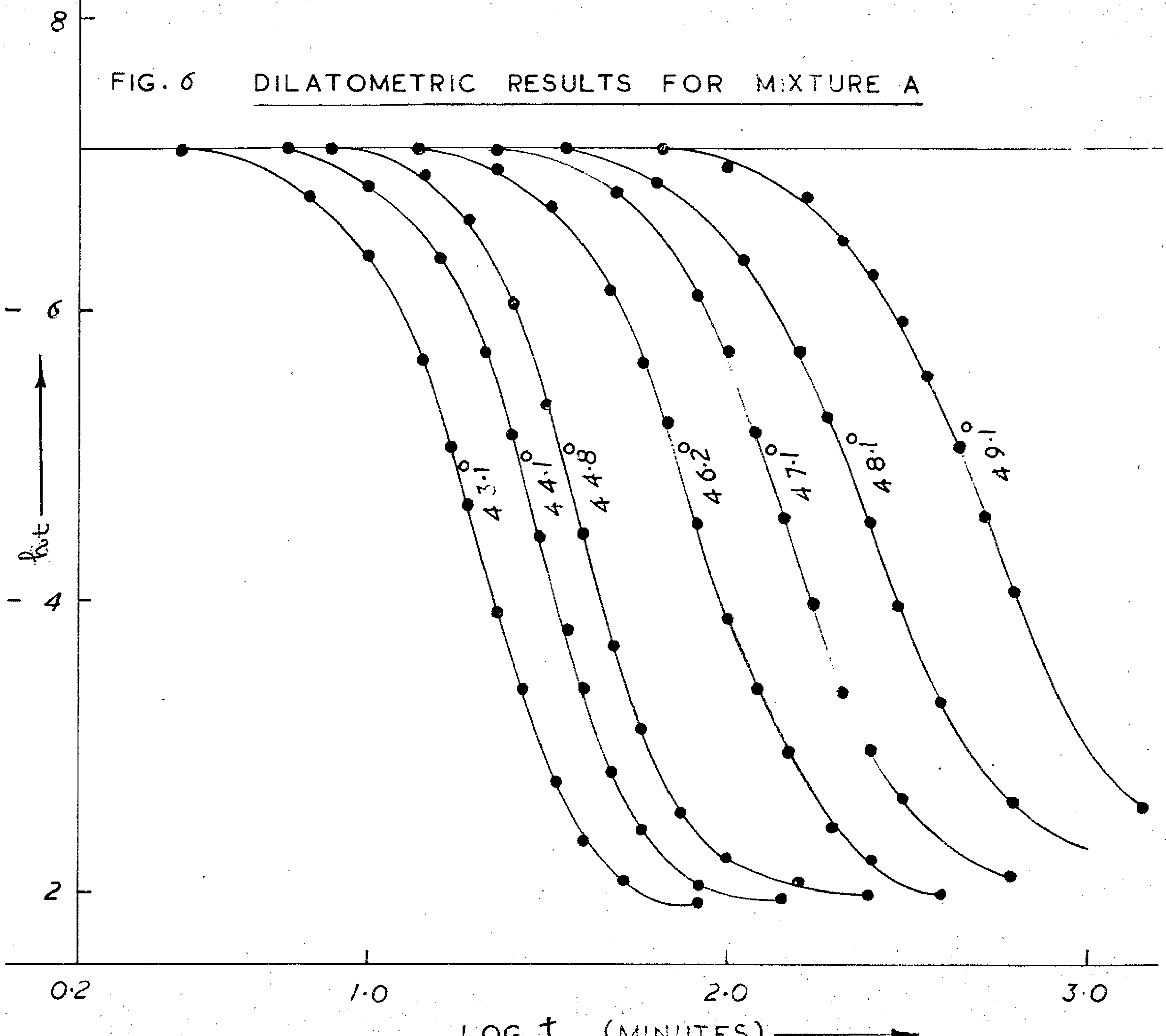

FIG.7 DILATOMETRIC RESULTS FOR MIXTURE B

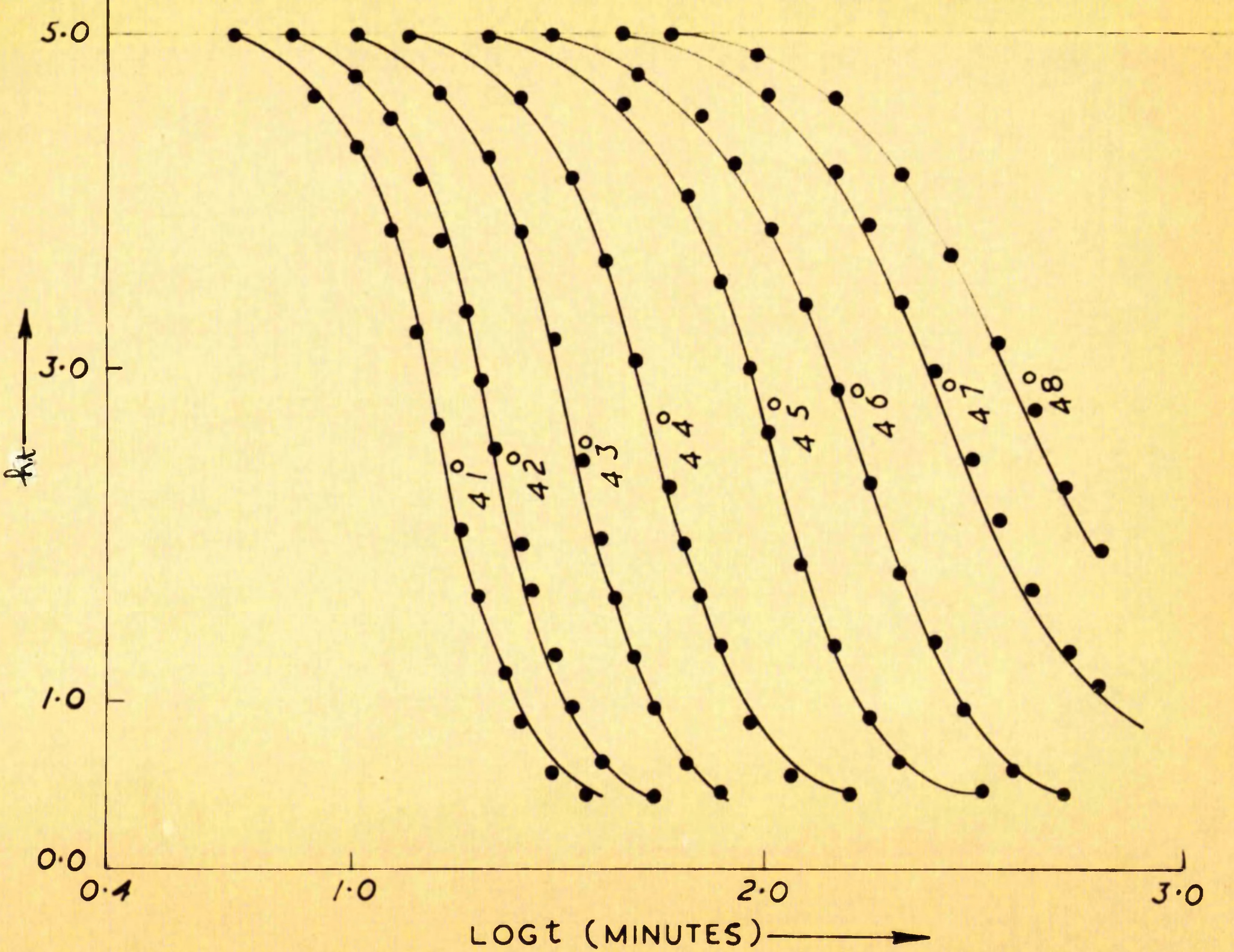

TABLE 7 - Summary of Dilatometric Results - Mixture C

T_c	ΔT	$h_0 - h_\infty$	r_i	$t_{1/2}$	
41.0	17	5.12	4	12.5	Constant Vol. change up to ΔT = 12
42.0	16	5.16	5	17.0	
43.0	15	5.15	6	28.0	
44.0	14	5.14	8	40.0	
45.0	13	5.19	12	67.0	
46.0	12	5.19	19	114.0	
47.0	11	5.12	30	214.0	
48.0	10	4.90	48	404.0	

TABLE 8 - Summary of Dilatometric Results - Mixture [illegible]

T_c	ΔT	$h_0 - h_\infty$	r_i	$t_{1/2}$	
40.0	17	5.22	6	25	Constant Vol. Change up to ΔT = 14
41.0	116	5.19	7	37	
42.0	15	5.12	10	59	
43.0	14	5.11	16	102	
44.0	13	5.05	30	195	
45.0	12	5.04	53	400	

FIG. 8 DILATOMETRIC RESULTS FOR MIXTURE C

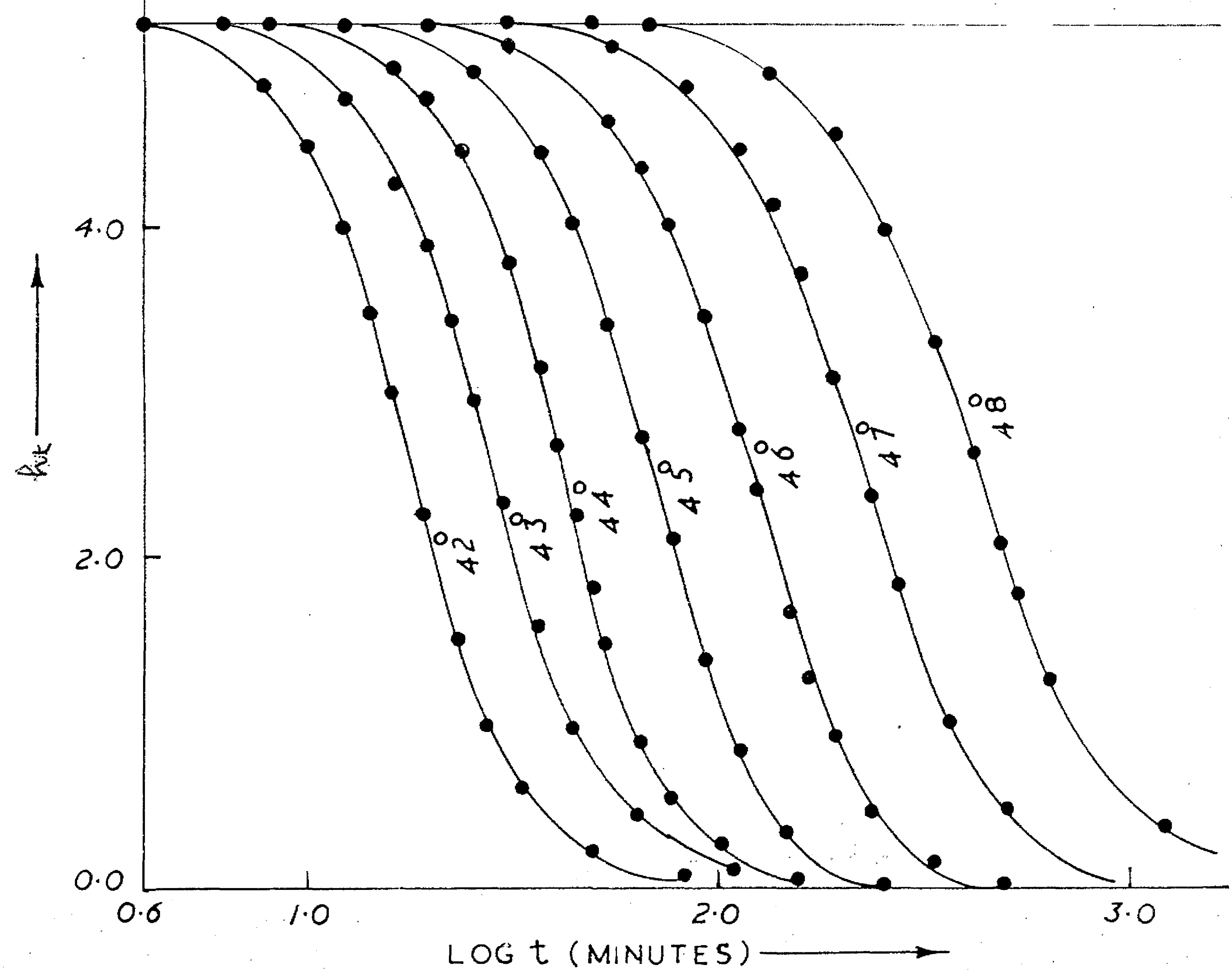

FIG. 9 DILATOMETRIC RESULTS FOR MIXTURE D

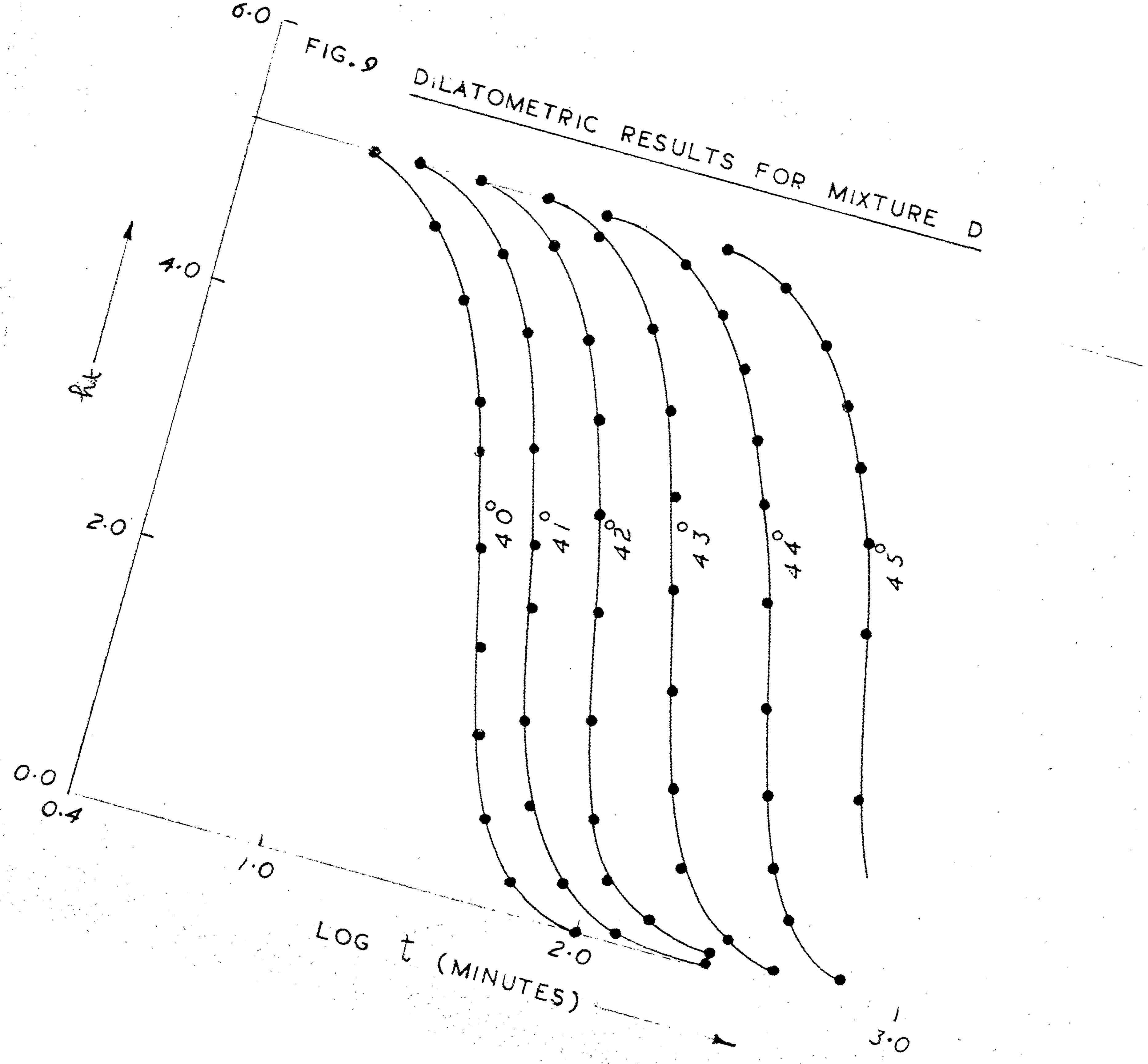

TABLE 9 - Summary of Dilatometric Results: Mixture E.

$T_{c.}$	ΔT	$h_0 - h_\infty$	r_1	$t_{1/2}$	
40	16.5	5.73	7	20	Constant Vol. Change up to ΔT = 1[illegible].5
41	15.5	5.72	10	33	
42	14.5	5.73	10	46	
43	13.5	5.64	16	83	
44	12.5	5.65	25	158	
45	11.5	5.51	63	370	

TABLE 10 - Summary of Dilatometreic Results - Mixture F.

$T_{c.}$	ΔT	$h_0 - h_\infty$	r_1	$t_{1/2}$	
39	17	4.04	8	22	Constant Vol. Change up to ΔT = 13
40	16	4.10	8	31	
41	15	4.03	10	46	
42	14	4.03	21	83	
43	13	4.03	25	136	
44	12	3.97	33	280	

FIG. 10 DILATOMETRIC RESULTS FOR MIXTURE E

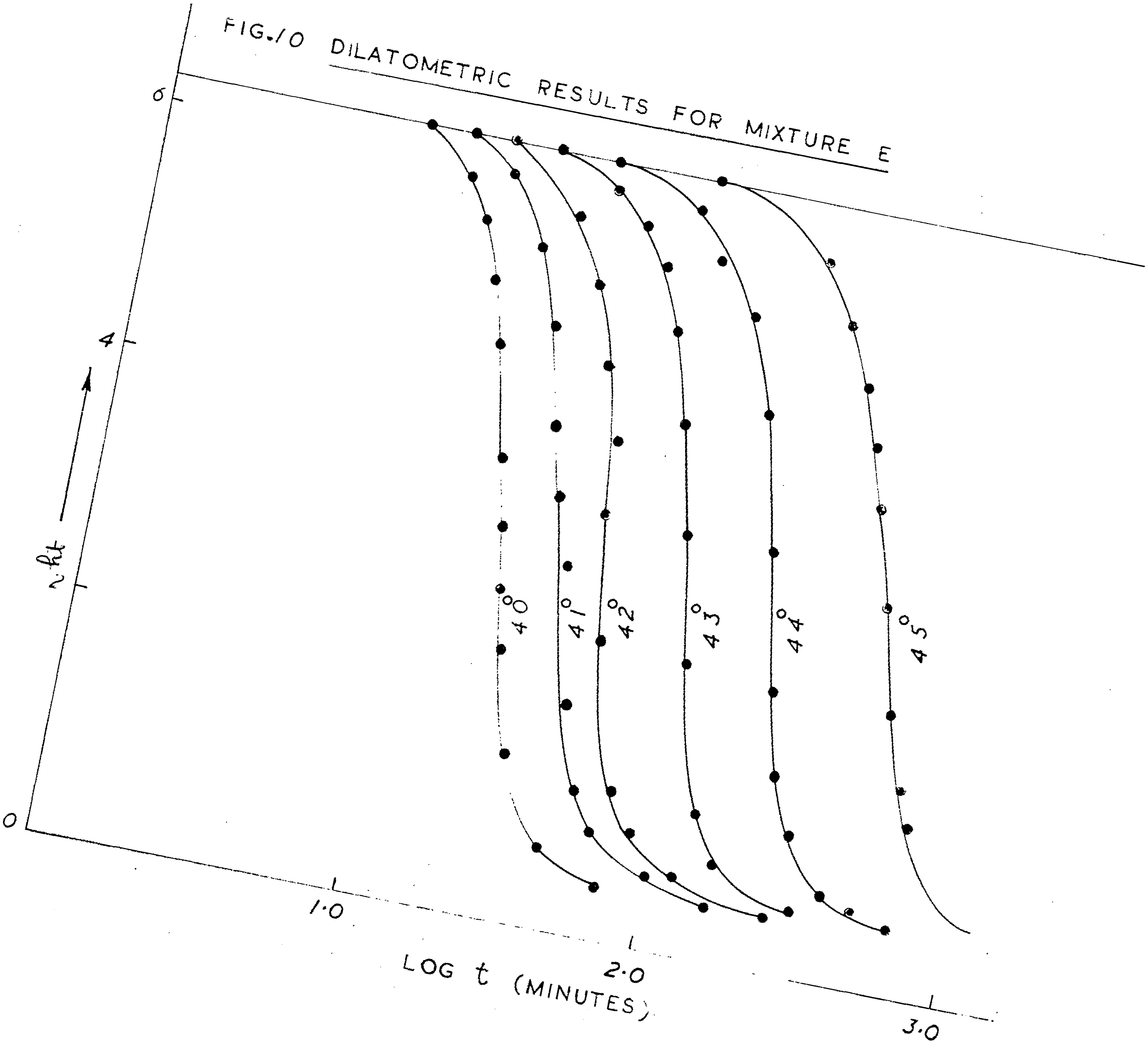

FIG. 11 DILATOMETRIC RESULTS FOR MIXTURE F

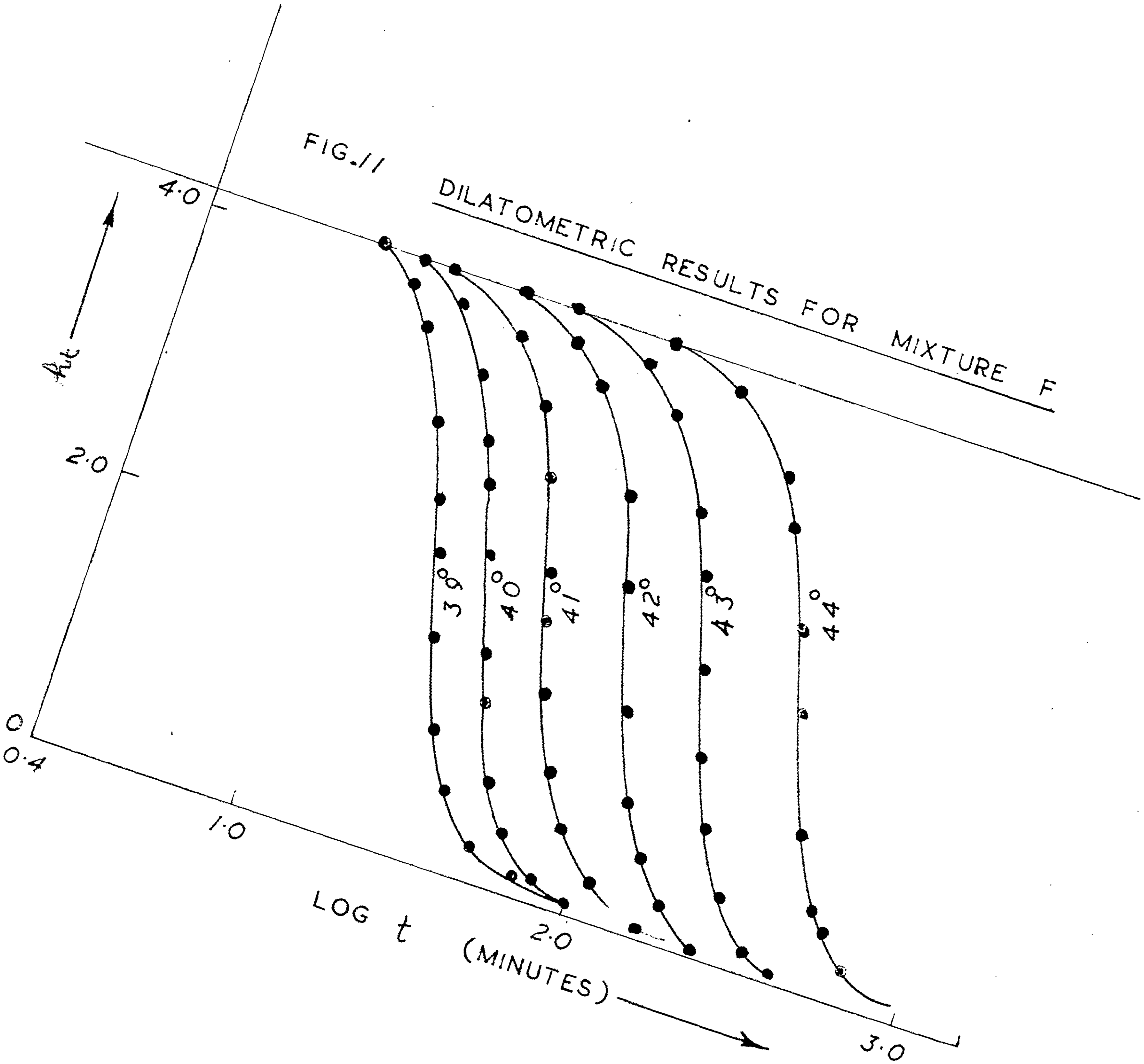

The range of temperature studied is, clearly, limited to ΔT = 10-17 i.e 8°C. It follows from the above tables (5-10) that the polymer-diluent systems have smaller r_i and $t_{1/2}$ at the same ΔT values compared with the bulk polymer. This can also be seen from tables (11-12). The r_i and $t_{\frac{1}{2}}$ for mixture (C) do not appear to be consistent with the other concentrations. The values of T_m^o are, however, uncertain to ± 1°C and an increase of T_m^o for this mixture by 1°C, thus increasing each value of ΔT by this amount would bring all the values for all the different concentrations into close agreement.

The results also show that the maximum crystallinity observed in these cases remains constant up to a value of ΔT of between 12-14 below which it begins to decrease gradually.

TABLE 11 – Induction Period (r_i) of Various Systems

ΔT	Bulk Polymer	A	B	C	D	E	F
11	–	53	53	30	–	–	–
12	–	30	40	19	53	63	33
13	63	16	30	12	30	25	25
14	36	11	21	8	16	16	21
15	19	8	13	6	10	10	10
16	10	6	10	5	7	10	8
17	8	3	7	4	6	7	8

TABLE 12 – Rate Constant ($t_{1/2}$) of Various Systems

ΔT	Bulk Polymer	A	B	C	D	E	F
11	–	530	440	215	–	–	–
12	–	250	274	114	400	370	280
13	320	150	156	67	195	158	136
14	158	83	99	40	202	83	83
15	80	39.5	52	28	59	46	46
16	44	29.5	35	17	37	33	31
17	28	19.5	21	12.5	25	20	22

C H A P T E R   V

(a) Microscopic Results

(b) Photographic Results

Microscopic Results

Growth Rates (G) of Pure Polymer.

The growth rates (G) of individual spherulites were measured and are given in the Fig.12A and correspond to the values in column 3 of Table 13. It was observed that at temperatures below 47°C, the number of spherulites was large and the growth fast. Hence rate measurements were carried out in the range 47-55°C, after which not only was the growth rate very low, but the induction period was also very large. It was found that at higher temperatures there was only one spherulite in the field of view.

The induction times varied from sample to sample and have not been included in Fig. 12.

The growth rate was found to vary with the thickness of the samples, as observed by earlier workers.[97] The figures (12 A, B) show the results where thickness reduces the G values by 50 per cent when it is changed from 100μ to 300μ.

The repeat runs on the samples at the same temperature, however, showed that most of the spherulites appeared in the same places each time. This behaviour was found to persist even when 3 or 4 runs were carried out and the duration of the melt was increased by 50% (i.e. 30 minutes). Nucleation appears to be heterogeneous in this case and in several cases reported earlier.[98]

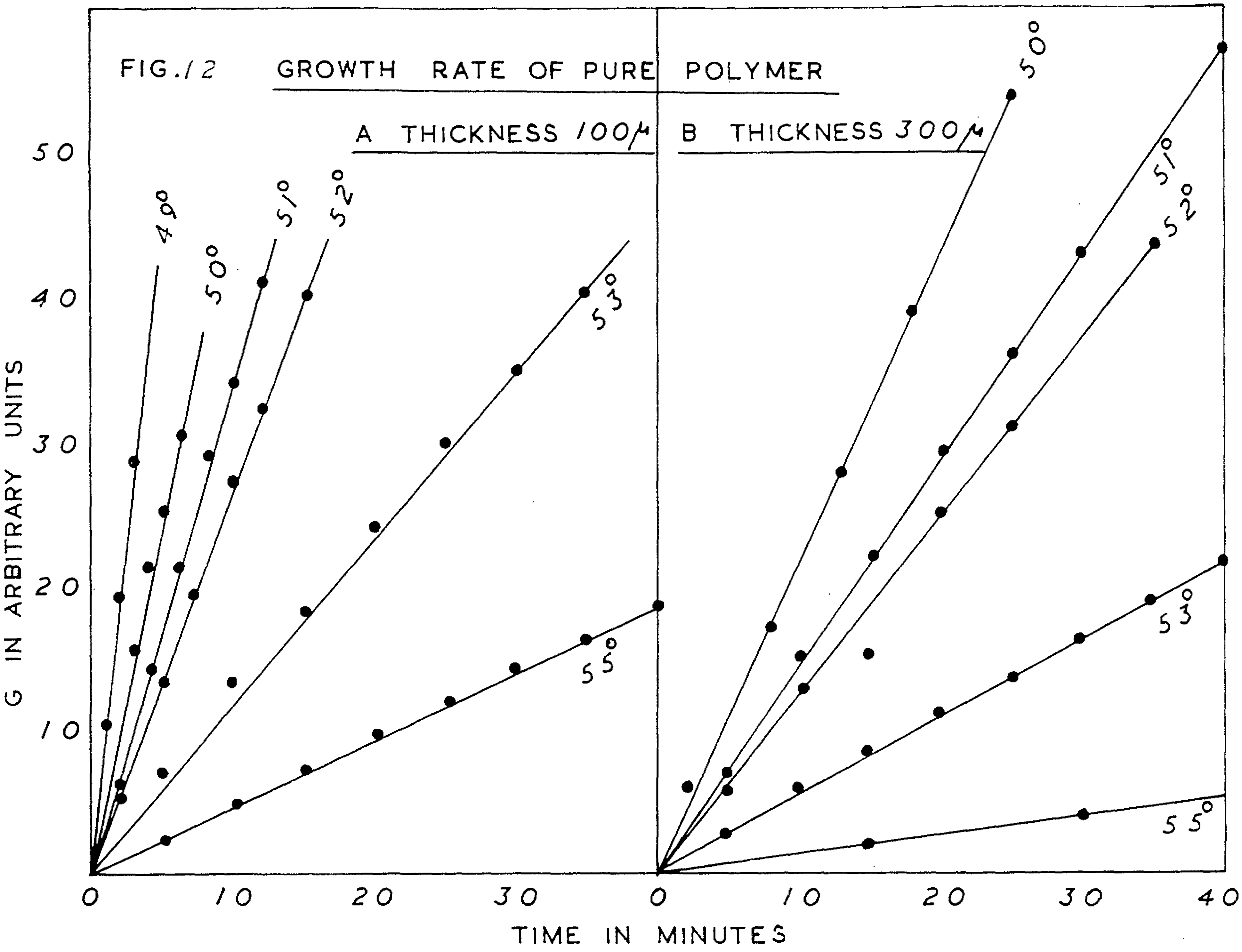

FIG. 12 GROWTH RATE OF PURE POLYMER
A THICKNESS 100μ
B THICKNESS 300μ
G IN ARBITRARY UNITS
TIME IN MINUTES
0
10
20
30
40
50
40°
50°
51°
52°
53°
55°

The nature of the spherulites in most cases was a mixed one where one could neither find a true maltese cross nor a well defined positive or negative charabter. These types of spherulites have been reported by Keith and Padden[27] in the case of polypropylene and by Price[99] in the case of carbowax 4000.Fronded structures were observed at lower supercoolings.

Growth Rates of Polymer-Diluent Systems

The growth rates of seven polymer-diluent mixtures are summarised in the table 14 and figures 13-19. They have been obtained by the method detailed in the experimental section and average of several separate runs is presented here. As with pure polymer, induction time has not been included in the figures.

The experimental uncertainty is unfortunately rather high and the only conclusion to be drawn is that for a given value of ΔT, G does not vary much as the concentration of the diluent is increased.

Number of Nuclei and Nucleation Rates-Pure Polymer

Column 5 of the table 13 shows the number of nuclei per $cm.^3$ observed in the pure polymer at various ΔT-values. The corresponding figure 20 for nucleation in the bulk polymer indicates that the number of nuclei increase linearly to a steady state value which remains constant until the crystallisation is complete. This behaviour is typical of polythene[100] and other polymers

TABLE 13 – Growth and Nucleation Rates of Pure Polyox

T°c	ΔT	G (Scale units/mt)	$G \times 10^{5}$ cm/mt	$N \times 10^{2}/cm^{3}$	$N/cm^{3}/$ mt	Log G	$\frac{1}{T\Delta T} \times 10^{4}$
47	19	15.5	37.00	5.7	44	-1.43	1.63
49	17	9.2	21.1	3.4	18	-1.67	1.84
50	16	5.00	11.5	3.4	-	-1.94	1.97
51	15	3.4	7.8	2.3	8	-2.11	2.11
52	14	2.5	5.7	2.4	-	-2.24	2.27
53	13	1.1	2.5	1.5	3	-2.60	2.48
55	11	0.45	1.0	0.4	1.6	-3.00	2.67

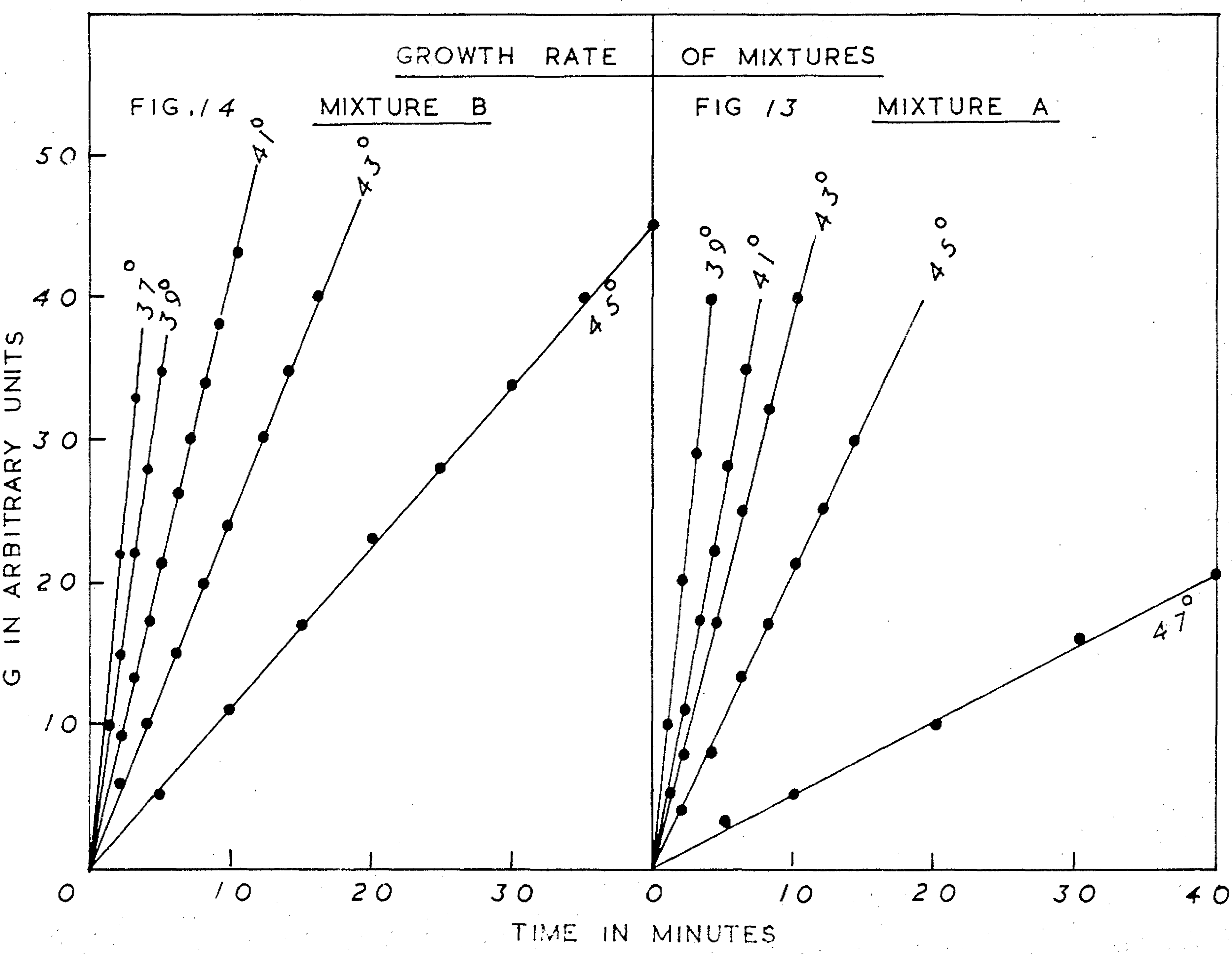

GROWTH RATE OF MIXTURES
FIG. 14 MIXTURE B
FIG 13 MIXTURE A
37°
39°
41°
43°
45°
47°
G IN ARBITRARY UNITS
TIME IN MINUTES
0
10
20
30
40
50

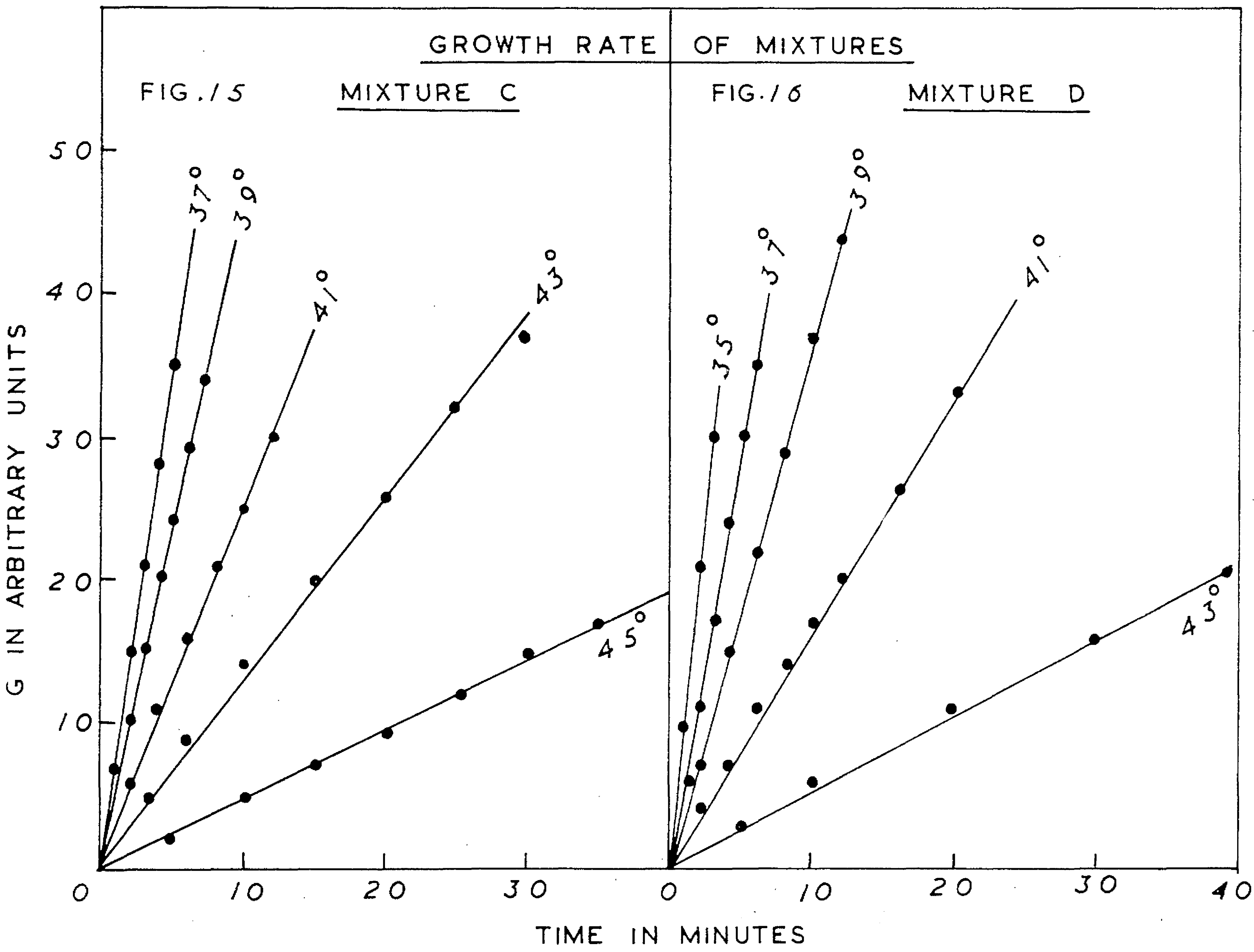
GROWTH RATE OF MIXTURES
FIG./5
MIXTURE C
FIG./6
MIXTURE D
G IN ARBITRARY UNITS
TIME IN MINUTES
0
10
20
30
40
50
37°
39°
41°
43°
45°
35°

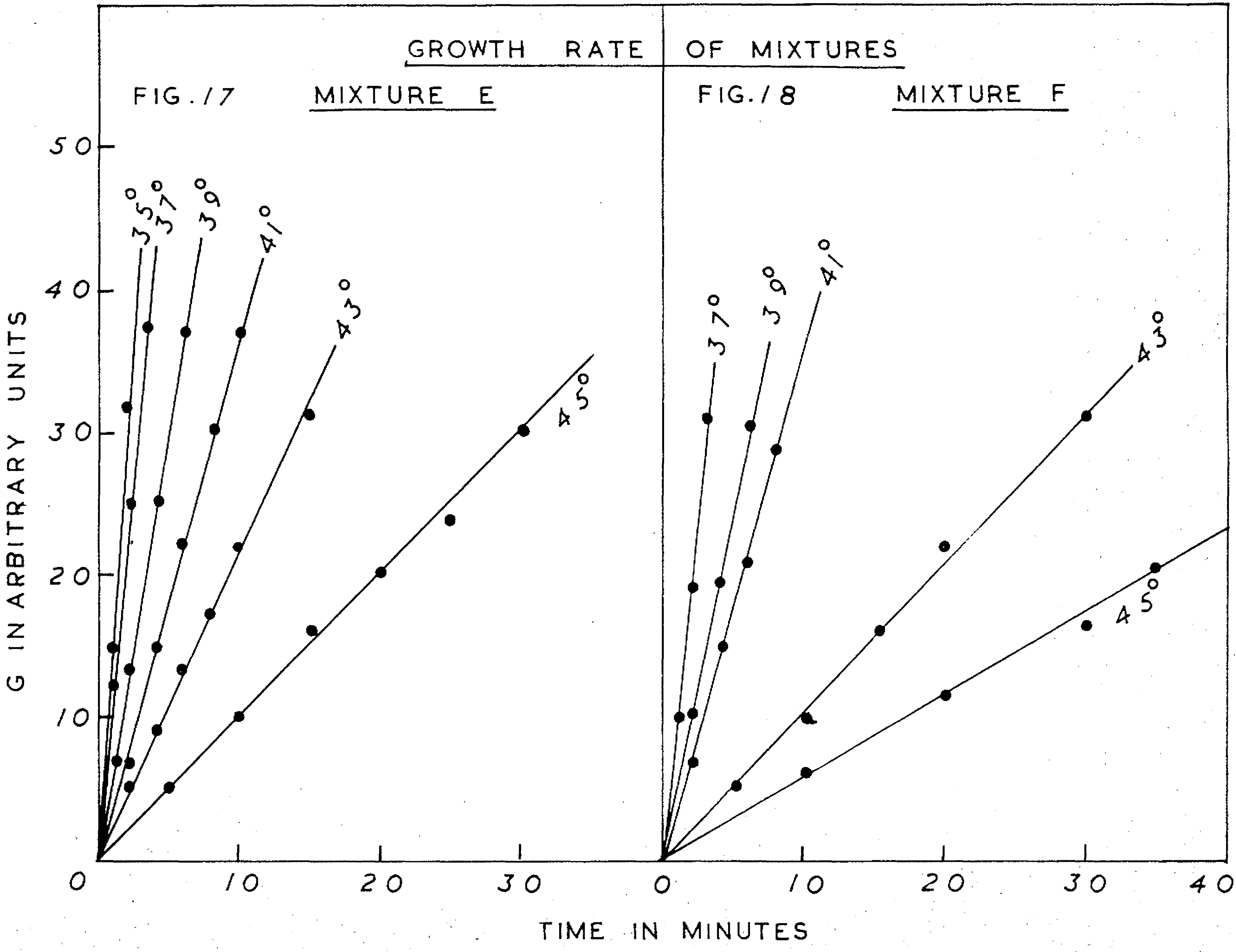

GROWTH RATE OF MIXTURES

FIG. 17 MIXTURE E

FIG. 18 MIXTURE F

FIG. 19

GROWTH RATE OF MIXTURE G

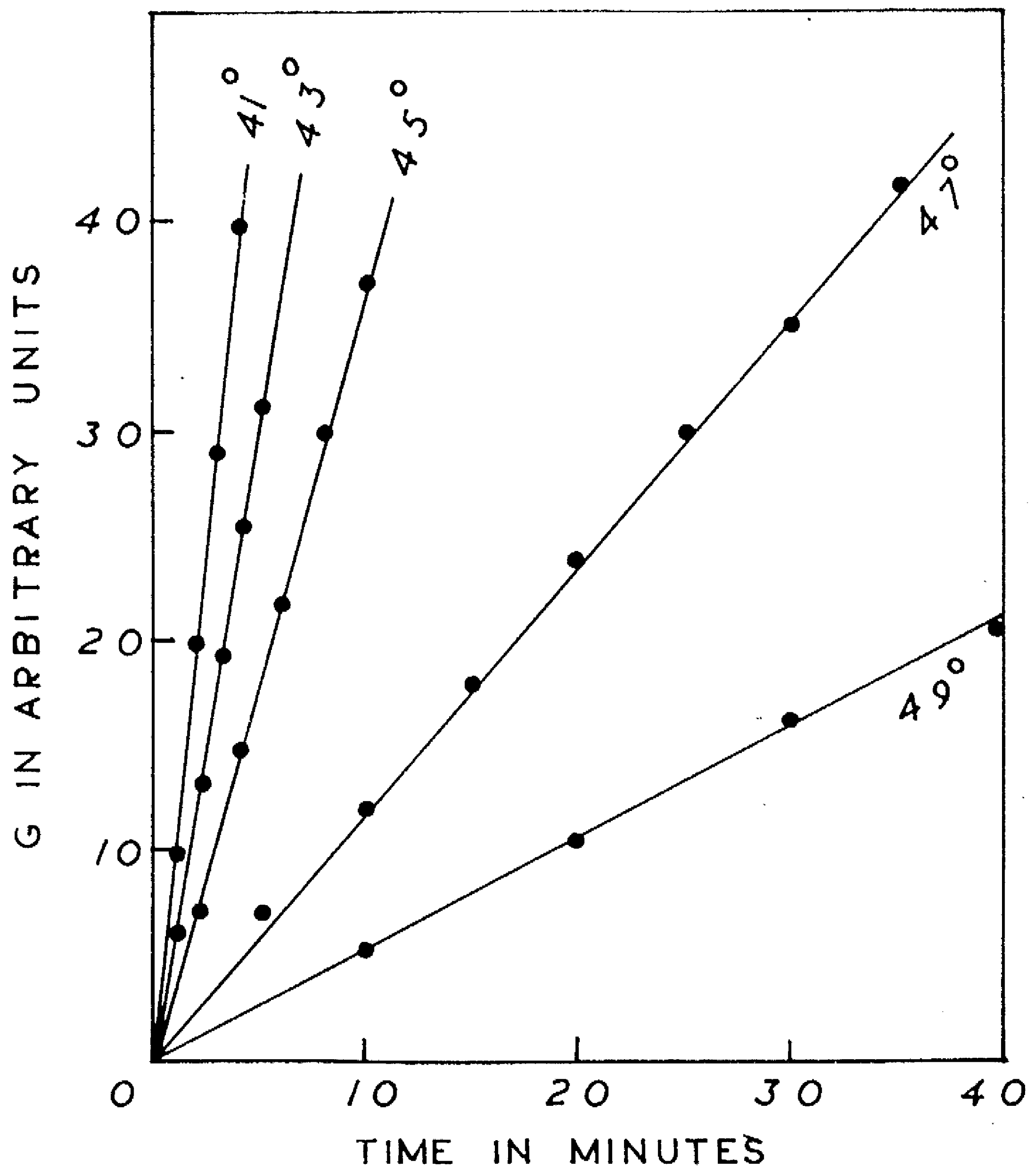

TABLE 14 - Growth Rates ($G \times 10^3$ cm/mt) of Polymer and Polymer-Diluent Systems.

ΔT	Polymer	G°	A	B	C	D	E	F
22	-	-	-	26.5	-	23.0	36.8	-
21	-	-	23.0	-	16.1	-	-	
20	-	23.0	-	17.2	-	13.8	27.8	-
19	37.0	-	13.8	-	11.5	-	-	23.0
18	-	13.0	-	9.2	-	8.0	14.0	-
17	21.1	-	9.2	-	5.7	-	-	11.6
16	11.5	8.0	-	5.7	-	3.45	6.9	-
15	7.8	-	4.6	-	2.7	-	-	8.1
14	5.7	2.8	-	2.5	-	1.2	4.6	-
13	2.5	-	1.2	-	1.2	-	-	2.3
12	-	1.2	-	-	-	-	2.3	-
11	1.0	-	-	-	-	-	-	1.2

° Composition of this system corresponds to 0.80 wt. fraction of Polymer

FIG 20

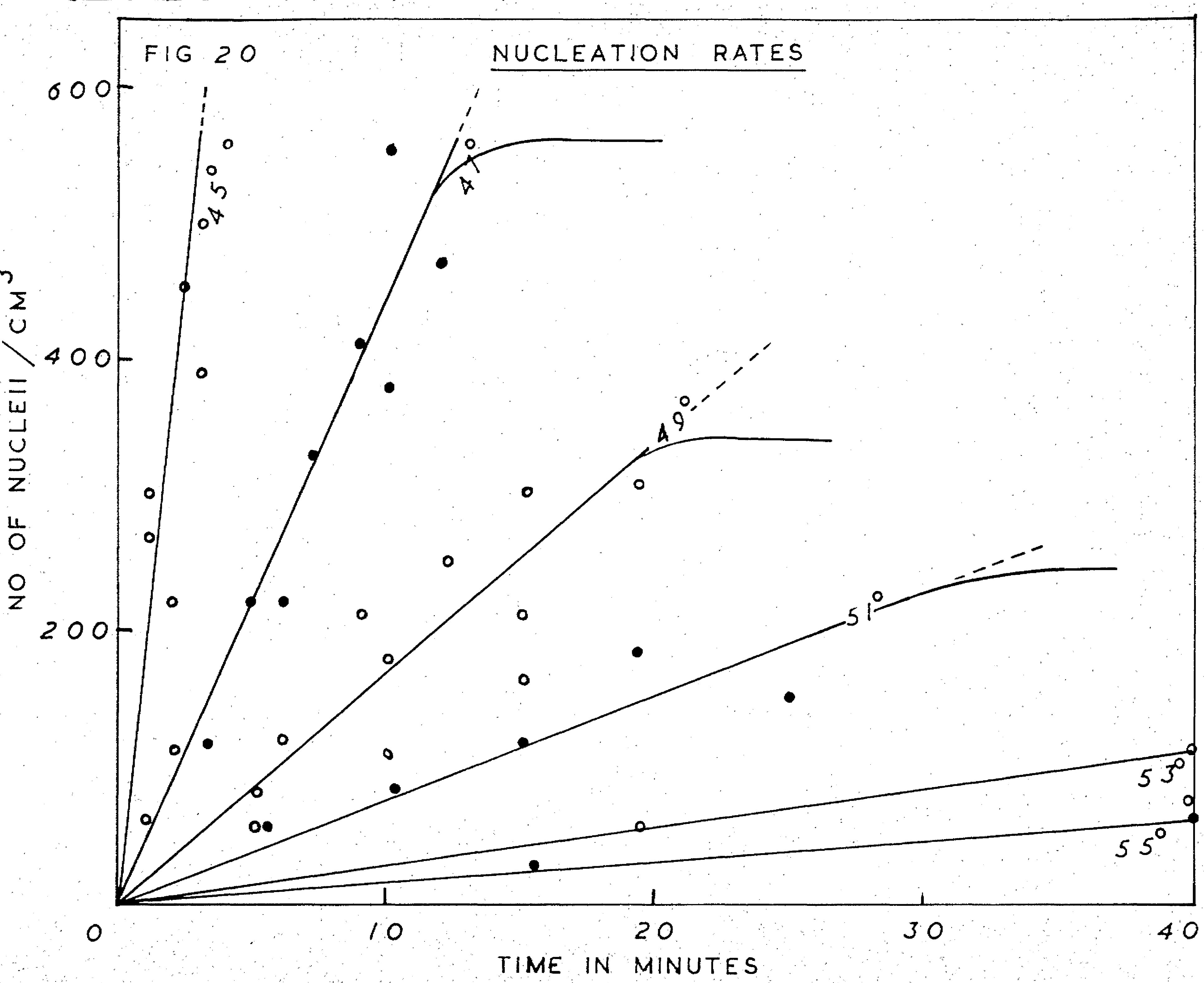
NUCLEATION RATES
NO OF NUCLEII / CM³
600
400
200
0
10
20
30
40
TIME IN MINUTES
45°
47
49°
51
53°
55°

showing initially random growth followed by pre-determined growth of the spherulites. The random nucleation suggests homogeneity of the sample.

Repeat runs, however, carried out on one sample at one temperature gave rise to memory effects similar to those noticed when attempting to measure growth rates. These memory effects are reduced at higher temperatures as is evidenced by the decreasing number of nuclei in the same sample at higher temperatures. The reverse process, i.e. examining a sample first at higher temperature and then at lower temperature, also gave the expected results of approximately doubling the number of nuclei per 2°C decrease in the temperature. It is clear from table 13 that nucleation is much less sensitive to temperature than is the growth rate.

Effect of Thickness on Nucleation.

McIntyre[9] pointed out the uncertainty in measuring the thickness of the sample and its effects on Nucleation process. It was confirmed that the thickness of the sample had a marked effect on nucleation as shown in the table 15, where N is the number of nuclei per cm.^{3}, and supported by the corresponding figure 21 for the constant temperature of 51°C. The t_v is the time, the first nucleus appeared. t_v seems inversely proportional to the sample thickness. Table 15 makes it clear

FIG 21 EFFECT OF THICKNESS ON NUCLEATION AT 51°C

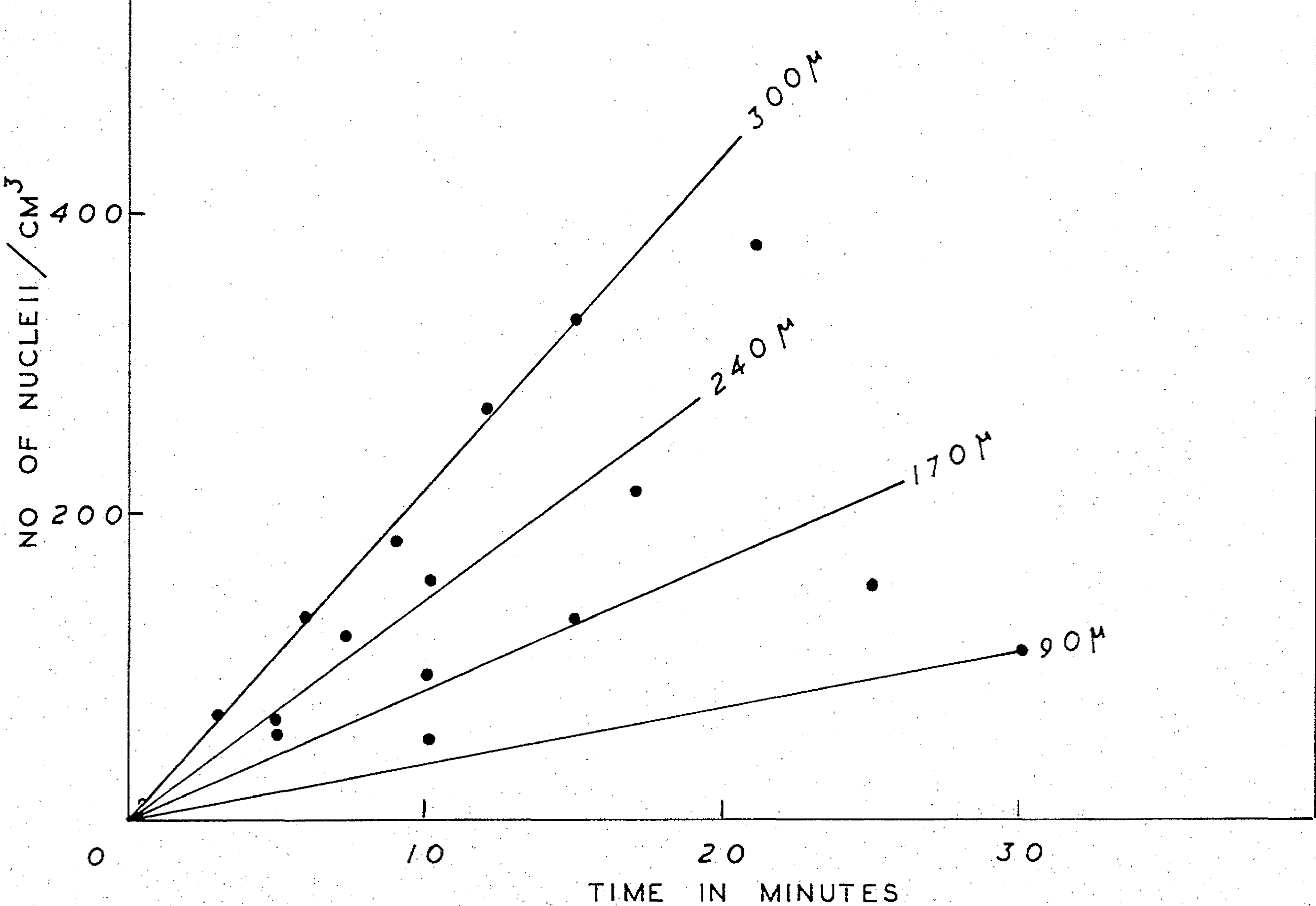

that the nucleation continues even after the dilatometric induction period r_i. t_n is the time at which new nuclei ceased to be formed.

The nucleation rates at various temperatures are given in columns 6 of the table 13. They have been calculated from initial slopes of the number of nuclei versus time plots of Fig. 20.

Table 15 - Effect of thickness on Nucleation at 51°C

Thickness (μ)	$NX10^3/cm^3$	t_v (min)	t_n (min)	Dilatometric r_i	Dilatometric $t_{1/2}$
80	1.10	20	30		
170	1.50	5	25	19	80
240	2.20	3	17		
300	3.80	2	21		

Nucleation in Polymer-Diluent Systems

The nucleation process in each of the six systems was studied. The results are presented in the Table 16. Although every attempt was made to study samples of equal thickness, but from the large scatter of results, it appears that this was not achieved. The interesting feature of the results is that the number of nuclei per unit volume for the mixtures does not appear to increase with decrease in temperature in a similar fashion to the pure polymer.

TABLE 16 - Number of Nuclei per cm^3 ($N \times 10^3$) in Polymer-diluent systems.

ΔT	Polymer	A	B	C	D	E	F
22	–	–	11 2	–	–		–
21	13.2	7.2	–	4.4	–	13.2	–
20	–	–	10.8	–	10.08	–	19.2
19	5.7	6.4	–	2.0	–	13.0	–
18	–	–	9.2	–	5.6	–	22.8
17	3.4	3.4	–	4.4	–	16.0	–
16	3.4	–	7.2	–	4.2	–	23.2
15	2.3	2.26	–	5.0	–	16.4	–
14	2.4	–	10.8	–	4.8	–	16.8
13	1.5	1.5	–	4.0	–	13.2	–
12	–	–	–	–	5.0	–	20.0
11	0.4	0.75	–	–	–	14.8	–
10	–	–	–	–	–	–	16.4

PHOTOGRAPHIC RESULTS

Pure Polymer

The photographic observations on the bulk polymer at different temperatures show that in most cases it can form four different types of spherulite. This behaviour has also been reported for polypropylene and nylon.

1. Negative spherulites at $\Delta T < 15$ in thin samples
2. Mixed spherulites in thick samples
3. Dendritic spherulites - mostly from solutions and at higher temperatures.
4. Ovalshaped dendritic spherulites at higher temperatures in thin samples.

Examples of the first two types are shown in the picture in Figure 22 while the latter two types are shown in Figure 25 and 26 respectively. Very occasionally at large degrees of supercooling (i.e. $\Delta T > 15$) in thin samples, positive spherulites were observed. These grew very quickly and were of extremely small size.

The dendritic spherulites have been reported in low molecular weight (i.e. 5500) PEO samples[99] while ovalshaped dendritic spherulites have been observed in polypropylene[101]. Spherulites growing in the pure polymer at lower temperatures have sharp boundaries between them, though this depends to a certain extent upon the thickness of the sample. At higher

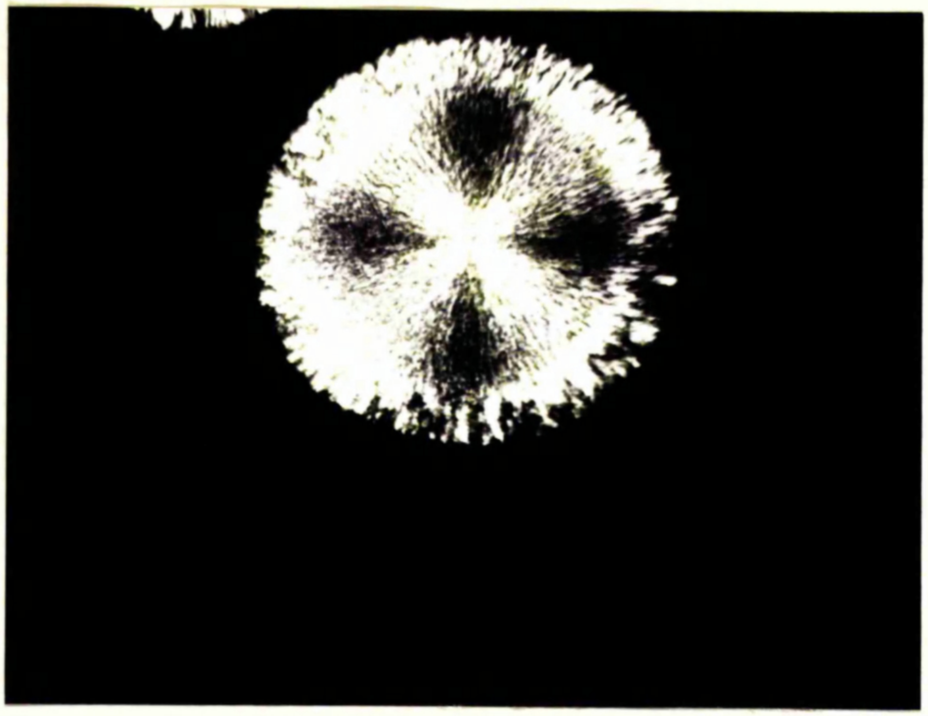

(a)

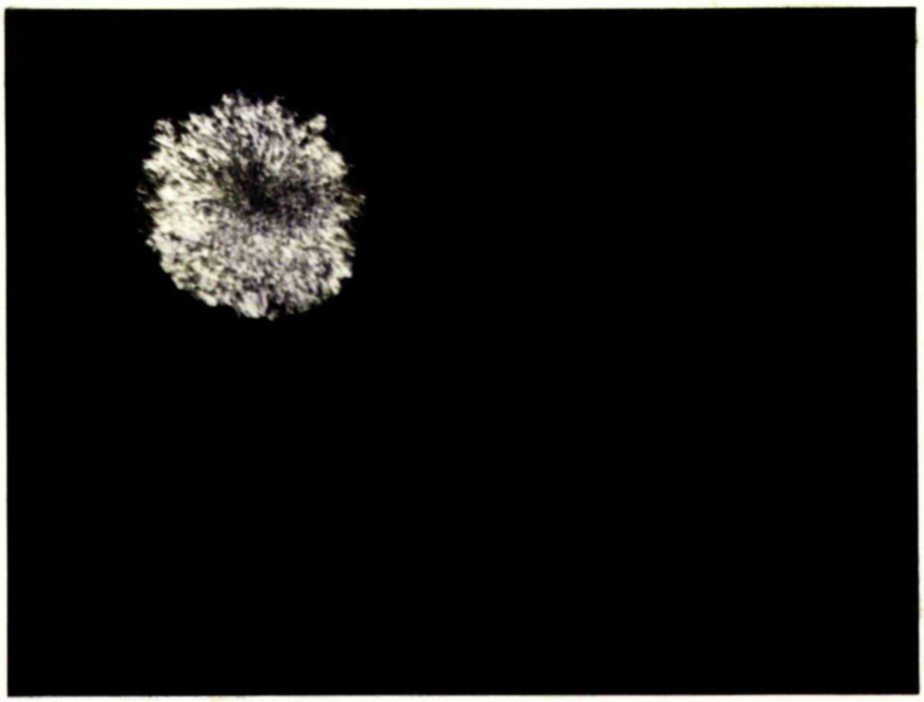

(b)

Fig. 22. Pictures showing (a) negative and (b) mixed spherulites of Pure Polymer at 53°C

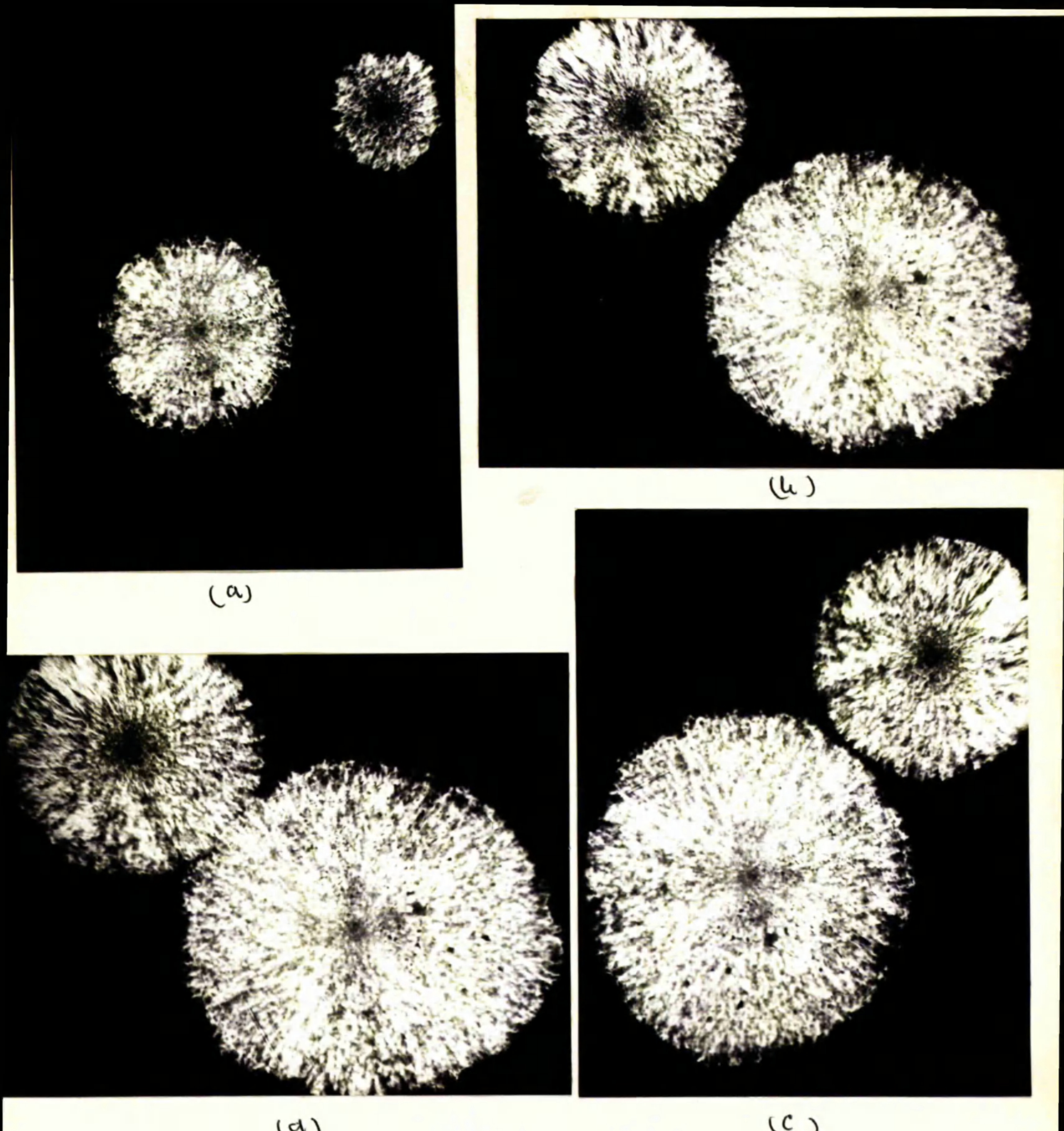

Fig. 23. Pictures showing growth of two spherulites at 53°C at (a) 0 min. (b) 10 min. (c) 13 min. and (d) 15 min.

temperatures, the nature of the spherulites changes and they are either negative or dendritic. In many cases the maltese cross is barely discernible. The ovalshaped dendritic spherulites were invariably obtained at $\Delta T \leq 11$ when spherulitic growth was very slow.

Price _et al_[85] reported a change in the growth rates of the spherulites when they are within 0.15 mm. of one another. This was confirmed and it was found that, sometimes, the size of the two abutting spherulites determined the change in speed, the smaller one growing at a higher speed as shown in the pictures of Fig. 23. The smaller spherulite was nucleated at a later time and grows at a faster speed. It can be seen from the graph in Fig. 24 that the growth of both spherulites decrease just before impact.

Polymer-Diluent Systems

Photographic records of four polymer-diluent systems were made. In order to cause a reasonable number of spherulites to nucleate in the field of view, the samples were held at room temperature for 30-55 seconds before transferring them to the hot stage. The following observations were made.

(a) The most common type of observation in polymer-diluent mixtures shows that two spherulites nucleated at the same time, and thus of equal size, continue to grow with identical

FIG 24 GROWTH RATE OF ABUTTING SPHERULITES AT $53^{\circ}C$ (PHOTOGRAPHIC)

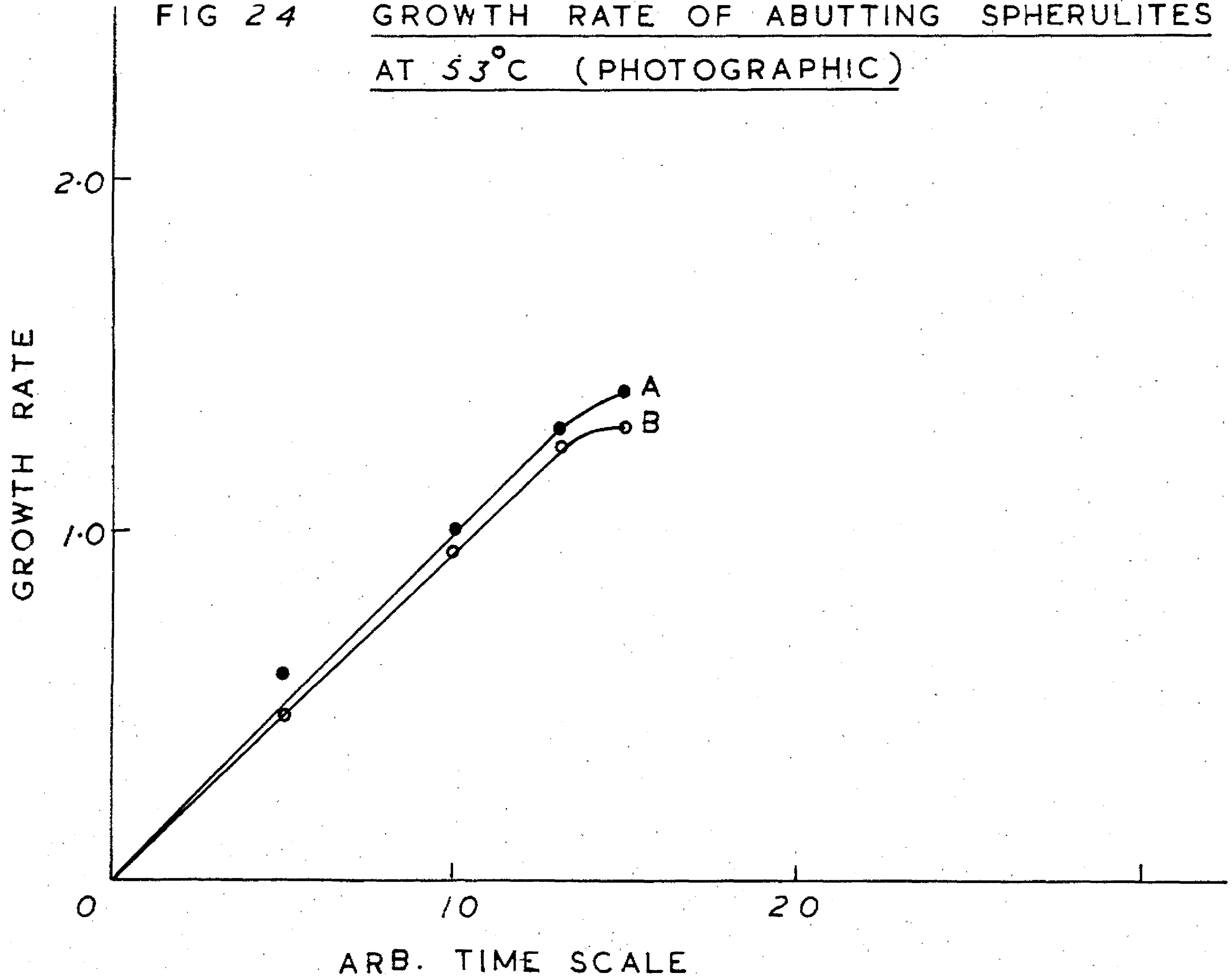

speeds until they meet. This is depicted in the pictures presented in Fig. 25.

(b) When two adjacent spherulites were obtained of unequal size, a similar phenomenon was observed to that seen in the pure polymer. Generally the smaller spherulite grows at a slightly greater rate right up to the point of impact.

(c) At higher temperatures, dendritic growth occurs causing the spherulites to grow in an oval form. The growth rate in these cases is not constant and varies with direction. The pictures given in the Fig. 26 depict two spherulites growing at T = 45°C in 1:1 (B) polymer-diluent system. The interesting feature is that for both the spherulites, the ratio of maximum rate of growth to minimum rate of growth is constant and equal to three. This effect was observed in numerous experiments.

(d) When dendritic spherulites are grown from mixtures, the edge of the growing spherulite tends to be irregular in form. In many cases, when two spherulites are about to touch, a bulge in one is seen to grow into a recess in the other. This is shown in the picture of Fig. 27. This effect was not observed for pure polymer in the temperature range investigated but photographs obtained by Price[99] on low molecular weight PEO, at ΔT = 11 seem to depict this phenomenon.

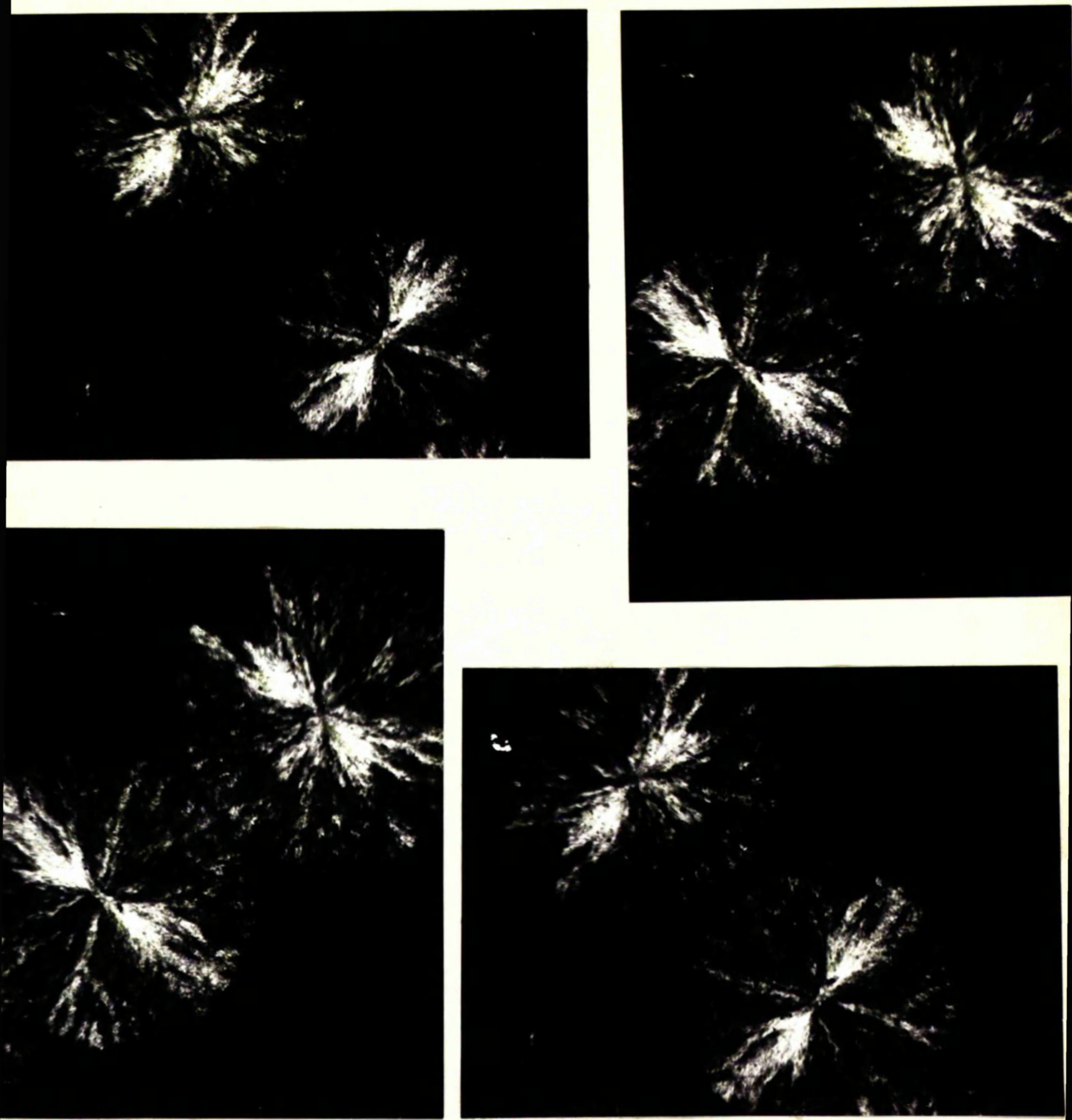

Fig. 25 Pictures showing growth of two equal-size dendritic spherulites at (a) 5 min. (b) 7 min. (c) 9 min. and (d) 11 min. - System C at 41°C

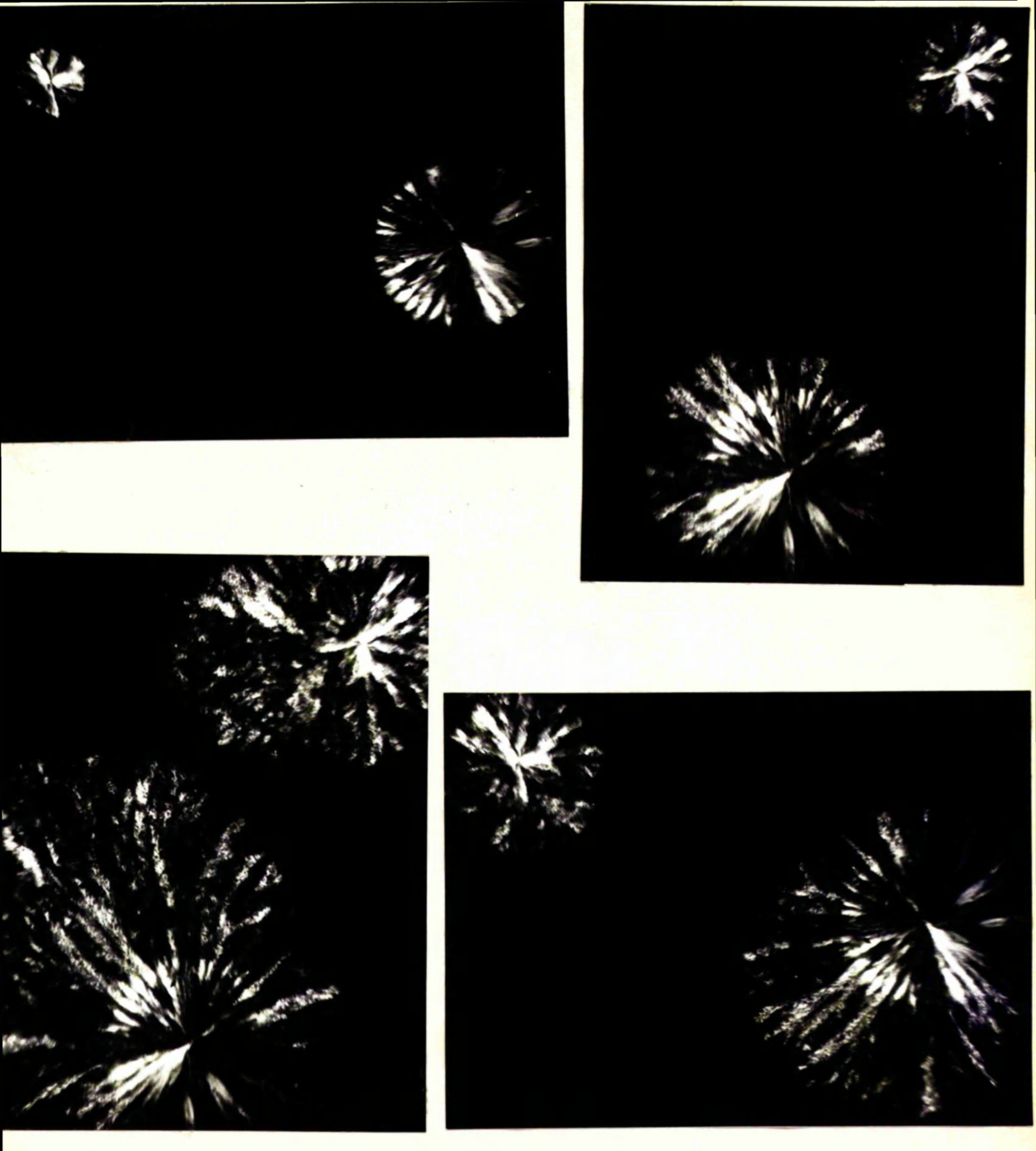

Fig. 26. Pictures showing ovalshaped growth for system A at 41°C at (a) 0 min. (b) 20 min. (c) 80 min. and (d) 175 min.

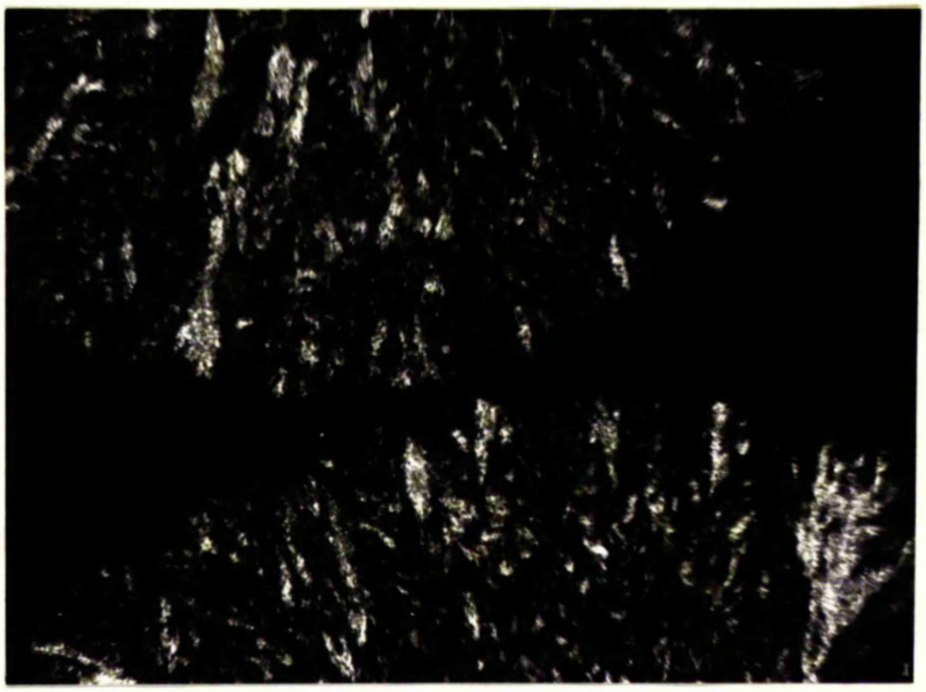

Fig. 27. Dendritic spherulite with bulge and recess

All the effects noted in the photographic examination, though interesting in themselves, will effect the overall crystallisation kinetics to a relatively minor extent.

C H A P T E R VI

DISCUSSION

Discussion

Pure Polymer - Values of 'n'

In all the experimental and theoretical comparisons, the zero on the time scale was taken to be the time when the temperature of the dilatometer and its contents reached that of the thermostat. In most cases, this was three minutes after the dilatometer was removed from the bath at 100°C.

The theoretical comparison of the dilatometric results for the pure polymer on the basis of the Avrami equation is given in figure (28) where log (-log θ) has been plotted against log t. The value of 'n' obtained in this way is 2.50 $\pm$ 0.1 for all temperatures.

The superposability of the crystallisation curves obtained at different temperatures on a logarithmic time scale and the linear growth rate of the crystalline phase have lent support for the theory that both the nucleation and growth processes are instantaneous. There seems, therefore, little theoretical justification for a separate induction period. At temperatures of crystallisation just below the melting point, it is found experimentally that the volume of the molten polymer remains virtually constant for a considerable time. If a sufficiently sensitive dilatometer were to be used, these apparent induction periods would vanish. Allen[89] and Magill[90] tried to exclude the induction period from their time scale for the crystallisation

FIG 28 AVRAMI PLOTS FOR PURE POLYMER WITH r_i

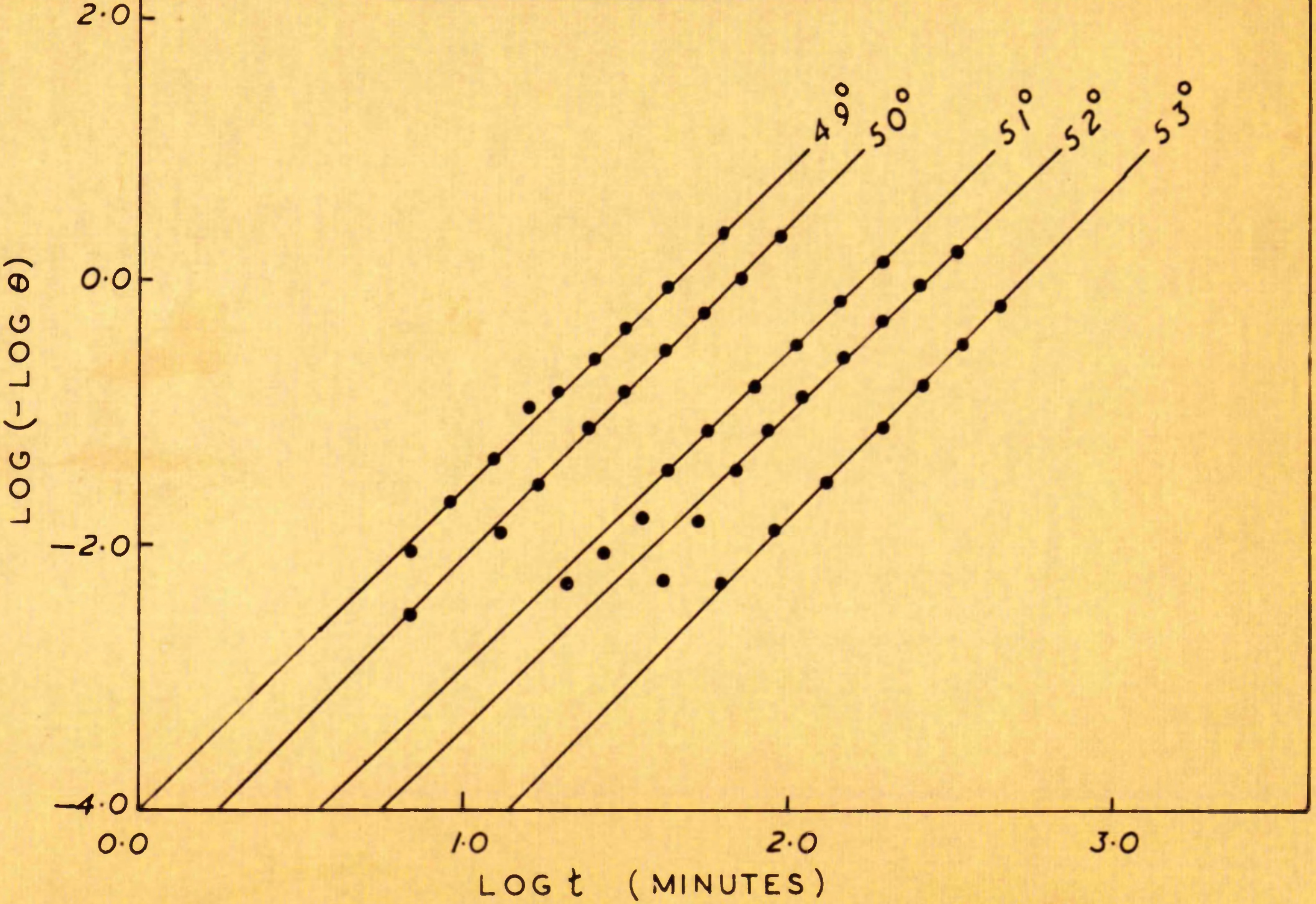

of PMMA, but they obtained erroneous values of 'n'. In spite of this, Rybnikar,[86] claimed two advantages for the exclusion of the induction period.

(i) The linearity of the Avrami plot is improved

(ii) 'Abnormal' values of 'n' change to integral values in agreement with the simple theory.

The Avrami plots for the present results constructed on this basis are shown in Fig.29 and it is seen that the exclusion of τ_i from the time scale has two effects. Firstly, there is a shift of the initial points towards the top side of the straight line thus decreasing the overall linearity. Secondly, there is decrease in the average slope of the line leading to reduced values of 'n'.

The average value of 'n', now, becomes 1.80 ± 0.15 which, though reduced, is still fractional. It is, therefore, clear that Rybnikar's findings are not substantiated by this work.

The Avrami plots, described above, allow an average value of 'n' to be calculated which may include lower or higher values at the start and at the end of the process. Equation (49b) has been used to calculate the values of 'n' for each stage of the crystallisation process as a function of Θ. In figure (30) 'n' against Θ is plotted for the pure polymer at 52°C including and excluding the induction period. When τ_i is included, it is seen that 'n' is constant for a range of Θ from 0.95 to 0.15.

FIG 29 AVRAMI PLOTS FOR BULK POLYMER (WITHOUT r_i)

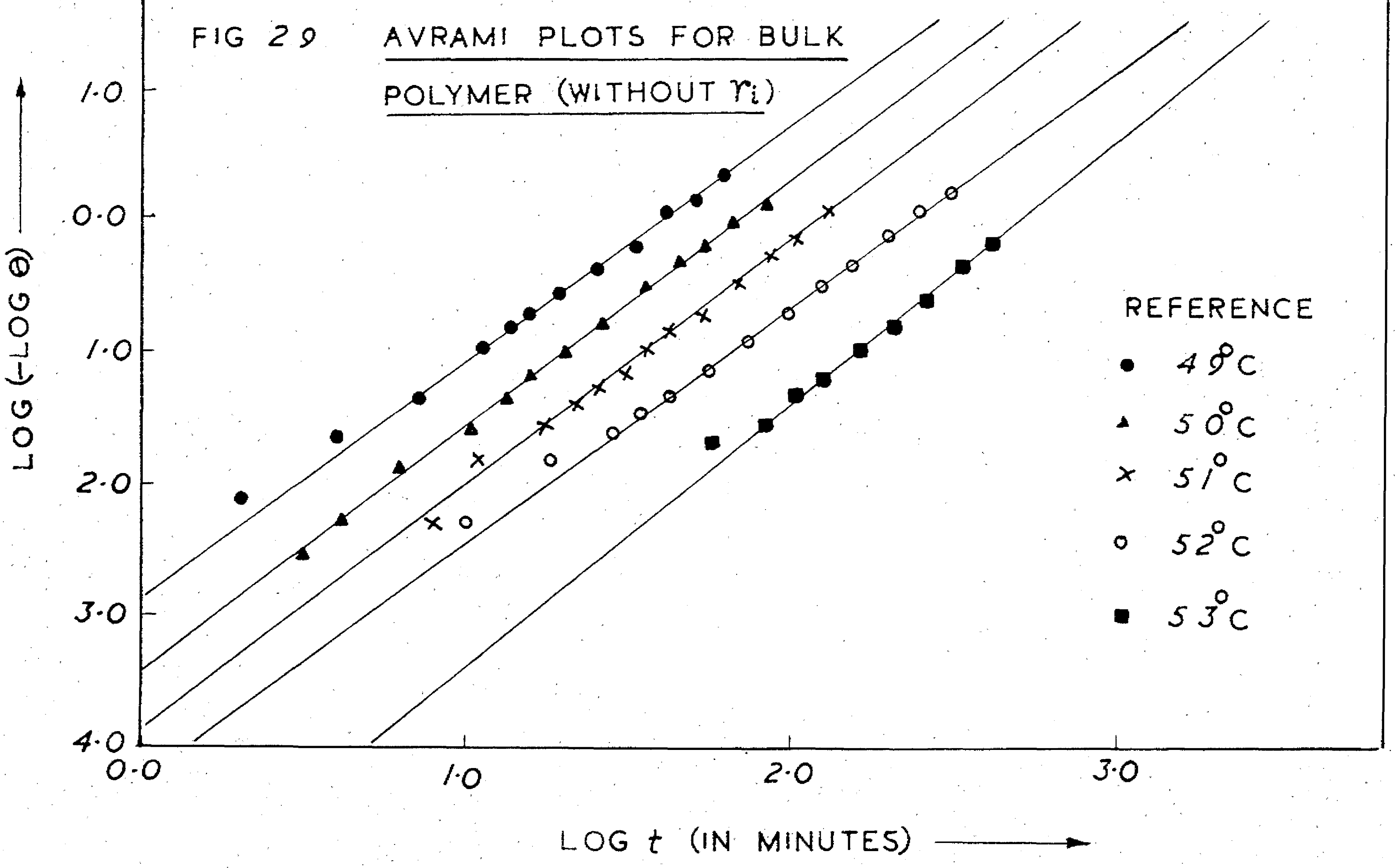

At the beginning and at the end of the crystallisation process, the experimental value of θ depends critically upon the value of h_0 and h_∞ selected. Bearing this in mind, it may well be that in this case 'n' is constant throughout the process.

In the other graph in fig.(30) where $x_{\frac{1}{2}}$ is excluded from the experimental time scale, it is seen that 'n' becomes a non-linear function of θ. This means that a plot of log (-log θ) against log. t should be curved. Equation (49b) is thus a more sensitive test of experimental results than this latter plot.

The value of $n = 2.5 \pm 0.1$ obtained for the crystallisation of pure PEO can be compared with the value of 3.0 obtained by Mandelkern and 2.0 obtained by Price. The polymer used by Price was low molecular weight material and he found that $n = 3$ or 4 in the initial stages of the crystallisation and fell to $n = 2$ after 5% of the process was completed. Sharples has also quoted a value of 2.0 for this polymer but no [redacted] details were given.

The main feature of the dilatometric measurements on the pure polymer is that not only is the Avrami exponent 'n' fractional, but it remains constant throughout the course of crystallisation. Fractional values of 'n' for many polymers have been reported recently. Many factors have been suggested to account for this phenomenon. Secondary crystallisation

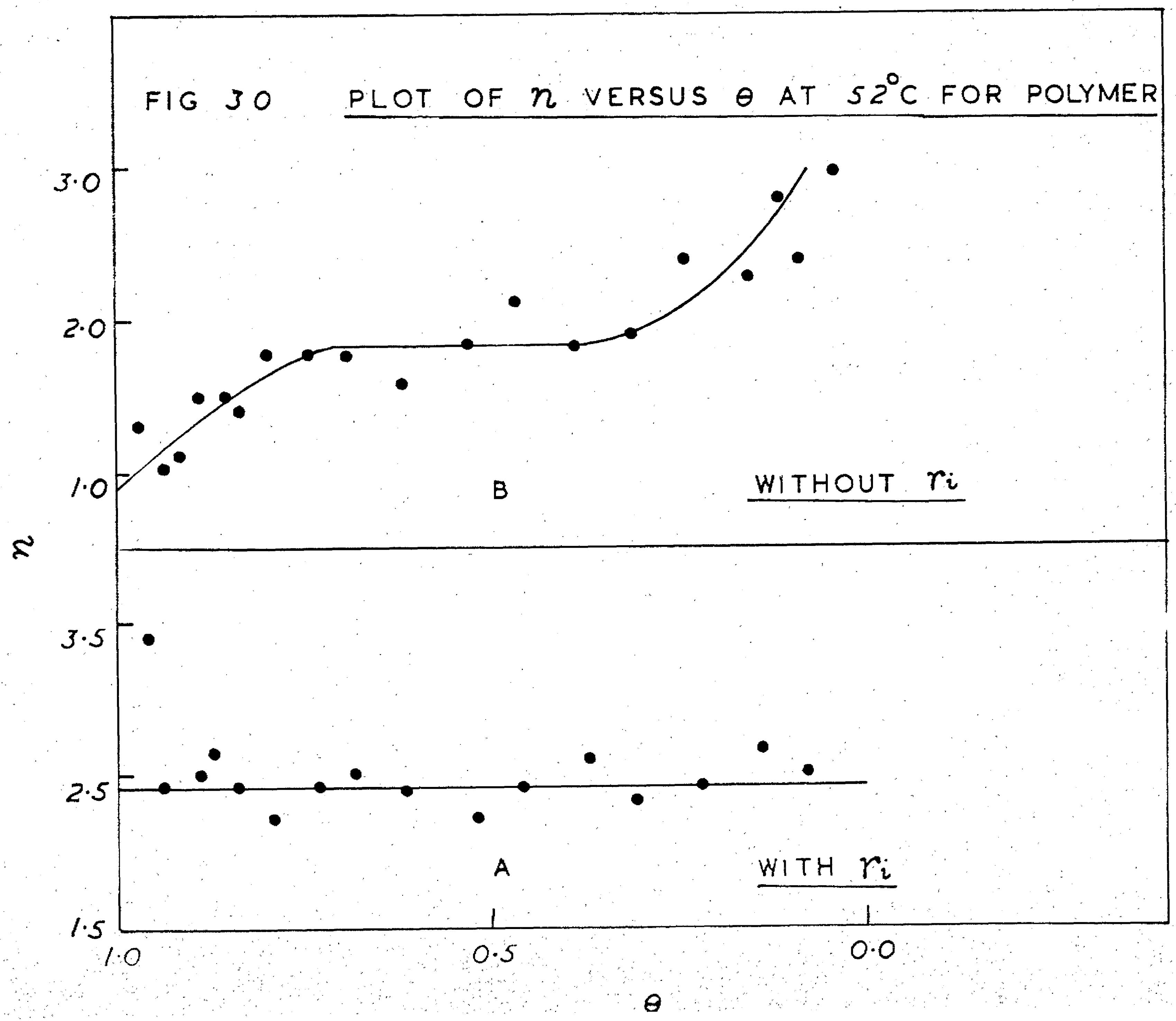
FIG 30 PLOT OF n VERSUS θ AT 52°C FOR POLYMER
3·0
2·0
1·0
3·5
2·5
1·5
n
B
WITHOUT r_i
A
WITH r_i
1·0
0·5
0·0
θ

is one of them, which seems to be absent in this case as is evident from the dilatometric curves. Persistence of nuclei or the presence of heterogeneities may also cause 'n' to be reduced and fractional. The process of nucleation might be concurrently[37] homogeneous and heterogeneous in which case the crystallisation behaviour will be complex. Sharples *et al.*[88] have analysed such a situation theoretically and have shown that though 'n' may become fractional, it will not remain constant during the crystallisation process. It seems evident in this case, that the crystallisation is mostly heterogeneous because spherulites have been found to appear at the same place on repeated crystallisation and melting. However, this does not exclude the possibility of homogeneous nucleation occurring simultaneously. Moreover, the nucleation results show that nucleation ceases after a certain time and, afterwards, there is only growth on nucleated sites. This behaviour could also lead to change in 'n', if the build up of nuclei continued during a considerable part of the crystallisation process. A comparison of Fig.(3)and (20) show that this is not the case and, at each temperature, a constant number of nuclei have been formed during the apparent initiation period before any significant decrease in the volume of the system has taken place.

The major portion of the crystallisation process which is observed dilatometrically takes place with pre-determined nuclei, so that the maximum value of 'n' to be expected is 3.0. Sharples et al after considering all the available evidence, have suggested that the most probable reason for a fractional and constant value of 'n' is that the density of the growing semi-crystalline spherulite is not constant but time-dependent. This would be rather difficult to prove experimentally and the actual time dependance of density would have to be a rather complex function in order to maintain 'n' constant throughout the process. The reason for appearance of fractional 'n' values awaits a satisfactory explanation.

The decrease in the rate of growth of two spherulites about to touch which has been observed in this and other work[38] is too small an effect to account for any major disagreement between Avrami theory and experiment. Any disagreement would tend to appear towards the end of the crystallisation process, and several instances of this were noted in the present studies, but were always just outside the experimental error. Keith[102] has recently suggested an explanation for the decrease in growth rate. Because of the nature of polymeric compounds, there are stereo-irregular or low molecular weight species present in the melt which are preferentially rejected by the crystallising units. In the melt, these species will be concentrated near the crystal faces. The crystallisable molecule must first diffuse through these layers. As the growing crystal surface advances into the melt, rejected impurities diffuse away from the surface and are left behind to accumulate in the interstices. The presence of and diffusion through these impurities cause the rate to slow down which accounts for the deviation from the Avrami theory.

Rate Constants - K

In table (17) are presented the rate constants K obtained from the intercepts of the Avrami plots based on the dilatometric results of Fig. 3. The corresponding microscopic rate constants obtained from the equation,

$$K \cong NG^3$$

are also given where the values of N and G are taken from table 13. It is seen that the microscopic rate constants are a factor of 10 higher than the rate constant measured dilatometrically. The difference most probably arises because the values of N and G used to calculate K(microscopic) are those for a sample 100 μ thick. A better and fairer comparison would be to measure N and G for a large number of thickness and to extrapolate to infinite thickness. These values could, then, be used to evaluate K to compare with the dilatometric value which is obtained on the polymer in bulk form.

TABLE 17 Crystallisation Rate Constants for Pure Polymer

ΔT	K_s (Dilatometric)	K (microscopic, using Nucleation density)	$\frac{K_s \text{(Micro.)}}{K_s \text{(Dil)}}$	K_s (Microscopic, using nucleation rate/min
19	1.4×10^{-3}	2.9×10^{-2}	20.9	2.2×10^{-2}
17	3.3×10^{-4}	3.24×10^{-3}	10.0	1.7×10^{-4}
16	2.3×10^{-5}	5.17×10^{-4}	22.4	-
15	2.9×10^{-5}	1.1×10^{-4}	4.0	3.7×10^{-6}
14	3.1×10^{-6}	4.4×10^{-5}	14.2	-
13	3.6×10^{-7}	2.4×10^{-6}	6.6	4.9×10^{-6}
11	-	4.0×10^{-8}	-	1.6×10^{-9}

TABLE 18 Comparative values at $\Delta T = 13$

Reference	K_s
Mandelkern[79]	3.9×10^{-6}
Present work	3.6×10^{-7}
Price *et al*[35]	1.19×10^{-11}

Dilatometric rate constants for PEO have been reported (Table 18) by previous workers. The results of Price *et al.* seem to be far too low while the present values are comparable with those obtained by Mandelkern. However, the extent of agreement which arises out of the comparison of the three sets of results, is that K determined both dilatometrically and microscopically is reduced by a factor of 10 per degree rise in temperature, and that there exists a ratio of approximately 10 between the microscopic and dilatometric K values at a given temperature. If the rate constants are calculated on the basis of nucleation rates derived from the initial slopes of fig. (20), it is found that they are lower than the dilatometric values by a factor of 10.

Polymer-diluent Mixtures - Values of 'n'.

The dilatometric curves obtained for the crystallisation of all the six systems resemble in their sigmoidal shape that of the pure polymer. Avrami analyses of all these systems (A-F) at a constant degree of supercooling, $\Delta T = 15$ are presented in figure (31). The plot for the pure polymer is also given in the figure. It is clearly seen by comparison, that the plots for the mixtures are non-linear. and confirm an earlier observation[110].

Analysis of the results according to equation (49b) is given

FIG 31

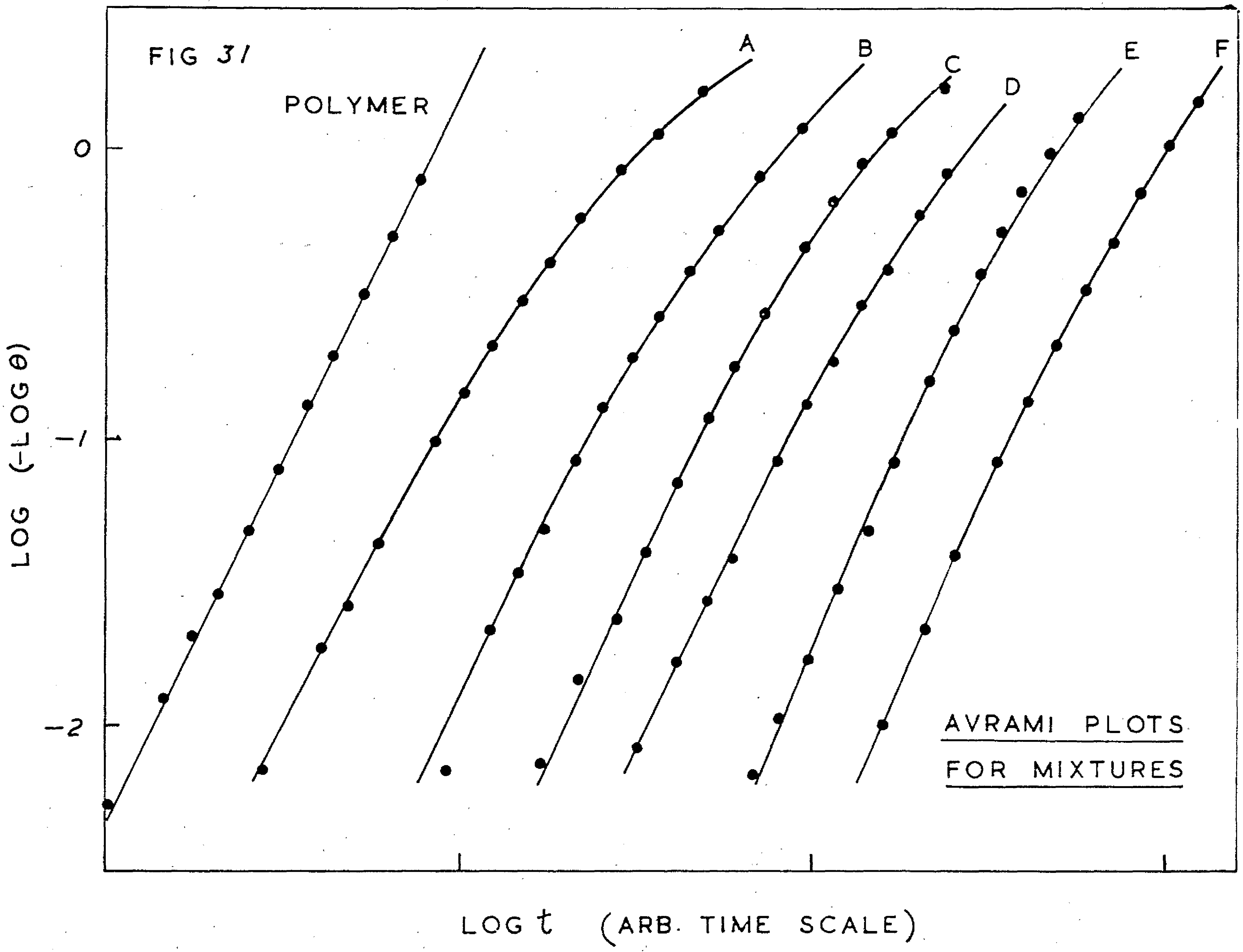
POLYMER
A
B
C
D
E
F
0
-1
-2
LOG (-LOG θ)
LOG t (ARB. TIME SCALE)
AVRAMI PLOTS
FOR MIXTURES

in figure (32) in the form of the Avrami exponenet, n, as a function of θ. For the four more concentrated solutions, 'n' seems to remain constant for the early part of the process where it is equal to 2.5 ± 0.1, identical to the value found for pure polymer over the whole crystallisation process. After a certain time, it begins to decrease in an approximately linear manner to a value of 1.3 ± 0.1 in all these systems. The main features of the plots in figure (32) are tabulated in table (19). It seems that as the concentration of the diluent is increased, the percentage of the total process over which 'n' is initially constant, decreases until at a weight fraction of polymer ≃ 0.15, the 'n' versus θ plots decreases continuously as θ decreases from 1.0 to 0.0. For the two most dilute solutions studied, the initial value of 'n' is 3.00, not 2.5.

It appears from the above evidence that when a polymer-diluent mixture starts to crystallise, the initial stage in the growth of the spherulites consists of virtually pure polymer. As the process continues, the uncrystallised material becomes less concentrated with respect to the polymer and the crystallising spherulite front becomes swollen with diluent as it advances. That the diluent is incorporated into the basic structure of the spherulite, is evident because even at the lowest concentration

TABLE 19 – Summary of n versus θ plots for Polymer-diluent systems

Mixture	Wt. fraction Polymer	Initial value of n	% Crystallisation for initial value of n	Final value of n
A	0.66	2.4	25	1.2
B	0.46	2.5	20	1.3
C	0.32	2.6	10	1.3
D	0.25	2.5	7	1.3
E	0.20	3.0	5	1.5
F	0.11	3.0	0	1.6
Pure Polymer	1.00	2.5	100	2.5

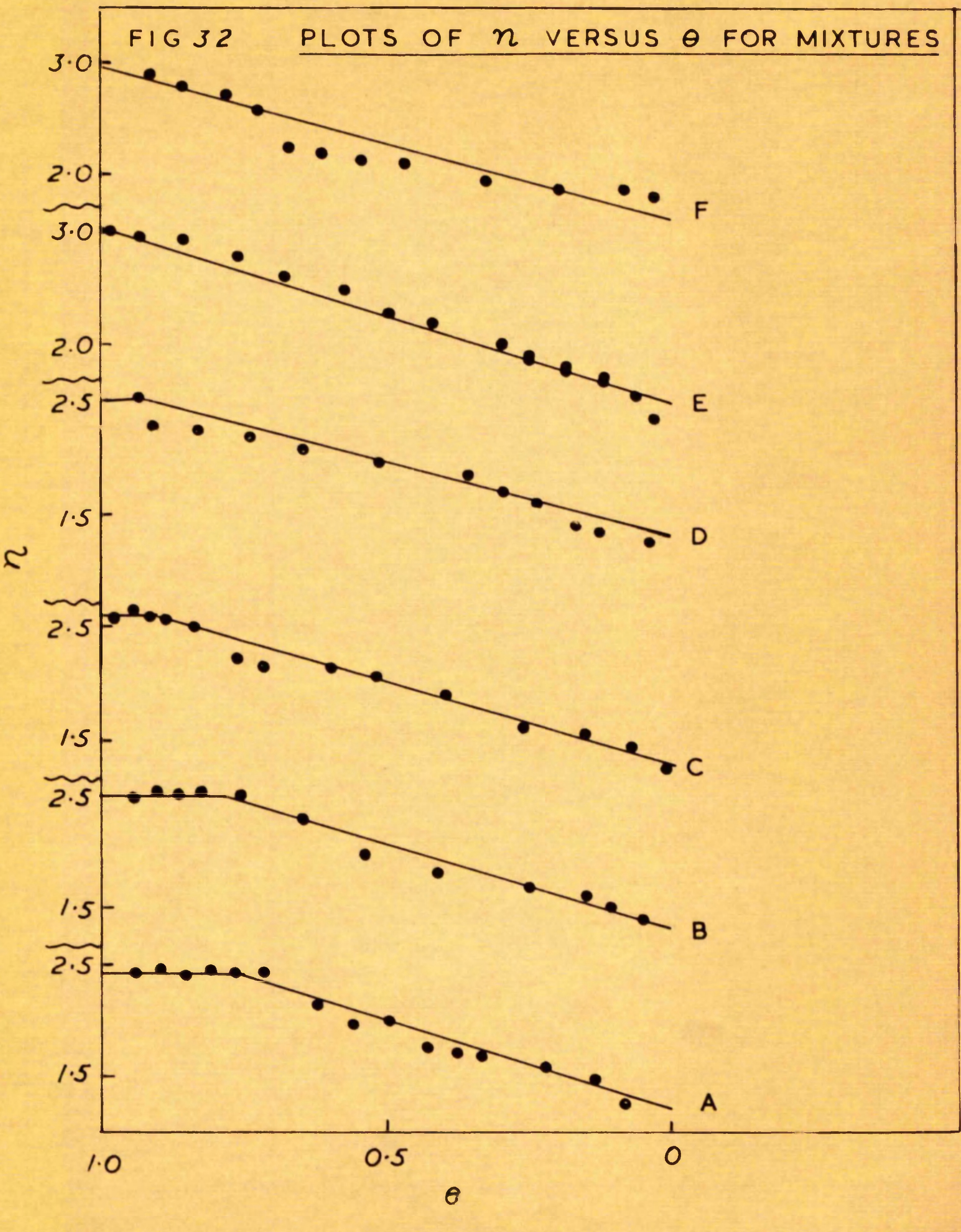
FIG 32 PLOTS OF n VERSUS θ FOR MIXTURES
3·0
2·0
3·0
2·0
2·5
1·5
2·5
1·5
2·5
1·5
2·5
1·5
n
F
E
D
C
B
A
1·0
0·5
0
θ

studied, visible phase separation did not occur, and the whole specimen became spherulitic throughout its mass. This latter process must account for the decrease in the value of 'n' from 2.5 to 1.3 and any theoretical analysis of the crystallisation process must take account of this factor. The original theory of crystallisation for solutions given by Mandelkern[79] did not allow for this fact but assumed that the density of the growing spherulite remained constant throughout the whole process.

The microscopic observation of the dendritic nature of spherulites formed from solutions suggests that the growing spherulite is not as dense as the normal one grown from pure polymer. Suggestions of the existence of a density composition gradient[103] and changing density[104,109] have recently been made, but they have not been subject to experimental verification. An attempt was, therefore, made to measure the variation in the density of a solution-grown spherulite as a function of its radius.

Several large spherulites grown between the cover-slips were selected and portions were cut out at increasing distances from their centres. In order to determine the concentration of polymer in each portion, the sections were weighed and then dissolved in a known volume of water filtered through Millipore filters. The viscosities of these solutions were determined using a micro-Ubbelode viscometer and from a knowledge of the viscosity concentration relationship for poly-ethylene oxide in water, the weight of polymer in each portion of the spherulite could be obtained. Unfortunately, the weight of the spherulite segments, and hence the concentration of the solutions were so low that their viscometric flow times only differed slightly, and no significant results could be obtained.

The apparent induction period of polymer-diluent systems is always less than that of the pure polymer at the same degree of supercooling. This can be seen from table (11). This suggests that it is easier for a nucleus to grow to a critical size in polymer-diluent systems. At high ΔT-values, however, the induction period seems to be independent of the concentration and the presence of the diluent, a fact supporting earlier results.[9b]

Rate Constants - K

Because of the non-linearity of the Avrami plots, values of K (dilatometric) can not be obtained. However, in many cases, $t_{1/2}$, i.e. time for half-change, has been used as a guide[10] for the rate constant according to the equation,

$$\ln 2 = \frac{K}{x\omega} \cdot t_{\frac{1}{2}}^{n}$$

which is another form of the Avrami equation where θ has been taken to be 0.5. This equation suggests that the rate constant is inversely proportional to $t_{1/2}$. The $t_{1/2}$ values for the

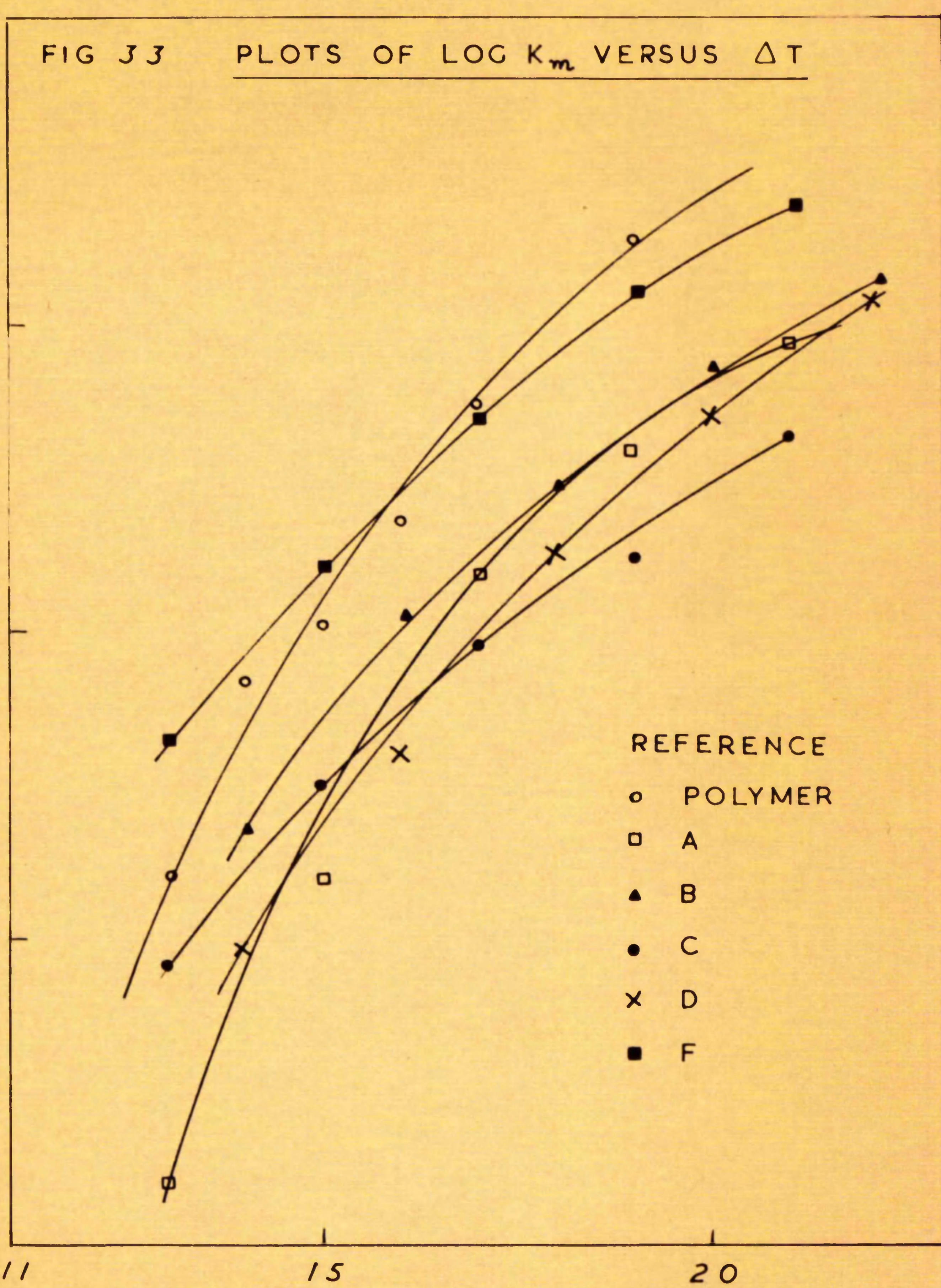
FIG 33 PLOTS OF LOG K_m VERSUS ΔT
LOG K_m
−2
−4
−6
−8
11
15
20
ΔT
REFERENCE
POLYMER
A
B
C
D
F

mixtures at various ΔT-values are presented in table (12) and it is seen that the growth rate as measured by $t_{\frac{1}{2}}$ is faster than that of the pure polymer until $\Delta T = 15$. At higher ΔT-values, however, it tends to be independent of the presence of the diluent and approaches that of the pure polymer.

The smaller induction period and faster growth rates suggest that crystallinity is favoured by the presence of an inert diluent and this is confirmed by the figures given in Column 7 of Table 2. It is seen from these figures that the volume change per $cm.^3$ of polymer increases with increasing dilution.

It is seen from the microscopic results on the polymer solutions presented in the form of plots of log K_m as a function of ΔT in fig. (33), that the rate constants for the more concentrated solutions are lower than those of the pure polymer at the same degree of supercooling. The rate constant for the most dilute solution, however, are very similar to those of the pure polymer. A similar feature can be seen from the 35 plot of log. G. as a function of $\frac{1}{T\Delta T}$ in figure (34). The results for the most dilute system are very similar to the pure polymer, while the linear plots for the other mixtures are parallel to the pure polymer plot and at some distance from it. The system D corresponding to a composition of 1:3 seems to be anomalous.

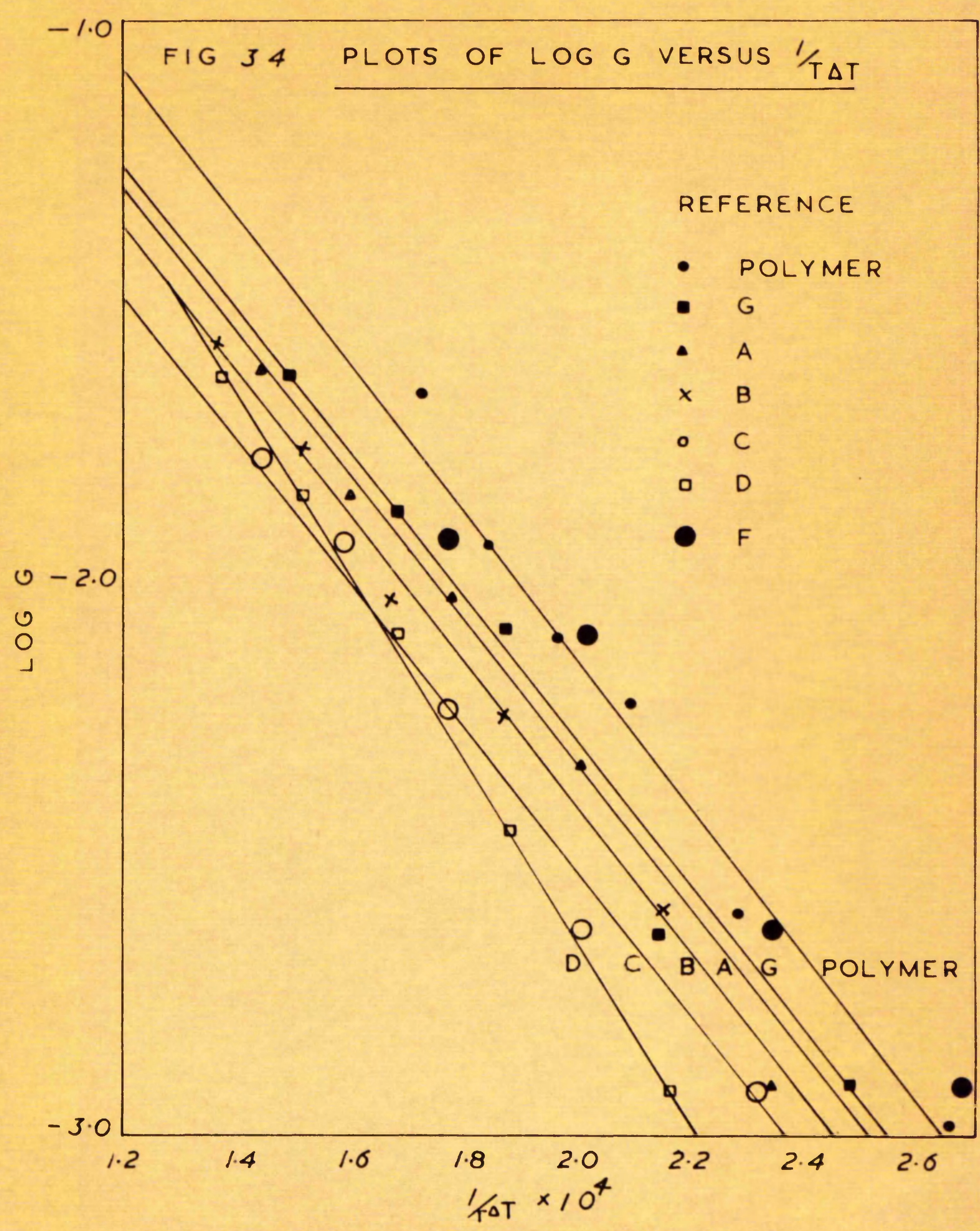

FIG 34 PLOTS OF LOG G VERSUS 1/TΔT
REFERENCE
POLYMER
G
A
B
C
D
F
D C B A G POLYMER
LOG G
-1.0
-2.0
-3.0
1.2
1.4
1.6
1.8
2.0
2.2
2.4
2.6
1/TΔT × 10⁴

In the only systematic dilatometric study of polymer-diluent mixtures, Mandelkern found that a plot of log K against $\frac{T_m^2}{T}\left(\frac{1}{\Delta T}\right)^2$, was curved. However, the observation of spherulitic growth in these systems means that the growth is most probably three dimensional. Mandelkern suggested that there is a fair amount of uncertainty in the determination of T_m° which may be as much as 3-5°C higher than the 'experimentally observed' T_m°. When the values of ΔT are estimated on this basis, his curves become linear within experimental error. It is seen, however, that even with this adjustment, the dilatometrically measured rate constants are unable to define the mechanism of growth uniquely. The plots of log G against $1/T\Delta T$ based on microscopic results, however, favour the two dimensional growth mechanism in both pure polymer and polymer diluent systems and supports other studies[106-7] where similar linear plots were obtained. It is concluded from these studies that the growth process in polymer solutions occurs by the same mechanism as applicable in the case of pure polymer.

It is seen from Table (11-12) that although $t_{1/2}$ and the induction periods for the solutions are smaller than those of the pure polymer at the same ΔT, the difference is not great and a shift of temperature of 1°C, which is the uncertainty in T_m°, would make all the rate constant similar. The addition of diluent increases the mobility of the polymer molecules and reduces the viscosity which, in turn, reduces the activation energy for transport, (E_D), thus an increase in the rate constant is to be expected. However, the thermodynamic term in the equation (54) will always be negative with increasing dilution because of the diffusional or osmotic[105] processes which are required to form a critical size nucleus. Thus, it seems that in homogeneous polymer-diluent systems, the nucleation might be slower, leading to the reduced rate constants at higher dilution. In cases like the present studies, where the nucleation is primarily heterogeneous, there is always a constant number of nuclei. Therefore, the major factor balancing the viscosity effects is the diffusion of the crystallisable molecules to the growing spherulitic boundary. Thus in heterogeneous systems, the crystallisation process seems to be primarily diffusion controlled.

Possible Modification of the Avrami Equation.

The overall crystallisation kinetics of pure poly-ethylene oxide can be well represented by the expression,

$$\ln \theta = -Kt^{2.5} \qquad \text{(i)}$$

All the basic assumptions used in the derivation of the Avrami equation have been proved experimentally except the restriction of constant spherulite density. It seems likely that failure to obey this last assumption is a probable reason for the time exponent, 'n,' to be constant and fractional in value. The experimental value of $n = 2.5$ can conceivably arise in one of the two ways, if a heterogeneous nucleation process is assumed.

The growth mechanism may be three dimensional with a density factor decreasing 'n' from 3 to 2.5 or

it could be two dimensional and the variation in density with time leading to an increase in 'n' from 2 to 2.5.

i.e. either,

$$\ln \theta = -At^{3}.Bt^{-1/2} \qquad \text{..................(iia)}$$

$$\text{or} \qquad \ln \theta = -A't^{2}.B't^{1/2} \qquad \text{..................(iib)}$$

No physically realistic choice of density as a function of time appears able to yield a final equation of the above form.

The attempts were made by modifying equation (41). For heterogeneous nucleation, and ρ_c, the density of the crystalline phase, now temperature dependent, equation (41) becomes,

$$V_c' = 4\pi/3\rho_L \; V_0.N.G^3,t^3\int_0^t \rho_c.dt' \qquad \text{..................(iii)}$$

where the symbols have their usual significance. By feeding in trial, time dependent functions for ρ_c, Avrami-type equations are found in the usual way, first integrating (iii) followed by differentiation and a subsequent, final integration.

If, for example, we choose,

$$\rho_c = C - Dt$$

where C and D are constants, we find,

$$\ln\theta = -xt^{3} + yt^{4} \qquad \ldots\ldots\ldots\ldots\ldots\ldots \qquad (iv)$$

where x and y are also time-independent constants.

This equation and other equations derived in a similar manner do not give a constant value of 'n' throughout the crystallisation process and must be rejected.

The dilatometric results for the polymer solutions can, with reasonable precision, be fitted to an empirical equation of the form,

$$\ln\theta = -Kt^{2.5(2-\theta)} \qquad \ldots\ldots\ldots\ldots \qquad (v)$$

The time exponent 'n' in this equation is, now, itself, time-dependent.

Once again, assuming that ρ_c is a function of time or of the extent of crystallisation, theoretical equations can be derived. However, no physically realistic density-time relationship can be found to give a theoretical equation approximating to equation (v).

In conclusion, on the basis of the above analysis, it must be concluded that a correct theory of crystallisation for both-pure polymer and polymer-diluent mixtures remains to be formulated.

An experimental study of the variation of spherulitic density with radius remains an urgent problem before more progress can be made. The present analysis, in fact, suggests that some factor other than the variation of density with time will have to be taken into account before a completely satisfactory theory is produced.

REFERENCES

1. Richards, R. B., J. Appl. Chem. 1, 370, (1951).
2. Flory, P. J., J. Cheml Phys. 15, 397, (1947).
3. Natta, G. and Corradini, P., J. Polymer Sc. 39, 29, (1959).
4. Morgan, L. B. in 'Progress in High Polymers' vol.1, (1961) edited by Robb and Peaker, Haywood and Co. London, pp.235.
5. Stuart, H. A. in 'Der Physik der Hochpolymer' vol.4, (1955), pp.353.
6. Leitner, M., Trans Faraday Soc., 51, 1015, (1955).
7. Gee, G., J. Polymer Sc., 2, 451, (1947).
8. Gent, A. N., Trans. Faraday Soc., 50, 521, (1954).
9. Mandelkern, L. (a) Chem. Reviews, 56, 903, (1956).
   (b) Growth and Perfection of Crystals, pp.467
10. Keller, A., ibid., pp.499
11. Keller, A., Macromol. Chem. 34, 1, (1959).
12. Stuart, H. A., J. pure and Appl. Chem. 5, 143, (1962).
13. Morgan, L. B., J. Appl. Chem., 4, 160, (1954).
14. Lindenmeyer, P. H., J. Polymer Sc., 1, 5, (1963).
15. Gupta, V. P. and Beevers, R. B. Chem. Reviews, 62, 665, (1962).
16. Farrow, G. and Ward, I. M., Polymer, 1, 331, (1960).
17. Kakudo, M. and Ullman, R., J. Polymer Sc. 45, 91, (1960).
18. Gupta, V. P. and Tobolsky, A. V., J. Chem. Phys., 36, 1999, (1962).
19. Till, P. H., J. Polymer Sc. 24, 301, (1957).

20. Magill, J. H. Research and Development, 11, 30, (1962).

21. Stuart, H. A. Ann. of N.Y. Aca. Sc. 83, 3, (1959).

22. Morse, H. W. and Donnay, J. D. H., American Minerologist, 21, 392, (1936).

23. Bunn, C. W. and Alcock, T. C., Trans Faraday Soc., 41, 317, (1945).

24. Morgan, L. B. et al., Phil. Trans., 247, 23, (1954).

25. Bosson, E. H. et al., J. Polymer Sc. 21, 151, (1956).

26. Morgan, L. B. et al. Atti del. Sym. Intern. Macromol. Chem. Milano, Turino, - Rei Sci (Suppl.) 25, 577, (1955).

27. Keith, H. D. and Padden, F. J., J. Appl. Phys., 30, 1479, (1959)

28. Levy, B., J. Appl. Polymer Sc. 5, 408, (1961).

29. Stankweather, H. W. jr., and Brookes, R. E., ibid, 1, 236, (1959).

30. Ohlberg, S. M., et al., ibid, 1, 114, (1959).

31. Flory, P. J., J. Chem. Phys., 17, 223, (1949).

32. Zaukelies, D. A., J. Appl. Phys., 33, 2797, (1962).

33. Richard, R. B. and Hawkins, S. W., J. Polymer Sc., 4, 515, (1949).

34. Price, F. P., J. Amer. Chem. Soc, 74, 311, (1952).

35. Price, F. P. et al., J. Phys. Chem., 65, 1743, (1961).

36. Sharples, A. et al., Nature, 194, 542, (1962).

37. Ravisicka, J., and Kovacs, A. J., J. Appl. Phys., 32, 2314, (1961).

38. Bernauer, F., Gedrittel Kristalle Berntrager, Berlin 1929, Hept 2.

39. Khowry, F., J. Polymer Sc. 26, 375, (1957).

40. Gahler, R. Naturwiss. 35, 284, (1948)

41. Zenkkel, E., et al., (a) Z. Elektrochem. 53, 4, (1949).
(b) Kolloid Z., 118, 86, (1950).

42. Keller, A., and Waring, J. R. S., J. Polymer Sc. 17, 447, (1955)

43. Fischer, E. W., Z. Nature Forsch. 12a, 753, (1957).

44. Clauer, G. C. et al., J. Polymer Sc., 20, 202, (1956).

45. Kean, J. J., and Stein, R. S., ibid., 17, 21, (1955).

46. Price, F. P. in Ref. 9b. pp. 533.

47. Geil, P. H. J. Polymer Sc. 47, 65, (1960).

48. Price, F. P., Ann. N.Y. Acad. Sc. 83, 20, (1959).

49. Keller, A. Nature, 169, 913 (1952).

50. Point, J. J. Bull. Aca. Roy. Belgique (a) 39, 453, (1953).
(b) 41, 974, 982, (1955).

51. Keller, A., J. Polymer Sc. 17, 291, 351, (1955).

52. Zenckel, E., et al, Kolloid, Z., 129, 19, (1952).

53. Schurr. G., J. Polymer Sc., 11, 385, (1953).

54. Keith, H. D. and Padden, F. J., ibid., 39, 123, (1959).

55. Keller, A., ibid., 39, 151, (1959).

56. Price, F. D., ibid., 37, 71, (1959).

57. Jaccoline, R., Nature, 176, 305, (1955).

58. Till, P. H., J. Polymer Sc. 24, 301, (1957).

59. Keller, A., Phil. Mag. 2, 1171, (1957).

60. Frank, F. C. 'Advances in Physics', 1, 91, (1952)

61. Renekar, D. H. and Geil, P. H., J. Appl. Phys., 31, 1916, (1960).

62. Neigisch, W. D., and Swan, P. R., ibid, 31, 1906, (1960)

63. Basette, D. C. et al. Nature, 184, 810, (1959)

64. Fischer, E. W., Ann. N.Y. Aca. Sc., 89, 620, (1961)

65. Peterlin A. and Fischer, E. W., Z. Physik, 159, 272, (1960).

66. Lawritzen, J. I. and Hoffman, I. D., J. Chem. Phys. 31, 1680, (1959).

67. Price, F. P., J. Polymer, Sc., 42, 49, (1960).

68. Fischer, E. W., et al., ibid, 34, 721, (1959).

69. Kargin, V. A., J. Pure and Appl. Chem., 4, 201, (1962).

70. Vogelsong, P. C., J. Polymer Sc. A1, 1055, (1963).

71. Popoff, B., Lat. V. Farm. Zuru. 1, (1934).

72. Buchedahl, N., J. Research Nat. Bur. Standards, 13, 411, (1934).

73. Avrami M., (a) J. Chem. Phys., 8, 212, (1940).

(b) ibid, 9, 177, (1941).

74. Becker, R. and Doring, W., Annal d. Physik, 24, 719, (1935)

75. Turnbull, D., and Fischer, J. C., J. Chem. Phys., 17, 71, (1949).

76. Burnet, B. B. and McDevitt, N. F., J. Appl. Phys., 28, 1101, (1957).

76a. Takanayagi, M. and Yamashita, T., J. Polymer Sc. 22, 572, (1956).

77. Hirai, N., ibid., 42, 213, (1960).

78. Evans, V. R., Trans Faraday Soc., 41, 365, (1945).

79. Mandelkern, L., J. Appl. Phys., 25, 830, (1954).

80. Banks, W., Gordon, M., Ree, R. J. and Sharples, A.,
Polymer, 4, 61, (1963)

81. Limbert, F. J., and Baer, E., J. Polymer Sc., A1, 3317, (1963).

82. Sharples, A. et al., Macromol. Chem., 59, 233, (1963).

83. Sharples, A. et al., Polymer, 4, 289, (1963).

84. Mandelkern, L., J. Appl. Phys. 26, 443, (1955).

85. Rybinkar, F., Coll. Czech. Chem. Comm. 26, 106, (1961)

86. Sharples, A. and Swinton, F. L., Polymer, 4, 119, (1963).

87. Hatano, M. and Kambara S., ibid, 2, 1,(1961).

88. Sharples, A., et al. unpublished work.

89. Allen, P. W., Trans. Faraday Soc., 48, 1178, 1952.

90. Magill, J. H., Polymer, 2, 221, (1961).

91. McIntyre, A. D., Ph.D. Thesis, Cornell University, 1956.

92. Flory, P. J., and Mandelkern, L.,
(a) J.Polymer Sc., 12, 97,(1954).
(b) Flory, P. J. et al. J. Amer. Chem. Soc., 72, 218, (1950).
(c) Flory, P. J. et al. ibid, 73, 2532,(1951)

93a. Mandelkern, L., and Quinn, F. A. Jr., ibid,80, 3178, (1958).

93b. Mandelkern, L., and Roberts, D. E. ibid, 77, 781, (1955).

94. Park, J. Associateship Thesis, R.C.S.T., 1961.

95. Smith K. L. and Cleve, R. van. Ind and Eng. Chem. 50, 10, (1958).

96. Wood, L. A. and Backdahl, N., J. Appl. Phys., 17, 362, (1946)

97. McLaren J. V., Polymer, 4, 175, (1963).

98. Sharples, et al. ibid, 3, 250, (1962)

99. Price, F. P., J. Polymer Sc., 57, 395, (1962).

100. Sharples, et al., Polymer (in press)

101. Inoue, M., J. Polymer Sc., 60, 81, (1962).

102. Keith, H. D. ibid., C3, 121, (1963).

103. Holland, V. F. and Lindenmeyer P. A., J. Polymer Sc., 57, 589, (1962).

104. Sabenda, J., et al., ibid., 57, 785, (1962)

105. Griffith, J.H. and Rauby, B.G., ibid., 38, 107, (1959)

106. Kahle, B. and Stuart, H. A. ibid., 40, 159, (1959).

107. Kenyon, A. S. et al., ibid., 40, 159, (1959)

108. Flory, P. J., J. Amer. Chem. Soc., 84, 2857, (1962).

109. Johnson, J. F. and Farrow, W. J. Appl Polymer Sc. 3 365, (1960).

110. Swinton, F. L. unpublished work.

111. Sharples, A and Banks W. Makromol Chem. 67, 42, (1963)

A P P E N D I C E S

APPENDIX A

Abbreviations

PE	Poly-ethylene
PEO	Poly-ethylene oxide
PEA	Poly-ethylene adipate
PETP	Poly-ethylene Terephthalate
PDMS	Poly-decamethylene Sebacate
PDTP	Poly-decamethylene Terephthalate
PHMA	Poly-hexamethylene Adipamide
PMP	Poly-methyl-1-pentene
PTFE	Polychloro-trifluoro-ethylene
PVA	Poly-vinyl Alcohol

APPENDIX B

List of Symbols

A	Area
B	Interaction parameter
D	Parameter between 0-1
d_1, d_3	Width and length of rectangular parallelopiped
E	Expected number
E_D , ED	Activation energy of viscous flow
ΔF	Free energy difference between liquid and crystalline states.
$\Delta F_{max.}$	Maximum free energy barrier, to be crossed over to attain a nucleus of critical size.
Δf_0	Bulk free energy of fusion/mole
G	Rate of growth
G_0	Frequency factor for growth
h_0, h_t, h_∞	Dilatometric heights at o, t and infinite times respectively
ΔH_u	Heat of fusion / per mole of repeating unit
ΔH_m	Heat of fusion/mole of segment
K	Crystallisation, rate constant (subscript s or d referring to spherical and disc growth respectively)
K_m, K_d	Microscopic and dilatometric rate constant respectively .
l	Length/thickness of the cylindrical discs. Length/

n_L	Melt viscosity near the crystal surface
n	Rate parameter defining the mode of growth
N	(a) Rate of formation of nuclei (b) No of polymer molecules
N_o	Frequency factor for nucleation.
$P(u)$	Patterson function
P_l, P_x, P_o	Any property undergoing change during crystallisation referring to liquid, semi-crystalline and crystalline states.
P	(a) Transition probability parameter for a bond in amorphous region to be followed by a bond in crystalline region. (b) No. of polymer chains.
r	Distance/radius
$r_{max.}$	Radius of critical size nucleus
R	Gas constant
T, T_c	Absolute temperature, Temperature of Crystallisation
T_m	Melting temperature of substance or mixtures
T_m°	Equilibrium melting temperature of polymer
ΔT	Degree of supercooling
t	Time
V_t, V_o	Volume of substance at t and o times respectively
v_o, v_t, v_∞	Volumes at o, t and infinite times respectively
v	Radial velocity

V_u	Molar volume of repeating unit
V_D	Molar volume of diluent
v_1	Volume fraction of the diluent
v_2	$(1-v_1)$ = volume fraction of the polymer
W_L, W_o	Mass untransformed at t and o times respectively
W_c, W_c'	Actual and effective mass transformed.
dW_c, dW_c'	Actual and effective mass crystallised during dt.
X_W	Equilibrium degree of crystallinity.
Z, ξ	No. of repeating units in length 'l'
α, θ	Fraction remaining uncrystallised at time t
ρ	Density
P_l, P_c	Density of liquid and crystal respectively
δ	P_l/P_c
N, N'	Nucleation density.
σ_s	Interfacial free energy unit area between liquid and crystal surfaces
σ_E	Interfacial free energy/unit area for end surfaces.

APPENDIX C

List of Tables

APPENDIX D

List of Figures